Extracellular and Intracellular Regulation of G Protein-Coupled Receptor Signaling

Joseph E. Rittiner

A dissertation submitted to the faculty of the University of North Carolina at Chapel Hill in partial fulfillment of the requirements for the degree of Doctor of Philosophy in the School of Pharmacy (Chemical Biology and Medicinal Chemistry)

Chapel Hill
2013

Approved by:

Alexander Tropsha

Mark J. Zylka

Stephen Frye

Ken McCarthy

T. Kendall Harden

ABSTRACT

Joseph E. Rittiner: Extracellular and Intracellular Regulation of G Protein-Coupled Receptor Signaling
(Under the direction of Dr. Mark J. Zylka)

Signaling through G protein-coupled receptors (GPCRs) is an essential part of cellular communication, and nearly half of modern pharmaceuticals target GPCRs in some way. GPCRs are also subject to extensive biological regulation, which is incompletely understood. Here, I examined both extracellular metabolic control of GPCR signaling, and intracellular feedback mechanisms which regulate downstream signal transduction and receptor desensitization. I first found that the nucleotide adenosine 5'-monophosphate (AMP) is an agonist of the A_1 adenosine receptor. Previously, AMP was thought to signal exclusively via hydrolysis to adenosine, and no AMP receptor was known to exist. Using a novel real-time assay of adenosine receptor activity, I showed that AMP directly activates A_1R independent of hydrolysis to adenosine, but that activation of the adenosine A_{2B} receptor required hydrolysis to adenosine. I also identified a histidine residue in the A_1R binding pocket critical for receptor activation by AMP, but not adenosine. These results suggest that some of the A_1R-mediated physiological effects attributed to adenosine may in fact be directly caused by AMP. Furthermore, I found that extracellular loop 2 partially determines A_1R sensitivity to AMP, and that AMP stimulation elicits differential activation of signaling cascades downstream of A_1R. In subsequent work, I found that the novel lipid kinase

diacylglycerol kinase eta (DGKη) positively modulates signaling downstream of muscarinic and purinergic GPCRs. This effect required DGKη catalytic activity, but only a minimal level of DGKη expression. DGKη expression also suppressed extracellular signal-related kinase (ERK) phosphorylation downstream of protein kinase C (PKC) and both activation and depletion of PKC abolished the DGKη effect on GPCR signaling, indicating that DGKη enhances GPCR signaling by suppressing PKC activation, likely reducing receptor desensitization. Enhanced expression of DGKη is linked to bipolar disorder (BPD), suggesting that increased DGKη activity contributes to the dysregulation of GPCR and PKC signaling in BPD and that DGKη inhibitors may have therapeutic potential for the treatment of BPD. Together, my work expands the current understanding of adenosine receptor signaling, implies an enhanced role for multiple endogenous ligands and functional selectivity in physiological GPCR signaling, and highlights GPCR-modulating enzymes as targets for drug discovery.

ACKNOWLEDGEMENTS

First of all, I would like to thank Mark, for providing me a temporary home, a sweet microscope, lots of advice, and infinite coffee. Thanks most of all for allowing me the freedom to explore my projects in my own way, and for help with my writing. Your patience has been appreciated. I would also like to thank the "prodrug meeting" (now with less prodrugs!) crew, Stephen, Jian, Bill, and Emily, for providing a sounding board for potential experiments and bringing invaluable real-world experience to the proceedings. And of course, thanks to Ilia for the samurai journey, you totally saved the day.

I would like to thank the members of the Zylka lab, past and present, for various opinions and advice, both scientific and extracurricular. It has been a strange treat to watch the lab triple in size since I've been here. Thanks for making the lab a wonderful environment to work in, because trust me, there are plenty of labs that aren't. I would not have survived without the various lab managers through the ages: Yvette, Brendan, Sarah, and Gabby; thanks for keeping everything running. Thanks also to Vicki, for swooping in at the perfect time to take my second project off my hands, so that I could focus on graduating without worrying about it. But most of all, thanks to Julie, for showing me how to work hard and keep a sense of humor, and for teaching me what medicinal chemistry is all about.

Lastly, and most importantly, I would like to thank my family for all of the love and support over the years. I know it probably seemed like I would be in grad school until the end of days, but it's over now, and I would have never made it without you. Mua!

TABLE OF CONTENTS

LIST OF TABLES

LIST OF FIGURES

LIST OF ABBREVIATIONS

A_1R – adenosine A_1 receptor

$A_{2A}R$ – adenosine A_{2A} receptor

$A_{2B}R$ – adenosine A_{2B} receptor

A_3R – adenosine A_3 receptor

αβ-met-ADP – α,β-methylene-ADP

ACP – deoxyadenosine 5'-monophosphonate

AC – adenylyl cyclase

AUC – area under the curve

BPD – bipolar disorder

cAMP – cyclic adenosine monophosphate

CCPA – 2-chloro-N^6-cyclopentyladenosine

CNS – central nervous system

CPA – N^6-cyclopentyladenosine

CPX – 8-cyclopentyl-1,3-dipropylxanthine

DAG – diacylglycerol

DGK – diacylglycerol kinase

DMT – N,N-dimethyltryptamine

EGFR – epidermal growth factor receptor

ERK – extracellular signal-related kinase

GDP – guanosine diphosphate

GPCR – G protein-coupled receptor

GRK – G protein-coupled receptor kinase

GTP – guanosine triphosphate

h – human

IP_3 – inositol 1,4,5-triphosphate

m – mouse

NT5E – ecto-5'-nucleotidase

PAP – prostatic acid phosphatase

PA – phosphatidic acid

PDE – phosphodiesterase

PIP_2 – phosphatidylinositol 4,5-bisphosphate

PKA – protein kinase A

PKC – protein kinase C

PLC – phospholipase C

PMA – phorbol-12-myristate-13-acetate

RGS – regulator of G protein signaling

SERCA – sarco/endoplasmic reticulum calcium ATPase

WT – wild-type

CHAPTER 1: A BRIEF INTRODUCTION TO GPCR SIGNALING

G protein-coupled receptors (GPCRs) are a fundamental part of cellular communication in all eukaryotic organisms. Indeed, the importance of GPCRs in biological signaling is difficult to overstate; they are responsible for an estimated 80% of all signal transduction across biological membranes (1). Furthermore, GPCRs are highly druggable proteins, and are an essential component of modern pharmacology. As of 2013, over 30% of the small-molecule drugs currently on the market target GPCRs in some fashion (2). As such, a thorough understanding of GPCR structure and function is crucial both in the investigation of biological signaling processes and in future drug discovery. As recognition of the importance of GPCR signaling, multiple researchers have received Nobel Prizes in Chemistry or Medicine for work on GPCR signaling, including Alfred Gilman and Martin Rodbell in 1994 for the discovery of G proteins, Richard Axel and Linda Buck in 2004 for the characterization of olfactory receptors, and Brian Kobilka and Robert Lefkowitz in 2012 for work examining the structure and signaling mechanisms of GPCRs.

GPCRs span the cellular plasma membrane, and a significant portion of a given GPCR exists within the interior of the lipid bilayer. As such, detailed information regarding GPCR structure was unavailable for many years, as their amphiphilic composition – which is stabilized by the lipid bilayer, but not stable in aqueous solution – makes GPCR crystallization extremely difficult. However, high resolution crystal structures of multiple GPCRs including rhodopsin (3-5), the β_2 adrenergic receptor (6-8), and the A_{2A} adenosine

receptor (9-11) have now been solved, providing a more complete understanding of GPCR structure and function.

The core structural component of all GPCRs is a series of 7 transmembrane α-helices, arranged in a roughly cylindrical bundle. These helices are traditionally numbered I-VII, in order from N- to C-terminus. The N-terminus of GPCRs is always located on the extracellular side of the plasma membrane, and is often heavily N-glycosylated; this complex glycosylation is required for proper expression and trafficking of GPCRs (12). Conversely, the C-terminus is located on the intracellular face of the plasma membrane, and is important for interactions with scaffolding and regulatory proteins. The proximal portion of the C-terminus consists of another α-helix (helix VIII) oriented parallel to the plasma membrane and anchored by palmitoylation of one or more conserved cysteine residues (13,14).

The transmembrane helices are connected by three extracellular and three intracellular loops (EL1-EL3 and IL1-IL3, respectively). Of the extracellular loops, EL2 is of particular interest, as it is stabilized by a highly-conserved disulfide bond with the extracellular end of helix III (15), and is often located in close proximity to the ligand binding site (16). Of the intracellular loops, IL2 and IL3 are the most noteworthy, as they constitute a significant portion of the G protein coupling interface. Furthermore, IL2 is anchored by a very highly conserved E/DRY series of residues at the cytoplasmic end of helix III, which is believed to be involved in stabilizing receptor conformational states (17). In the vast majority of GPCRs, the ligand binding pocket is located between the extracellular ends of the transmembrane helices, within the plasma membrane. However, the members of a small subfamily, the class C GPCRs, have a large N-terminal ligand binding domain that extends into the extracellular space (18).

GPCRs signal primarily through interactions with heterotrimeric G proteins. As implied by the name, heterotrimeric G proteins are composed of three subunits, α (alpha), β (beta), and γ (gamma). The Gα subunits are homologous to the Ras family of small GTPase signaling proteins (19), and function in a similar fashion. However, unlike small GTPases, Gα subunits are tethered to the plasma membrane by N-terminal myristoylation and/or palmitoylation (20). In their inactive state, Gα subunits bind a molecule of guanosine diphosphate (GDP), and form a complex with Gβ, Gγ, and a coupled GPCR. Upon ligand binding, GPCRs undergo a conformational change which causes the release of GDP from the coupled Gα subunit, where it is replaced by a molecule of guanosine triphosphate (GTP) from the cytosol. The precise characteristics of this conformational change have only recently begun to be elucidated. As currently understood, agonist binding causes an outward motion in the cytoplasmic ends of transmembrane helices V and VI, creating a cavity into which the C-terminus of the coupled Gα subunit extends (8,21).

GTP binding causes a conformational change in Gα, which results in the dissociation of the Gα subunit from the coupled GPCR and the other G protein subunits. In their active, GTP-bound state, Gα subunits diffuse freely throughout the plasma membrane, where they interact with and activate various membrane-bound second messenger proteins (Fig. 1.1). G protein signaling is terminated by the enzymatic hydrolysis of Gα-bound GTP into GDP, which causes the Gα subunit to revert back to its inactive conformation and re-associate with the β and γ subunits of the heterotrimeric G protein complex (22). In isolation, Gα subunits catalyze GTP hydrolysis very poorly. However, signal termination is facilitated by a large family of regulator of G protein signaling (RGS) proteins, which greatly enhance the rate of GTP hydrolysis through interactions with active Gα subunits (23).

Figure 1.1

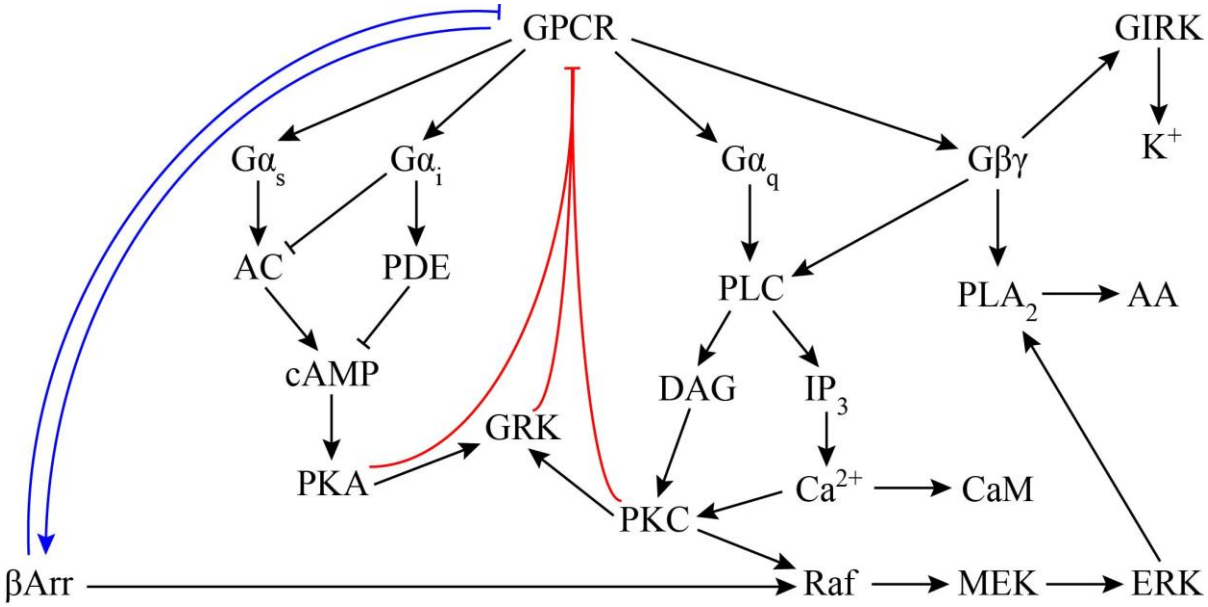
GPCR
GIRK
Gαs
Gαi
Gαq
Gβγ
K+
AC
PDE
PLC
PLA2
AA
cAMP
DAG
IP3
GRK
PKA
Ca2+
CaM
PKC
βArr
Raf
MEK
ERK

Figure 1.1. Selected signaling pathways downstream of GPCR activation.

GPCR = G protein-coupled receptor. $G\alpha_s$ = Gs-family alpha subunit. $G\alpha_i$ = Gi-family alpha subunit. $G\alpha_q$ = Gq-family alpha subunit. $G\beta\gamma$ = G protein free beta-gamma complex. AC = adenylyl cyclase. PDE = phosphodiesterase. cAMP = 3'-5'-cyclic adenosine monophosphate. PKA = protein kinase A. PLC = phospholipase C. DAG = diacylglycerol. IP_3 = inositol-1,4,5-triphosphate. Ca^{2+} = calcium ion. CaM = calmodulin. PKC = protein kinase C. GRK = G protein-coupled receptor kinase. GIRK = G protein-coupled inward-rectifying potassium channel. K^+ = potassium ion. PLA_2 = phospholipase A2. AA = arachidonic acid. βarr = β-arrestin. Raf = Raf kinase. MEK = mitogen-activated protein kinase/ERK kinase. ERK = extracellular signal-related kinase. *Normal arrow*, activation/enzymatic production. *Flat arrow*, inhibition/enzymatic degradation. *Red*, GPCR phosphorylation. *Blue*, phosphorylation-dependant β-arrestin interaction.

Numerous downstream signaling pathways can be activated after stimulation of a given GPCR, determined mainly by the type of Gα subunit coupled to the receptor (Fig. 1.1). The Gα subunits of heterotrimeric G proteins are grouped into 4 main families, Gs, Gi, Gq, and G12, based on sequence homology and signaling activity (24). Of these, the Gs and Gi families signal primarily by modulating intracellular levels of cyclic adenosine monophosphate (cAMP). The Gs (stimulatory) family contains two members: $G\alpha_s$, which is ubiquitously expressed, and $G\alpha_{olf}$, which is exclusively expressed in the olfactory system and is responsible for signal transduction through the large olfactory subfamily of GCPRs (25). Activation of Gs-family Gα subunits leads to stimulation of adenylyl cyclase (AC), which converts ATP into cAMP, raising intracellular concentrations of cAMP (Fig. 1.1). Elevated cyclic AMP leads to the activation of protein kinase A (PKA), which phosphorylates multiple downstream effectors.

The Gi (inhibitory) family contains 5 members: $G\alpha_i$, $G\alpha_o$, $G\alpha_z$, $G\alpha_t$ (transducin), and $G\alpha_{gust}$ (gustducin). While the $G\alpha_i$, $G\alpha_o$, and $G\alpha_z$ subunits are widely expressed, transducin is exclusively expressed in the vision system, and couples to the light sensitive GPCRs rhodopsin and the three cone opsins (26). Similarly, gustducin is exclusively expressed in the taste and gastrointestinal systems (27,28). Activation of Gi-family Gα subunits leads to inhibition of adenylyl cyclase and the stimulation of phosphodiesterase (PDE) enzymes which hydrolyze cAMP (Fig. 1.1). Both of these activities decrease intracellular levels of cAMP, leading to a suppression of PKA activity and its associated downstream effectors. Activation of transducin more specifically results in the stimulation of a cyclic guanosine monophosphate (cGMP)-specific phosphodiesterase, leading to the closing of cGMP-gated cation channels, a critical step in visual signal transduction (29).

The Gq family contains 5 members: $G\alpha_q$, $G\alpha_{11}$, $G\alpha_{14}$, $G\alpha_{15}$, and $G\alpha_{16}$. The Gq family transduces signals using an entirely different second messenger system than the Gs and Gi families (Fig. 1.1). Activation of Gq-family Gα subunits leads to the stimulation of phospholipase C (PLC), which catalyses the hydrolysis of phosphatidylinositol-4,5-bisphosphate (PIP_2) into inositol-1,4,5-triphosphate (IP_3) and diacylglycerol (DAG). IP_3 activates IP_3 receptors on the endoplasmic reticulum, leading to the release of intracellular calcium stores and an increase in cytosolic calcium concentration. DAG activates conventional and novel isoforms of protein kinase C (PKC), leading to the phosphorylation of multiple downstream effectors (30), including MAP kinase cascades which culminate in the phosphorylation and activation of extracellular signal-related kinase (ERK). Elevated calcium also activates multiple downstream effectors, including conventional isoforms of PKC (30) and calmodulin-regulated proteins (31).

The G12 family contains two members: $G\alpha_{12}$ and $G\alpha_{13}$. The G12 family signals primarily via downstream activation of the Rho family of GTPases (32), and is poorly understood compared to the Gs, Gi, and Gq families. All GPCRs identified thus far that couple to the G12 family also couple to one of the other Gα families (32), suggesting that G12 may function in a secondary signaling role (G12 not shown in Fig. 1.1).

The GPCR-coupling selectivity of Gα subunits is primarily determined by the extreme C-terminal 5 amino acids (33,34), which extend into a cavity formed between the intracellular ends of the GPCR transmembrane helices upon receptor activation (8). However, the structural determinants of Gα-coupling selectivity of GPCRs are more complex, broadly encompassing the intracellular loops, intracellular regions of the transmembrane helices, and the proximal portion of the C-terminus. Most GPCRs

preferentially couple to a single Gα family, but many GPCRs can couple to multiple Gα families under certain circumstances. For example, Gα-coupling selectivity (and binding to other intracellular proteins) in a single activated GPCR can be directed by the structure of the activating agonist, a phenomenon known as functional selectivity (35). GPCR coupling selectivity can also be influenced by dimerization or oligomerization of the receptor (36).

The other two members of the heterotrimeric G protein complex, Gβ (beta) and Gγ (gamma), form an obligate dimer and as such are usually referred to together as the G beta-gamma complex, or simply Gβγ. There are currently 5 known isoforms of Gβ, and 11 known isoforms of Gγ (37), which can form numerous combination of Gβγ pairs with different signaling properties (38). Gβγ is tethered to the plasma membrane by farnesylation or geranylgeranylation of the C-terminus of Gγ (20), and binds the inactive, GDP-bound state of Gα subunits. Upon guanine nucleotide exchange, Gβγ is released from Gα; free Gβγ diffuses along the plasma membrane and activates downstream effectors independently of Gα. The signaling roles of free Gβγ are poorly understood, at least compared to the current understanding of Gα signaling. The most well-characterized activity of free Gβγ is gating the opening of G protein coupled inward rectifying potassium channels (GIRKs) (39). However, free Gβγ can also activate PLC (40,41), and phospholipase A2 (42), among other downstream effectors (Fig. 1.1).

After activation, GPCRs are phosphorylated by downstream effector kinases at multiple locations on the intracellular loops and C-terminus (Fig 1.1, *red*). GPCRs are directly phosphorylated by both PKA (43) and PKC (44), as well as by G protein-coupled receptor kinases (GRKs), which are themselves activated by Gβγ, PKA, and PKC (45,46). This feedback mechanism can have multiple effects on GPCR function, with the particular

fate of receptor signaling depending on the pattern of phosphorylation and the specific receptor (47). Among these regulatory effects, GPCR phosphorylation can directly and indirectly cause uncoupling of the GPCR from Gα subunits, leading to a termination of signaling downstream of GPCR activation (48), a process known as desensitization. In some cases, GPCR phosphorylation may also modify receptor ability to couple to different Gα subunits (49), effectively redirecting GPCR signaling to different downstream pathways (50), though this is somewhat controversial (51). Lastly, and perhaps most importantly, GPCR phosphorylation promotes the recruitment of β-arrestin proteins to activated GPCRs (Fig. 1.1, *blue*), which has multiple signaling functions.

β-arrestin binding to GPCRs occludes the interface required for Gα subunit coupling, leading to receptor uncoupling and desensitization (52). Additionally, β-arrestin acts as a scaffolding protein, recruiting proteins required for endocytosis, such as clathrin (53) and AP-2 (54), to the GPCR signaling complex. As such, β-arrestin is important in both short-term (receptor desensitization by disruption of G protein coupling) and long-term (receptor internalization through endocytosis) negative regulation of receptor activity. β-arrestins can also recruit enzymes which terminate second messenger signaling downstream of GPCR activation. For example, β-arrestins recruit PDEs (which hydrolyze the second messenger cAMP) downstream of $G\alpha_s$ signaling (55), and diacylglycerol kinases (which phosphorylate the second messenger DAG) downstream of $G\alpha_q$ signaling (56). Lastly, β-Arrestin recruitment actually stimulates other downstream signaling pathways, such as MAP kinase cascades leading to ERK phosphorylation (Fig. 1.1) (57).

In addition to β-arrestins, GPCRs interact with numerous other scaffolding and accessory proteins, including ion channels, 14-3-3 proteins, PDZ-domain proteins, A-kinase

anchoring proteins, and others (58). Apart from the regulation of GPCR signaling itself, these associations are important for receptor trafficking, localization, and cytoskeletal anchoring in lipid rafts and signaling complexes (58,59). As partially detailed in Figure 1.1, which presents only a very limited view, GPCRs can influence a staggering number of intracellular signaling pathways. The what, when, and where of these downstream signaling events, and thus their integration into biological signaling networks, is subject to very complex and detailed regulation, about which we understand very little. Indeed, given the tremendous importance of GPCRs in nearly every type of extracellular and intracellular signaling, the current scientific understanding of GPCR signaling and regulation is incomplete at best. As such, further efforts to characterize the endogenous regulation of GPCR signaling are of the utmost importance in developing a better understanding of the molecular bases of normal biological signaling. However, a better understanding of the role of GPCRs in *abnormal* biological signaling is even more critical, given the enormous potential – both past and future – of GPCRs as targets for therapeutic drug discovery.

CHAPTER 2: THE NUCLEOTIDE AMP IS AN ADENOSINE A_1 RECEPTOR AGONIST

INTRODUCTION

Adenosine and adenine nucleotides regulate diverse physiological processes (60,61). Adenosine activates four distinct G protein-coupled receptors, the so called P1 purinergic receptors: adenosine A_1 receptor (A_1R, ADORA1), adenosine A_{2A} receptor (A_{2A}R, ADORA2A), adenosine A_{2B} receptor (A_{2B}R, ADORA2B), and adenosine A_3 receptor (A_3R, ADORA3). A_1R and A_3R are $G_{i/o}$-coupled and inhibit adenylate cyclase when activated while A_{2A}R and A_{2B}R are G_s-coupled and stimulate adenylate cyclase.

While mammals have numerous P2 purinergic receptors for ATP and ADP, no receptor for their hydrolysis product (AMP) has been definitively identified. GPR80/GPR99 was originally classified as an adenosine and AMP receptor (62), however this finding has now been discounted (63,64). AMP has diverse physiological effects, suggesting a receptor for AMP could exist (65-74).

Complicating studies with AMP is the fact that cells express multiple enzymes that hydrolyze extracellular AMP to adenosine, including ecto-5'-nucleotidase (NT5E, CD73), Prostatic acid phosphatase (PAP, ACPP) and several alkaline phosphatases (75-78). Genetic deletion or pharmacological inhibition of individual ectonucleotidases reduces, but does not always eliminate, the physiological effects of AMP (65,67,70,72,79). And, the most

commonly used ectonucleotidase inhibitor α,β-methylene-ADP (αβ-met-ADP) inhibits NT5E, but it does not inhibit PAP (70).

Many of the physiological effects of AMP are lost in A_1R knockout mice or can be blocked with adenosine receptor antagonists (65,67,70,72-74), suggesting adenosine is the active ligand. However, given the challenges associated with inhibiting all ectonucleotidases in complex tissues (79), direct activation of adenosine receptors by AMP cannot be so easily ruled out.

Extracellular AMP originates from multiple endogenous sources (75), and nucleotide release and hydrolysis can be rapid (79,80). Endogenous AMP could thus directly modulate diverse adenosine-receptor dependent processes, including cardiovascular disease, cancer, neurotransmission and gliotransmission (60,61,81-83).

To rigorously study direct and indirect effects of AMP on adenosine receptors, we developed a novel cell based assay utilizing chimeric G proteins to visualize human (h)A_1R and $hA_{2B}R$ activation in real-time and at single cell resolution. We also used a non-hydrolyzable AMP analog to rule out the effects of AMP hydrolysis. Surprisingly, we found that AMP directly activated hA_1R, but not $hA_{2B}R$, and activation was independent of hydrolysis to adenosine. Our study thus indicates that A_1R is a receptor for the naturally occurring nucleotide AMP as well as a receptor for adenosine.

MATERIALS AND METHODS

Materials

Adenosine (A9251), AMP (01930), inosine (I4125), 2-chloro-N^6-cyclopentyladenosine (C7938), N^6-cyclopentyladenosine (C8031), α,β-methylene adenosine 5'-diphosphate (αβ-met-ADP; M3763), and pertussis toxin (P7208) were purchased from Sigma-Aldrich. Pyridoxalphosphate-6-azophenyl-2',4'-disulfonic acid (PPADS; 0625) and suramin (1472) were purchased from Tocris Bioscience. Stock solutions of adenosine (10 mM), AMP (10 mM), αβ-met-ADP (50 μM), PPADS (10 mM), and suramin (10 mM) were made in Hank's balanced salt solution assay buffer (HBSS, Gibco catalog #14025, supplemented with 9 mM HEPES, 11 mM D-glucose, 0.1% fatty-acid free bovine serum albumin, pH 7.3) and frozen at -80°C in single use aliquots. All other compounds were dissolved in HBSS assay buffer at final concentration immediately before use.

Molecular Biology

Full-length expression constructs for human A_1R (GenBank accession #AY136746) and human $A_{2B}R$ (GenBank accession #AY136748) were obtained from the Missouri S&T Clone Collection (www.cdna.org). Human A_1R point mutants were generated by PCR-based mutagenesis. Chimeric G protein constructs ($G\alpha_{q\text{-}i5}$ and $G\alpha_{q\text{-}s5}$) and the mouse transmembrane (TM)-PAP (nt 64-1317 from GenBank accession # NM_207668) expression construct were previously described (76,84,85). Full-length expression constructs of mouse NT5E (nt 47-1777 from GenBank accession # NM_011851.3) and mouse A_1R (nt 1070-2053 from GenBank accession # NM_001008533) were generated by RT-PCR using C57BL/6

dorsal root ganglia cDNA as template. The TM-PAP and NT5E expression constructs hydrolyzed AMP when transfected into HEK293 cells (assessed using enzyme histochemistry; data not shown for NT5E and previously shown for TM-PAP (76)). PCR-generated constructs have a Kozak consensus sequence, were cloned into pcDNA3.1(+) and were sequence verified.

Calcium Imaging

HEK293 cells were grown on polylysine-coated glass bottom culture dishes (MatTek Corp, P35G-0-10-C) in Dulbecco's modified Eagle's medium (DMEM) containing 10% Fetal Bovine Serum, 100 U/mL penicillin and 100 μg/mL streptomycin. Cells were transfected with Lipofectamine Plus (Invitrogen) in DMEM containing 1% Fetal Bovine Serum, which was replaced with fresh growth media after 4 hours. The total amount of DNA per transfection was adjusted to 1 μg by adding pcDNA 3.1(+). 100 ng of pCS-Venus was included in each transfection to identify transfected cells. Following transfection (~24 hours), cells were washed two times in Hank's balanced salt solution assay buffer (HBSS, Gibco catalog #14025, supplemented with 9 mM HEPES, 11 mM D-glucose, 0.1% fatty-acid free bovine serum albumin, pH 7.3), then loaded for one hour at room temperature with 2 μM Fura-2 AM (Invitrogen, F-1221) and 0.02% Pluronic F-127 (Invitrogen, P3000-MP) in assay buffer. Cells were washed three times with assay buffer, incubated for 30 minutes at room temperature, and were imaged on a Nikon Eclipse Ti microscope.

A Sutter DG-4 light source (excitation 340 nm / 380 nm; emission 510 nm) and Andor Clara CCD camera were used to image calcium responses. Assay buffer was

refreshed immediately prior to imaging. Antagonists were added in assay buffer 3 minutes prior to imaging. Starting solution was aspirated and agonist solution added after 40 seconds of baseline imaging. We manually pipetted and aspirated solutions for all calcium imaging experiments. Only cells which expressed visible Venus protein, did not saturate the camera at a 40 ms exposure time, and had low (< 0.6) baseline Fura-2 ratios were analyzed. 500 ms excitation at 340 nm and 250 ms excitation at 380 nm were used for all experiments.

Calcium responses were analyzed in two ways. To create real-time response profiles, the Fura-2 fluorescence intensity ratio (340 nm/380 nm) at each time point was averaged over all transfected cells in each condition and then normalized relative to the average baseline fluorescence ratio before agonist addition. Calcium responses were also quantified by calculating the area under the curve (AUC) extending 1 minute from agonist addition, relative to the baseline fluorescence ratio, on a cell-by-cell basis. AUC values were then averaged over all cells in each condition. Calcium response profiles and AUC data are presented as mean ± s.e.m. To create dose response curves, GraphPad Prism was used to fit a variable slope dose response equation to the average AUC values for each agonist concentration.

Cyclic AMP GloSensor Assay

Cyclic AMP determinations were made using a modified GloSensor luciferase detection system (Promega). Low passage, subconfluent HEK293T cells (ATCC CRL-11268) grown in DMEM without phenol red (Gibco #31053) and supplemented with 10% Fetal Bovine Serum (Gibco #26140) were reverse transfected by spotting a calcium

phosphate DNA complex mixture containing 12.5 ng each of GloSensor 22F plasmid (Promega #E2301) and human A_1R plasmid in 25 mM HEPES at pH 7.1, 140 mM sodium chloride, 0.75 mM disodium monophosphate and 250 mM calcium chloride. Cells were immediately added at a density of 20,000 cells per well using a Multidrop 384 (Titertek) to 384 well white, clear bottom tissue culture plates (Corning #3707). Cell plates were incubated for 24 hours at 37^{o}C and 5% CO_2. Sixteen point, 1:3 dilutions curves of test compounds starting at 100 µM final concentration were diluted to 4x final concentration in HBSS (Gibco #14175) supplemented with 2 mM HEPES, pH 7.5 and then added to the cell plates with a Multimek automated liquid handling device (Nanoscreen, Charleston, SC). Following a 10 minute incubation at room temperature, 50 µM 3-isobutyl-1-methylxanthine (Sigma) and 175 nM (-)-isoproterenol hydrochloride (Sigma) were added by Multimek. Seven minutes later, GloSensor cAMP reagent (Promega #E1291) containing 2% luciferin and supplemented with 0.2% NP40 (Tergitol, Sigma) to permeabilize the cells was added by Multimek along with a final 5 µL addition of 100% Ethanol (Decon Labs) to eliminate bubbles. Luminescence was read on an Envision plate reader (Perkin Elmer) for 15 minutes. Data from 95% of Vmax for isoproterenol (~10 minutes post GloSensor reagent addition) were normalized for scale to 100% response equivalent to the response of 1 µM 2-chloro-N^6-cyclopentyladenosine and 0% response equal to the response from the isoproterenol alone.

Cortical Neuron Dissociation and Culture

Embryonic cortical neurons were cultured as previously described (86). Briefly, cortices from ~E16.5 embryos were dissected and digested in dissociation medium (DM) (98

mM Na_2SO_4, 30 mM K_2SO_4, 5.8 mM $MgCl_2$, 0.25 mM $CaCl_2$, 1 mM HEPES, 20 mM D-glucose, 0.125 mN NaOH, and 0.001% phenol red) containing 0.32 mg/mL L-cysteine (Sigma, W326305) and 20 U/mL papain (Roche, 10108014001) at 37°C for 20 minutes with occasional mixing. After digestion, cortices were washed twice with DM containing 1 mg/mL BSA (Sigma, A3912) and 1 mg/mL trypsin inhibitor (Sigma, T9128), followed by incubation in DM containing 10 mg/mL BSA and 10 mg/mL trypsin inhibitor for 2 minutes. Prepared cortices were then suspended in plating media (Neurobasal-A, Gibco, 10888) containing 4.5% FBS, 2% B27 (Gibco, 17504), 100 U/mL penicillin, 100 µg/mL streptomycin, and 2 mM L-glutamine) and gently disrupted by pipetting 15-20 times. The dissociated neurons were counted in a hemocytometer and plated at 1×10^6 cells/well in polylysine/laminin-coated 6-well plates containing plating media.

Neuron Treatment and cAMP ELISA Assay

After 1 day in vitro, neuron plating media was replaced with serum-free plating media (otherwise identical) for 1 hour. Afterwards, the media was replaced with Neurobasal-A containing 1 mM ACP or 1 µM N^6-cyclopentyladenosine (CPA) (Sigma, C8031) for 30 minutes. For untreated conditions, media was replaced with Neurobasal-A containing no additives. For antagonist conditions, 100 µM 8-cyclopentyl-1,3-dipropylxanthine (CPX) (Tocris, 0439) was added 15 minutes before agonist addition, and agonist solutions also contained 100 µM CPX. Following incubation, forskolin (Sigma, F6886) was added, to a final concentration of 10 µM. After a final 15 minute incubation, the media was aspirated, and the neurons were washed twice in ice-cold Dulbecco's phosphate buffered saline (PBS)

(Sigma, D8537). Then, lysis buffer (provided with cAMP ELISA Kit) (R&D Systems, KGE002B) was added, and the neurons were scraped and collected.

The cAMP ELISA assay was performed according to manufacturer's instructions. Briefly, cells were subjected to 2 freeze/thaw cycles from -20°C to room temperature to ensure cell lysis. Cells were then centrifuged at 600 x g for 10 minutes and the supernatant was isolated. Neuron samples and cAMP standards were added to a microplate containing immobilized cAMP antibody, followed by a labeled cAMP conjugate. After incubation and washes, a substrate solution was added, causing a colorimetric reaction proportional to the quantity of bound cAMP conjugate. After incubation, stop solution was added, and absorbance was measured on a BioTek Synergy HT plate reader. Standard curve fitting and sample analysis was performed using GraphPad Prism.

Immunohistochemistry

HEK293 cells were grown on poly-D-lysine (Sigma, P0899)-coated coverslips and transfected using Lipofectamine Plus with 1 µg (per coverslip) of wild-type or mutant hA_1R. 24 hours after transfection, the cells were washed twice with PBS and fixed for 15 minutes with 4% paraformaldehyde in PBS. The cells were then washed 3 times with PBS for 5 minutes and permeablized with 0.05% Triton-X-100 (Fisher, BP151) in PBS for 20 minutes. The cells were washed three times (5 minutes/wash) and blocked with 5% normal goat serum (NGS) in PBS for 30 minutes. Cells were then incubated with a 1:250 dilution of rabbit anti-hA_1R primary antibody (Santa Cruz Biotechnology, sc-28995) in 10% NGS for 2 hours, and washed three times (10 minutes/wash) with 10% NGS. The cells were then incubated in the

dark for 1 hour with a 1:1000 dilution of Alexa 546-conjugated Goat anti-rabbit secondary antibody (Invitrogen, A11010) in 10% NGS. Cells were washed three times with PBS and mounted on glass slides. The following day, the slides were imaged on an Olympus FV1000 confocal microscope. Dissociated cortical neurons were immunostained for mA_1R in the same way, except that incubation with primary antibody was conducted at 4°C overnight.

RESULTS

Chimeric G proteins can be used to visualize adenosine receptor activation in real time

Activation of G_i-coupled A_1R or G_s-coupled $A_{2B}R$ is typically quantified by measuring ligand-evoked decreases or increases in intracellular cAMP, respectively. However, these assays entail lysing cells at different times post-stimulation, hence these assays have limited temporal resolution and no cellular resolution. In an effort to develop a real-time readout of adenosine receptor activation, we co-transfected HEK293 cells with vectors encoding hA_1R and $G\alpha_{q\text{-}i5}$ (Gqi), a chimeric G protein that couples G_i-coupled receptors to phospholipase C (PLC) activation and calcium mobilization (Fig. 2.1) (85). In parallel, we co-transfected HEK293 cells with vectors encoding $hA_{2B}R$ and chimeric $G\alpha_{q\text{-}s5}$ (Gqs), to couple $hA_{2B}R$ to PLC and calcium mobilization (Fig. 2.1) (84). As controls, we found that adenosine (1 mM) did not evoke calcium mobilization in untransfected HEK293 cells or in cells expressing hA_1R alone, $hA_{2B}R$ alone, Gqi alone or Gqs alone. However, a saturating concentration of adenosine (1 mM) evoked rapid onset calcium responses that slowly decayed in cells co-expressing hA_1R + Gqi or $hA_{2B}R$ + Gqs (Fig. 2.2 A,B), indicating adenosine receptor activation can be monitored in real-time at cellular resolution.

Figure 2.1

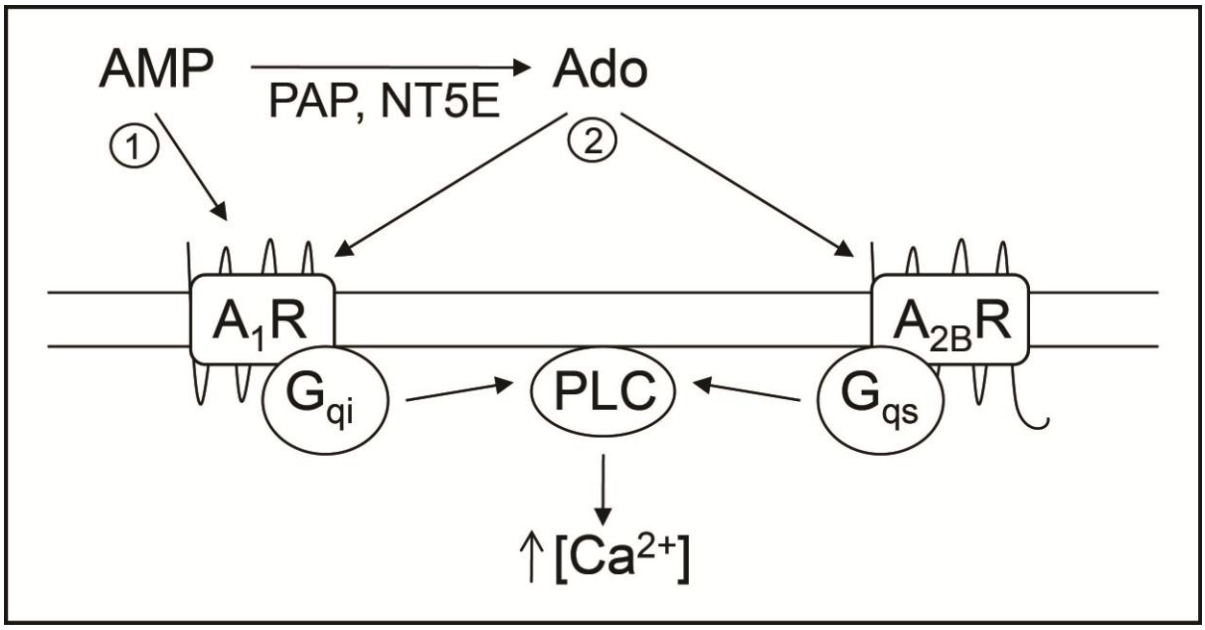

Figure 2.1. Real-time visualization of adenosine receptor activation and ectonucleotidase activity.

G_i-coupled A_1R and G_s-coupled $A_{2B}R$ do not mobilize intracellular calcium when activated in most cell types, including HEK293 cells. However, when A_1R or $A_{2B}R$ are co-expressed with chimeric G proteins that couple to phospholipase C (PLC; G_{qi}, G_{qs}, respectively), receptor stimulation can be visualized in real-time using the calcium-sensitive dye Fura-2. PAP and NT5E hydrolyze extracellular AMP to adenosine. Real-time visualization allowed us to show that (1) AMP directly activates A_1R whereas (2) AMP activates $A_{2B}R$ indirectly via ectonucleotidase-catalyzed hydrolysis to adenosine.

AMP activates hA$_1$R independent of ectonucleotidases whereas hA$_{2B}$R activation is ectonucleotidase-dependent

Since no AMP receptors have been definitively identified, we next hypothesized that AMP would only mobilize calcium in adenosine receptor-expressing cells after hydrolysis to adenosine by PAP or NT5E ectonucleotidases (Fig. 2.1). To test this hypothesis, we co-transfected cells with hA$_1$R + Gqi vectors along with the membrane-bound ectonucleotidases PAP or NT5E. These ectonucleotidases were enzymatically active when expressed in HEK293 cells (see Materials and Methods). To our initial surprise, 1 mM AMP evoked calcium responses in hA$_1$R + Gqi-expressing cells that were indistinguishable in onset and magnitude from calcium responses evoked by 1 mM adenosine, and co-expression of PAP or NT5E did not modify AMP-evoked responses (Fig. 2.2A). Similar results were observed in cells co-expressing mouse A$_1$R + Gqi (Fig. 2.3). These AMP-evoked calcium responses were dependent on overexpressed A$_1$R as AMP had no effect in HEK293 cells when Gqi was expressed alone (Fig. 2.2A, Fig. 2.3). Rapid activation of A$_1$R was not due to contaminating levels of adenosine (adenosine was undetectable in our AMP stock solution based on high performance liquid chromatography analysis). Instead, our data suggested that a nucleotide (AMP) could directly activate the adenosine A$_1$ receptor.

In contrast, adenosine (Fig. 2.2B, *grey*) and AMP (Fig. 2.2B, *blue*) evoked kinetically distinct calcium responses in hA$_{2B}$R + Gqs co-expressing HEK293 cells. Specifically, adenosine evoked a rapid onset calcium response that peaked shortly after agonist addition, while AMP elicited a gradual calcium response that began approximately 15 seconds after agonist addition. Co-expression of PAP or NT5E significantly augmented the speed and magnitude of the AMP response (Fig. 2.2B, *green*, *purple*), suggesting these enzymes

accelerated hydrolysis of AMP to adenosine. Although HEK293 cells endogenously express $hA_{2B}R$ (62,87), AMP did not evoke calcium responses in cells expressing Gqs alone (Fig. 2.2B, *black*). Taken together, these data suggest that AMP only activates $hA_{2B}R$ indirectly following hydrolysis to adenosine.

To directly test if AMP activates hA_1R or $hA_{2B}R$ as a result of ectonucleotidase activity, we repeated our experiments in the presence of α,β-methylene-ADP (αβ-met-ADP), a high-potency (Ki = 5 nM) NT5E inhibitor (88). We found that αβ-met-ADP did not inhibit adenosine- or AMP-evoked calcium responses in cells co-expressing hA_1R + Gqi (with or without overexpressed ectonucleotidases) (Compare Fig. 2.2A to Fig. 2.2C), further suggesting that AMP stimulates hA_1R directly. In contrast, 10 μM αβ-met-ADP completely inhibited the calcium response caused by AMP in $hA_{2B}R$ + Gqs-expressing cells (Fig. 2.2D, *blue*) but did not inhibit the adenosine-evoked calcium response (Fig. 2.2D, *grey*). αβ-met-ADP also significantly reduced the calcium response caused by AMP in NT5E co-expressing cells (Fig. 2.2D, *purple*) and marginally inhibited the calcium response caused by AMP in PAP co-expressing cells (Fig. 2.2D, *green*).

Figure 2.2

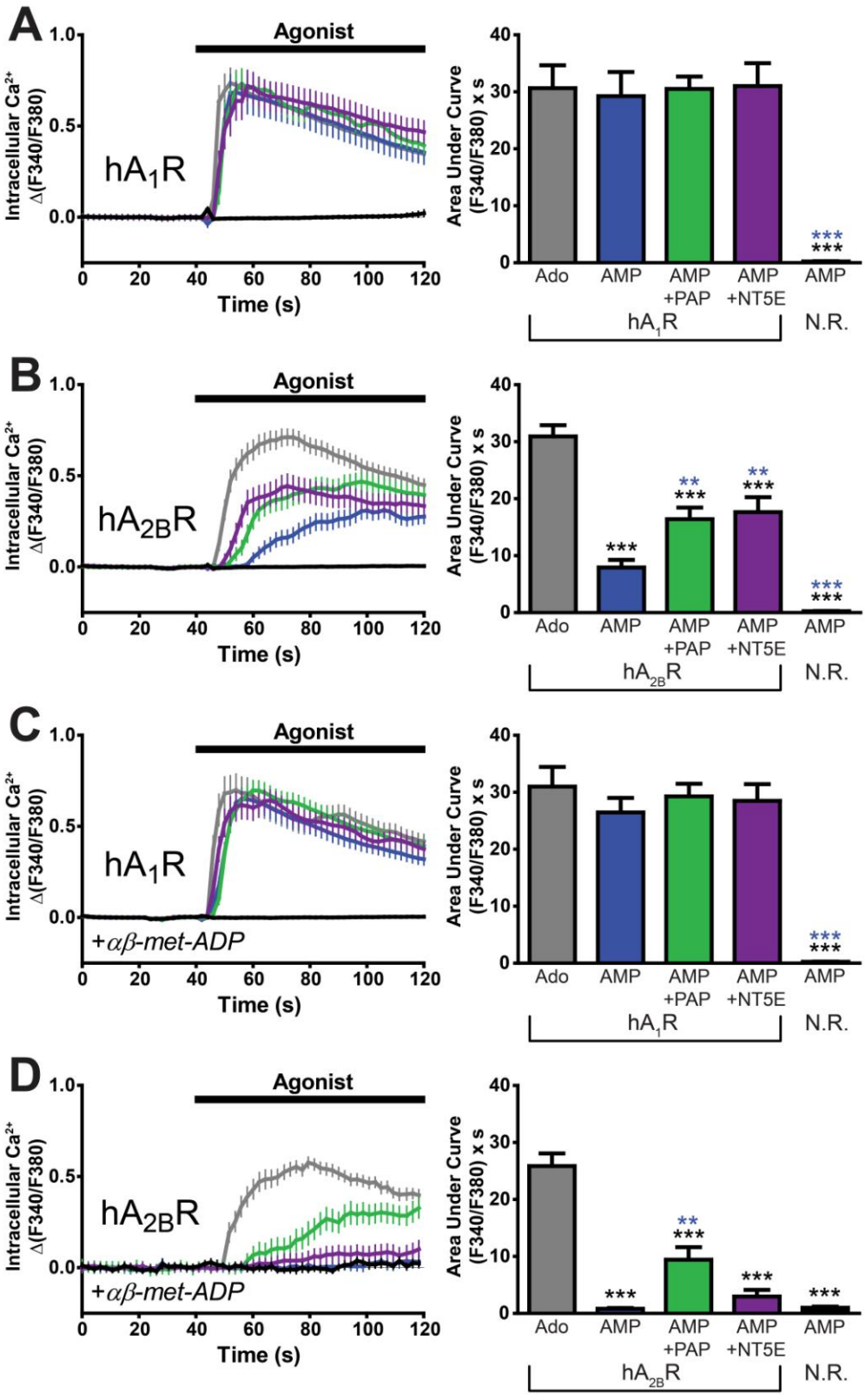
A
B
C
D
Agonist
Intracellular Ca2+ Δ(F340/F380)
hA1R
hA2BR
+αβ-met-ADP
Time (s)
Area Under Curve (F340/F380) x s
Ado
AMP
AMP +PAP
AMP +NT5E
AMP
hA1R
hA2BR
N.R.

Figure 2.2. AMP directly activates hA_1R whereas AMP activates $hA_{2B}R$ indirectly via ectonucleotidase-catalyzed hydrolysis to adenosine.

Calcium mobilization responses in HEK293 cells expressing (A, C) Gqi ± hA_1R or (B, D) Gqs ± $hA_{2B}R$. (C, D) Cells were incubated with the competitive NT5E inhibitor αβ-met-ADP (10 μM) for 3 minutes and then were stimulated with 1 mM agonist in the presence of 10 μM αβ-met-ADP. (*Black*) 1 mM AMP in the absence of a transfected adenosine receptor, but in the presence of the respective chimeric G protein. Area under curve (AUC) measurements extended for 1 minute from agonist addition. Paired t tests were used to compare AUC data. *Black asterisks*, statistically significant difference compared to adenosine stimulation. *Blue asterisks*, statistically significant difference compared to AMP stimulation (in receptor-expressing cells). *, $p < 0.05$; **, $p < 0.005$; ***, $p < 0.0005$. All data are the average of two experiments performed in duplicate. n = 20-74 cells per condition. All data, including calcium traces, are presented as means ± standard error.

Figure 2.3

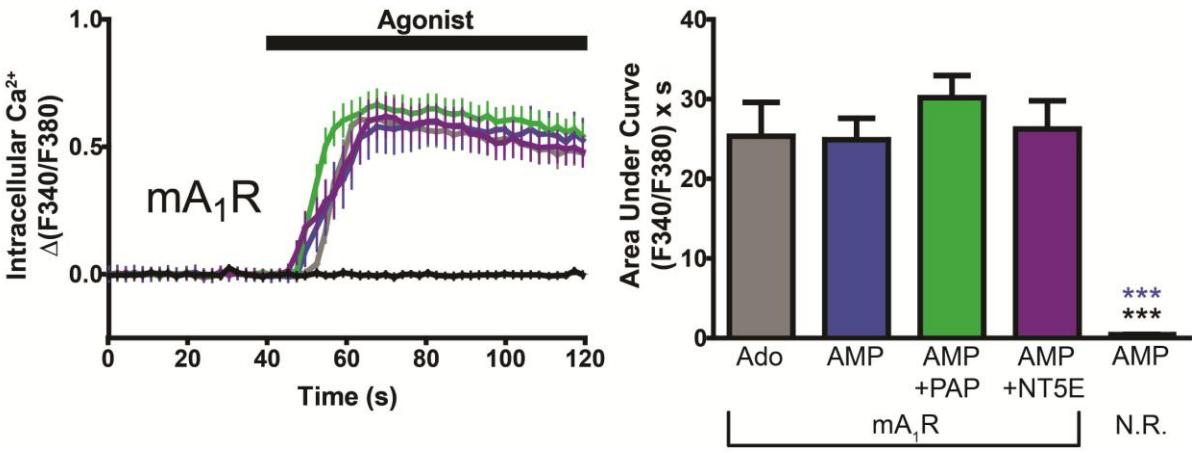
Agonist
Intracellular Ca2+ Δ(F340/F380)
mA1R
1.0
0.5
0.0
0
20
40
60
80
100
120
Time (s)
Area Under Curve (F340/F380) x s
40
30
20
10
0
***
***
Ado
AMP
AMP +PAP
AMP +NT5E
AMP
mA1R
N.R.

Figure 2.3. AMP activates mouse A_1R.

Calcium mobilization responses in HEK293 cells expressing Gqi ± mA_1R. Agonists: (*Grey*) 1 mM adenosine. (*Blue*) 1 mM AMP. (*Green*) 1 mM AMP in PAP co-expressing cells. (*Purple*) 1 mM AMP in NT5E co-expressing cells. (*Black*) 1 mM AMP in the absence of a transfected adenosine receptor, but in the presence of Gqi. Area under curve (AUC) measurements extended for 1 minute from agonist addition. Paired t tests were used to compare AUC data. *Black asterisks*, significant difference compared to adenosine stimulation. *Blue asterisks*, significant difference compared to AMP stimulation (in A_1R-expressing cells). ***, $p < 0.0005$. All data are the average of three experiments. n = 18-34 cells per condition. All data, including calcium traces, are presented as means ± standard error.

A non-hydrolyzable AMP analog activates hA_1R but not $hA_{2B}R$

We next sought to determine if 5'-deoxyadenosine monophosphonate (ACP), a non-hydrolyzable analog of AMP (88), could also activate hA_1R (Fig. 2.4 A,B). We found that 1 mM ACP evoked a rapid onset calcium response in hA_1R + Gqi-expressing cells (Fig. 2.4C, *solid line*) but no response in $hA_{2B}R$ + Gqs-expressing cells (Fig. 2.4C, *dashed line*). ACP, AMP and adenosine also evoked rapid calcium responses in COS7 cells expressing hA_1R + Gqi, but not Gqi alone, indicating that all of these compounds activate hA_1R when expressed in a different cell line (Fig. 2.5).

Figure 2.4

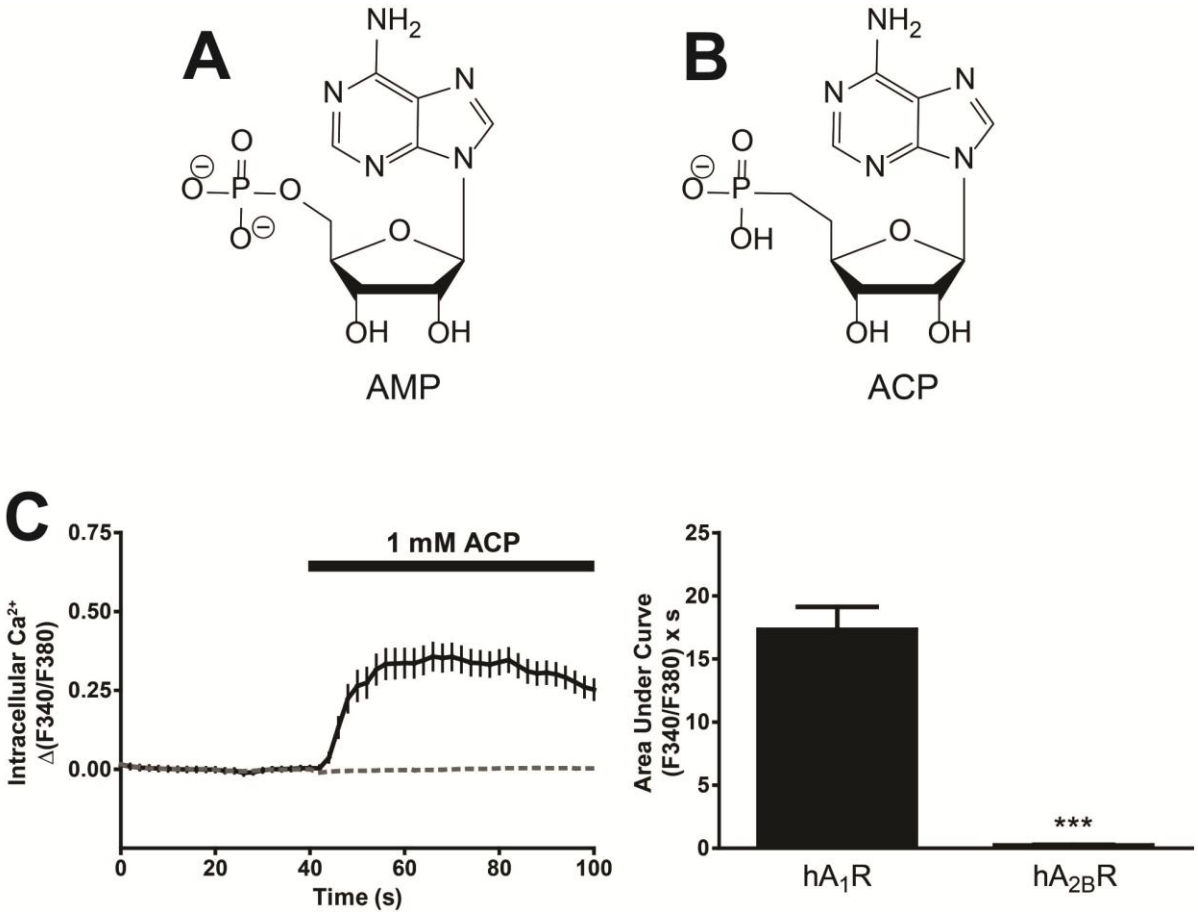
A
B
AMP
ACP
C
1 mM ACP
Intracellular Ca2+
Δ(F340/F380)
Time (s)
Area Under Curve
(F340/F380) x s
***
hA1R
hA2BR

Figure 2.4. A non-hydrolyzable AMP analog activates hA_1R but not $hA_{2B}R$.

A and B) Structures of (A) AMP and (B) the non-hydrolyzable analog ACP at physiological pH. C) Calcium mobilization responses elicited by 1 mM ACP in HEK293 cells expressing (*solid line*) hA_1R + Gqi or (*dashed line*) $hA_{2B}R$ + Gqs. Cells expressing Gqi alone did not respond to ACP. AUC measurements extended for 1 minute from agonist addition. Paired t tests were used to compare AUC data. ***, $p < 0.0005$. Data are the average of one ($hA_{2B}R$) or two (hA_1R) experiments performed in duplicate. n = 28-73 cells per condition. All data, including calcium traces, are presented as means ± standard error.

Figure 2.5

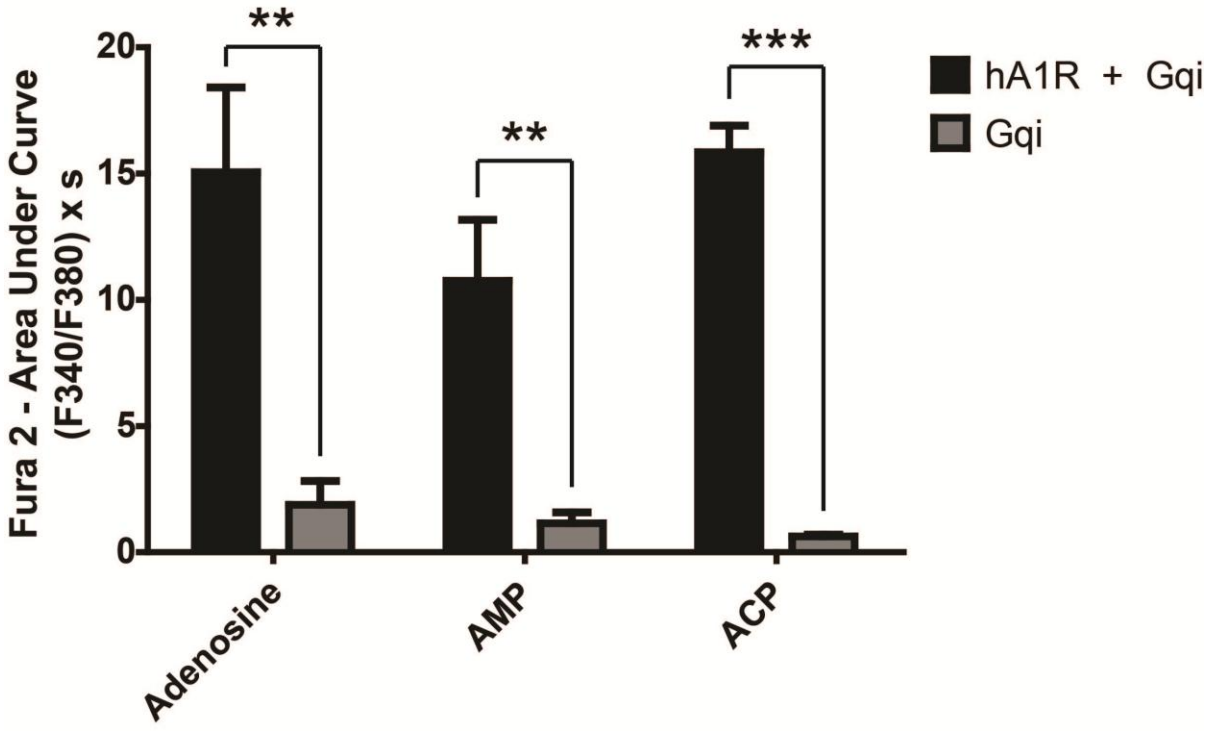
**
**
***
20
15
10
5
0
Fura 2 - Area Under Curve
(F340/F380) x s
hA1R + Gqi
Gqi
Adenosine
AMP
ACP

Figure 2.5. Adenosine, AMP and ACP stimulate calcium mobilization in COS7 cells.

Calcium mobilization in COS7 cells expressing (*black*) hA_1R + Gqi or (*grey*) Gqi alone, and stimulated with the indicated compounds (at 1 mM). AUC measurements extended for 1 minute from agonist addition. Paired t tests were used to compare AUC data in the presence and absence of transfected hA_1R. **, $p < 0.005$; ***, $p < 0.0005$. All experiments performed in duplicate. n = 15-21 cells per condition. All data are presented as means ± standard error.

Adenosine and AMP are equipotent hA_1R agonists

Since our experiments above were performed using a single concentration of agonist, we next performed dose-response experiments to determine agonist potency in hA_1R + Gqi-expressing cells (Fig. 2.6). We found that adenosine stimulated calcium responses with an EC_{50} of 1.41 μM (Table 1), a value consistent with previously published measurements (71,89). Interestingly, the EC_{50} and E_{max} of AMP in the absence or presence of αβ-met-ADP (to ensure AMP was not hydrolyzed by endogenous NT5E) were not significantly different from those of adenosine (Fig. 2.6, Table 1). The non-hydrolyzable analog ACP had an EC_{50} of 26.1 μM, 15 fold higher than AMP. This reduced potency relative to AMP could reflect the charge difference between the phosphonate and phosphate groups (monoanionic verses dianionic at neutral pH, respectively, Fig. 2.4). The adenosine deamination product inosine had an EC_{50} of 38.1 μM, 27 fold higher than adenosine. The high potency A_1R agonist 2-chloro-N^6-cyclopentyladenosine (CCPA) evoked calcium responses with an EC_{50} of 3.32 nM. The Hill slopes of all dose responses were near 1.

To test the potency of these compounds in an assay that does not depend on the use of chimeric G proteins, we utilized a modified Promega GloSensor assay (Fig. 2.7, see Materials and Methods for assay details). This assay measures agonist effects on isoproterenol-evoked cAMP accumulation using a luminescent reporter construct, and is conducted in cells containing only endogenous G proteins. When stimulating hA_1R-expressing cells with adenosine, we observed a bimodal dose response, with adenosine inhibiting cAMP accumulation at low concentrations and stimulating cAMP accumulation at high concentrations (Fig. 2.7B). The latter response was likely due to activation of G_s-coupled A_2 receptors, which HEK293 cells endogenously express (62,87). Indeed, adenosine

stimulated additional cAMP accumulation in cells transfected with empty vector (Fig. 2.8B). This bimodal response prevented us from obtaining an EC_{50} value for adenosine.

In contrast, CCPA, AMP, ACP, and inosine exclusively inhibited cAMP accumulation in hA_1R-expressing cells (Fig. 2.7 A, C-F) but had no effects in cells transfected with empty vector (Fig. 2.8 A, C-E). Incubation with 100 ng/ml pertussis toxin for 16 hr post-transfection abolished the A_1R-mediated inhibition of cAMP accumulation by adenosine, AMP, and CCPA (data not shown), confirming that signaling was mediated through endogenous G_i proteins. The rank order of agonist potency was similar between cAMP accumulation assays and calcium mobilization assays (Table 1). The EC_{50} values of AMP were not significantly different in the presence or absence of 10 μM αβ-met-ADP (Fig. 2.7 C,D), further indicating AMP stimulates hA_1R/G_i-coupled signaling directly and independent of hydrolysis to adenosine. Moreover, AMP did not produce a bimodal response like adenosine, arguing that the signaling effects of AMP were specific to hA_1R and not due to hydrolysis to adenosine.

Figure 2.6

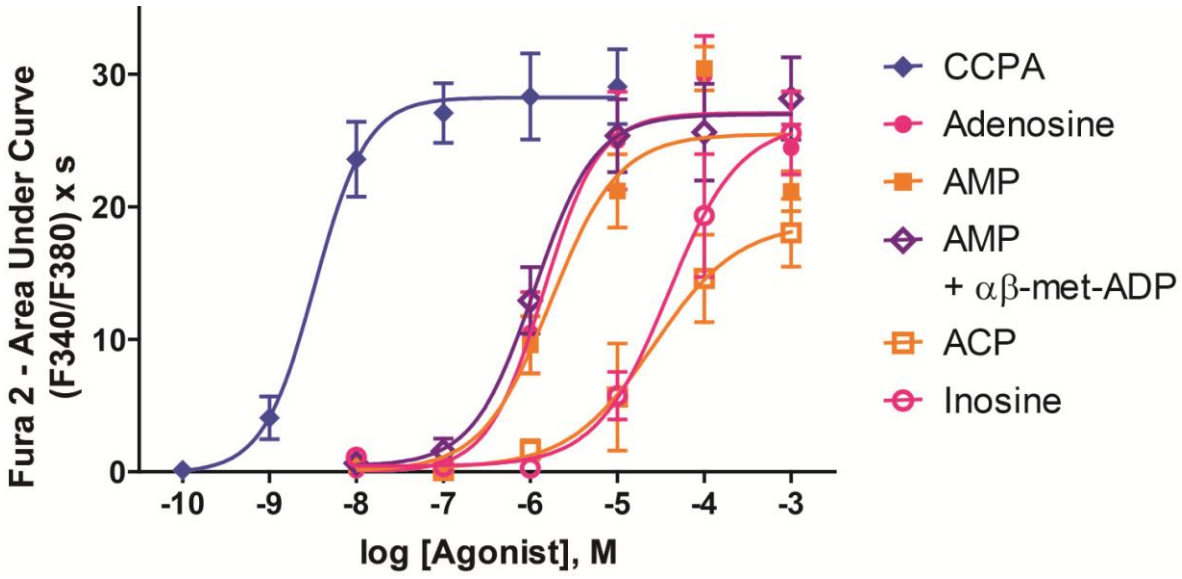
Fura 2 - Area Under Curve
(F340/F380) x s
30
20
10
0
-10
-9
-8
-7
-6
-5
-4
-3
log [Agonist], M
CCPA
Adenosine
AMP
AMP
+ αβ-met-ADP
ACP
Inosine

Figure 2.6. Dose-response curves for adenosine, AMP and related analogs at hA_1R.

Calcium mobilization in HEK293 cells expressing hA_1R + Gqi and stimulated with the indicated compounds. For AMP + αβ-met-ADP condition, cells were incubated with 10 μM αβ-met-ADP for 3 minutes and then were stimulated with AMP in the presence of 10 μM αβ-met-ADP. AUC measurements extended for 1 minute from agonist addition. All experiments performed in duplicate. n = 19-45 cells per condition. All data are presented as means ± standard error.

Figure 2.7

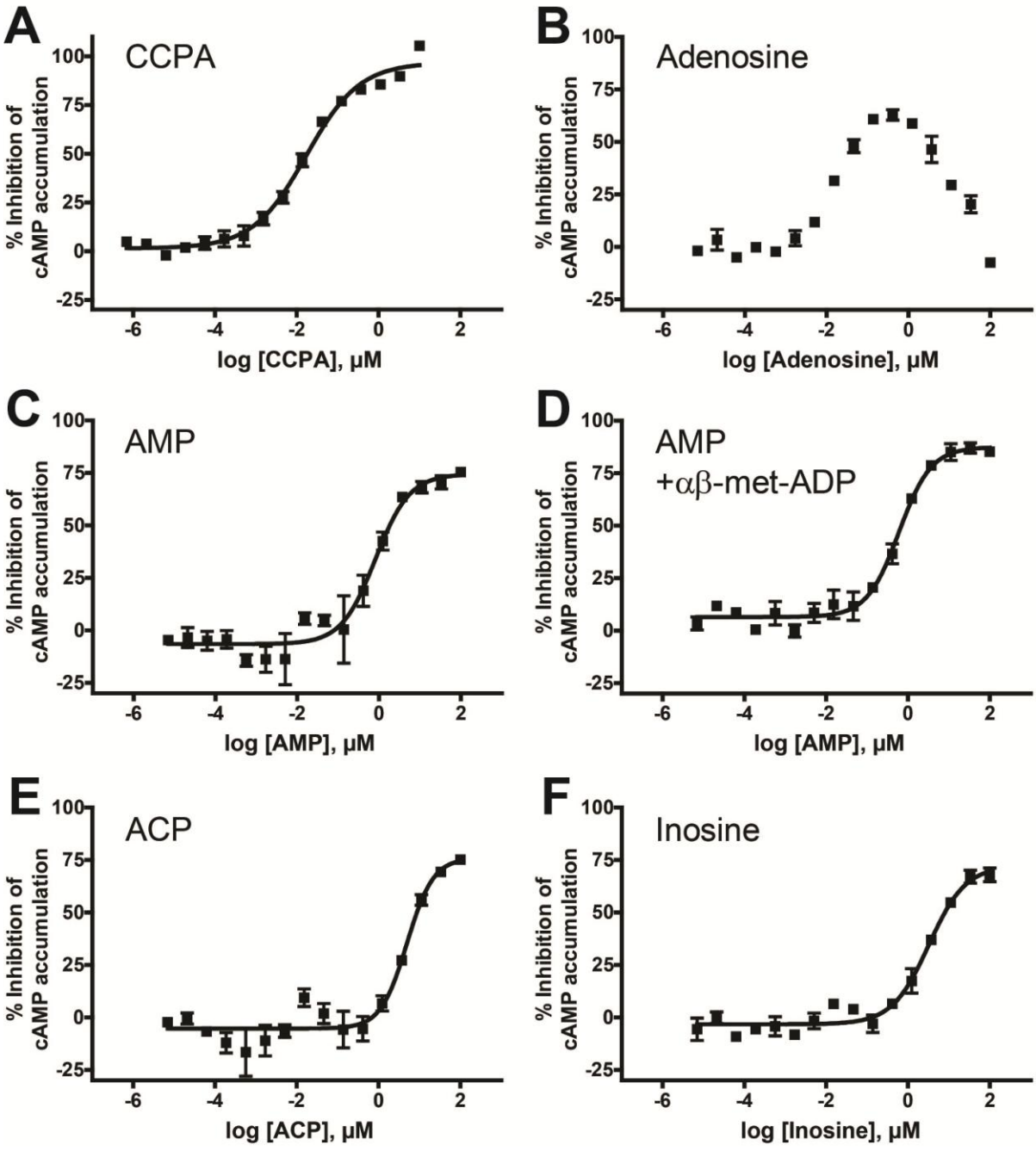
A
CCPA
% Inhibition of cAMP accumulation
log [CCPA], µM
B
Adenosine
log [Adenosine], µM
C
AMP
log [AMP], µM
D
AMP
+αβ-met-ADP
log [AMP], µM
E
ACP
log [ACP], µM
F
Inosine
log [Inosine], µM

Figure 2.7. Adenosine, AMP and related analogs inhibit cAMP accumulation in hA_1R-expressing cells.

HEK293T cells were co-transfected with a vector encoding hA_1R and GloSensor 22F plasmid then stimulated with (A) CCPA, (B) adenosine, (C) AMP, (D) AMP in the presence of 10 μM αβ-met-ADP, (E) ACP, or (F) inosine. Cells were incubated with test compound for 10 minutes, then 175 nM (-)-isoproterenol was added for 7 minutes to stimulate cAMP accumulation. Following incubation, GloSensor cAMP reagent was added and luminescence was measured. Data were normalized such that 100% inhibition is equal to the response at the maximal concentration of CCPA and 0% is equal to the response from isoproterenol alone. All experiments were performed in duplicate. All data are presented as means ± standard deviation.

Figure 2.8

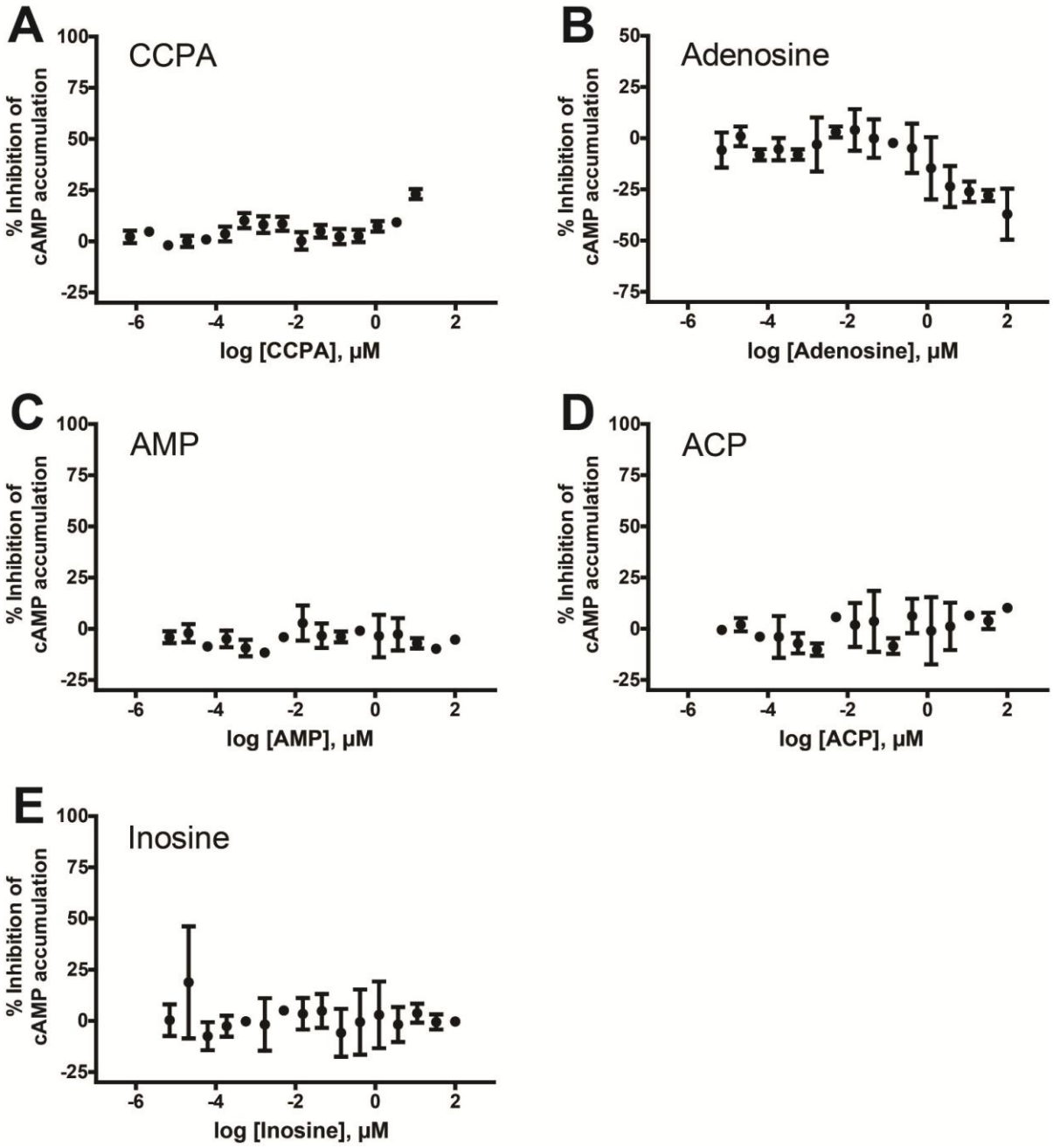
A
CCPA
% Inhibition of cAMP accumulation
100
75
50
25
0
-25
-6
-4
-2
0
2
log [CCPA], µM
B
Adenosine
% Inhibition of cAMP accumulation
50
25
0
-25
-50
-75
-6
-4
-2
0
2
log [Adenosine], µM
C
AMP
% Inhibition of cAMP accumulation
100
75
50
25
0
-25
-6
-4
-2
0
2
log [AMP], µM
D
ACP
% Inhibition of cAMP accumulation
100
75
50
25
0
-25
-6
-4
-2
0
2
log [ACP], µM
E
Inosine
% Inhibition of cAMP accumulation
100
75
50
25
0
-25
-6
-4
-2
0
2
log [Inosine], µM

Figure 2.8. Adenosine, AMP and related analogs do not inhibit cAMP accumulation in cells lacking hA_1R.

HEK293T cells were co-transfected with empty expression vector and GloSensor 22F plasmid then were stimulated with (A) CCPA, (B) adenosine, (C) AMP, (D) ACP, and (E) inosine. Cells were incubated with test compound for 10 minutes, then 175 nM (-)-isoproterenol was added for 7 minutes to stimulate cAMP accumulation. Following incubation, GloSensor cAMP reagent was added and luminescence was measured. All data were normalized such that 0% is equal to the response from isoproterenol alone. All experiments performed in duplicate. All data are presented as means ± standard deviation.

Table 1

hA_1R dose responses for Ca^{2+} mobilization assay and Glosensor assay

	Ca^{2+} mobilization		Inhibition of cAMP accumulation
Agonist	EC_{50} (μM)	E_{max} (%)*	EC_{50} (μM)
CCPA	0.00332	104.3 ± 2.0	0.0171
Adenosine	1.41	100	--
AMP	1.69	94.1 ± 14.1	0.816
AMP#	1.11	99.6 ± 3.3	0.601
ACP	26.1	69.4 ± 3.2	4.95
Inosine	38.1	97.2 ± 3.6	3.22

* Relative to adenosine; # In presence of 10 μM αβ-met-ADP

ACP inhibits forskolin-evoked cAMP accumulation in embryonic mouse cortical neurons

Since the experiments above relied upon overexpression of adenosine receptors, to further assess physiological relevance, we next sought to determine if the non-hydrolyzable AMP analog (ACP) could activate native A_1R and native downstream signaling components in a primary cell type. We selected mouse embryonic cortical neurons because AMP directly activates mA_1R (Fig. 2.3), mA_1R is highly expressed (Fig. 2.9A) and A_1R activation regulates the physiology of cortical neurons (83). We utilized a cAMP ELISA assay to measure the second messenger that is downstream of G_i-coupled mA_1R. In addition, we used ACP to ensure that no adenosine was produced from endogenously expressed ectonucleotidases.

Stimulation of cortical neurons with the adenylyl cyclase activator forskolin (10 μM) for 15 minutes increased intracellular cAMP concentration by 10-fold compared to baseline (Fig. 2.9B, *blue*). The concentration of cAMP in neurons treated with 1 mM ACP for 30 minutes prior to forskolin stimulation was decreased 34.9% compared to neurons treated with forskolin alone (Fig 2.9B, *green*), and cAMP concentration decreased 57.2% in neurons treated with 1 μM N^6-cyclopentyladenosine (CPA; Fig 2.9B, *purple*), a high potency A_1R agonist. In addition, the potent A_1R antagonist CPX (100 μM) completely blocked the effects of ACP and CPA, as evidenced by no decrease in cAMP concentration compared to forskolin alone (Fig 2.9C). Thus, these data indicate that a nonhydrolyzable AMP analog can directly activate endogenous signaling pathways downstream of endogenously expressed A_1R (i.e. in cells that were not subjected to any genetic manipulation).

Figure 2.9

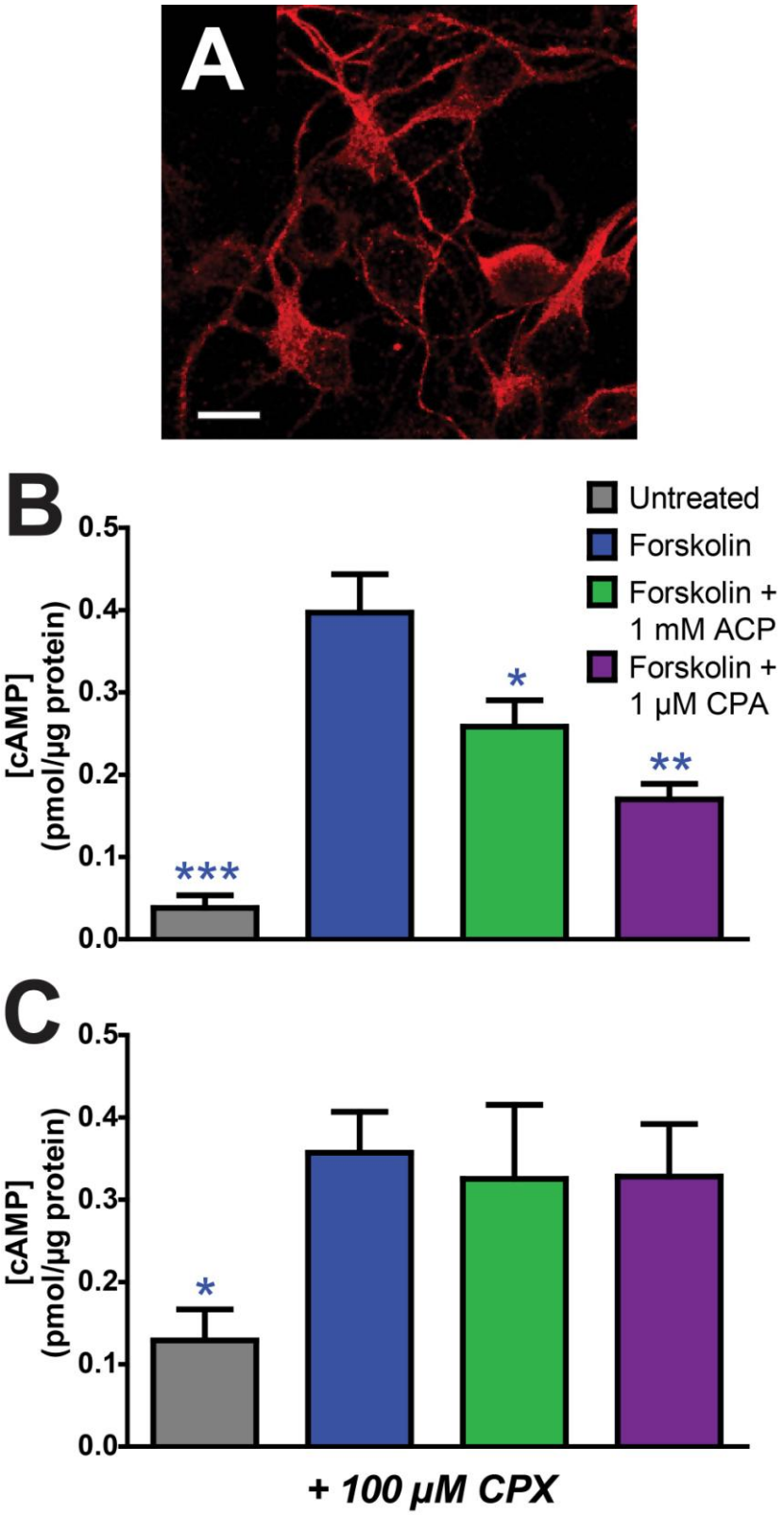
A
B
[cAMP]
(pmol/µg protein)
0.5
0.4
0.3
0.2
0.1
0.0
***
*
**
Untreated
Forskolin
Forskolin +
1 mM ACP
Forskolin +
1 µM CPA
C
[cAMP]
(pmol/µg protein)
0.5
0.4
0.3
0.2
0.1
0.0
*
+ 100 µM CPX

Figure 2.9. ACP inhibits cAMP accumulation in mouse embryonic cortical neurons.

Embryonic cortical neurons were dissociated and plated at approximately embryonic day 16.5. A) Confocal image of cortical neurons immunostained with an anti-A_1R antibody. Scale bar = 10 µm. B and C) After 1 day in vitro, neurons were incubated for 30 minutes with 1 mM ACP or 1 µM CPA in the (B) absence or (C) presence of 100 µM CPX. Neurons were then stimulated with 10 µM forskolin for 15 minutes, washed, and lysed. Cell lysates were then applied to a cAMP ELISA assay according to manufacturer's instructions. cAMP concentrations were normalized to total protein using a BCA protein assay. *Blue asterisks*, statistically significant difference compared to forskolin stimulation alone. *, $p < 0.05$; **, $p < 0.005$; ***, $p < 0.0005$. Data are the average of four (- CPX) or two (+ CPX) experiments performed in duplicate. All data are presented as means ± standard error.

AMP stimulates hA$_1$R independent of P2Y receptors

HEK293/T cells express multiple P2Y receptors (64,90) and P2Y receptors can heterodimerize with A_1R, imparting a P2Y-like pharmacology on A_1R (91-93). In addition, P2Y receptors can be stimulated by AMP analogs but not by AMP (94). Thus, we evaluated whether AMP-evoked calcium responses in hA_1R-expressing cells could be blocked with non-selective P2Y antagonists (PPADS or suramin). We found that stimulation of untransfected HEK293 cells with 10 μM ATP elicited a rapid calcium response (Fig. 2.10A, *grey*). This response was blocked completely by 100 μM PPADS (Fig. 2.10A, *blue*) and by 100 μM suramin (Fig. 2.10A, *green*). However, the same concentrations of PPADS or suramin did not block calcium responses in hA_1R + Gqi-expressing cells that were stimulated with 10 μM adenosine (Fig. 2.10B) or 10 μM AMP (Fig. 2.10C). These data thus indicate that AMP signals directly through hA_1R, independent of P2Y receptor activity.

His251 and His278 in the ligand binding pocket are required for AMP to directly activate hA$_1$R

The crystal structures of an adenosine receptor ($hA_{2A}R$) co-crystallized with adenosine and an adenosine analog were recently reported (10,11). From these structural views of the ligand binding pocket, we selected two positively charged histidine residues (H251 and H278; conserved in hA_1R) as possibly important for interacting with the negatively charged phosphate of AMP. We then mutagenized each of these histidine residues to a nonpolar residue (alanine), to generate hA_1R-H251A and hA_1R-H278A. We

confirmed that each mutant receptor was expressed and membrane-localized to the same extent as wild-type hA_1R (Fig. 2.11 A-C).

Next, we measured adenosine and AMP potency at the mutant receptors with our calcium mobilization assay (Fig. 2.11D). We performed these experiments in the presence of 10 μM αβ-met-ADP to prevent AMP from slowly being hydrolyzed to adenosine. In cells expressing hA_1R-H251A + Gqi, adenosine stimulated calcium mobilization with an EC_{50} of 1.80 μM, essentially identical to what we observed when stimulating wild-type hA_1R with adenosine (Table 1). Likewise, mutation of H251 did not affect binding of a radiolabled agonist to bovine A_1R (95). In contrast, the potency of AMP in hA_1R-H251A + Gqi-expressing cells was drastically reduced, so much so that we could not obtain a complete dose response. In cells expressing hA_1R-H278A + Gqi, we observed a very weak response after stimulation with 1 mM adenosine, but no response at lower concentrations. Furthermore, stimulation with 1 mM AMP elicited no response. This is also consistent with a previous report, which showed that mutation of H278 abolished agonist binding (95). Taken together, our results provide compelling evidence that adenosine and AMP activate hA_1R directly, with activation requiring an agonist binding pocket residue (H278) that is conserved in all adenosine receptors. Furthermore, the positively charged H251 residue is critical for activation of hA_1R by a negatively charged nucleotide (AMP) but not by adenosine. Importantly, these mutagenesis experiments conclusively rule out the possibility that adenosine and AMP stimulate calcium mobilization through any other receptor in HEK293 cells.

Figure 2.10

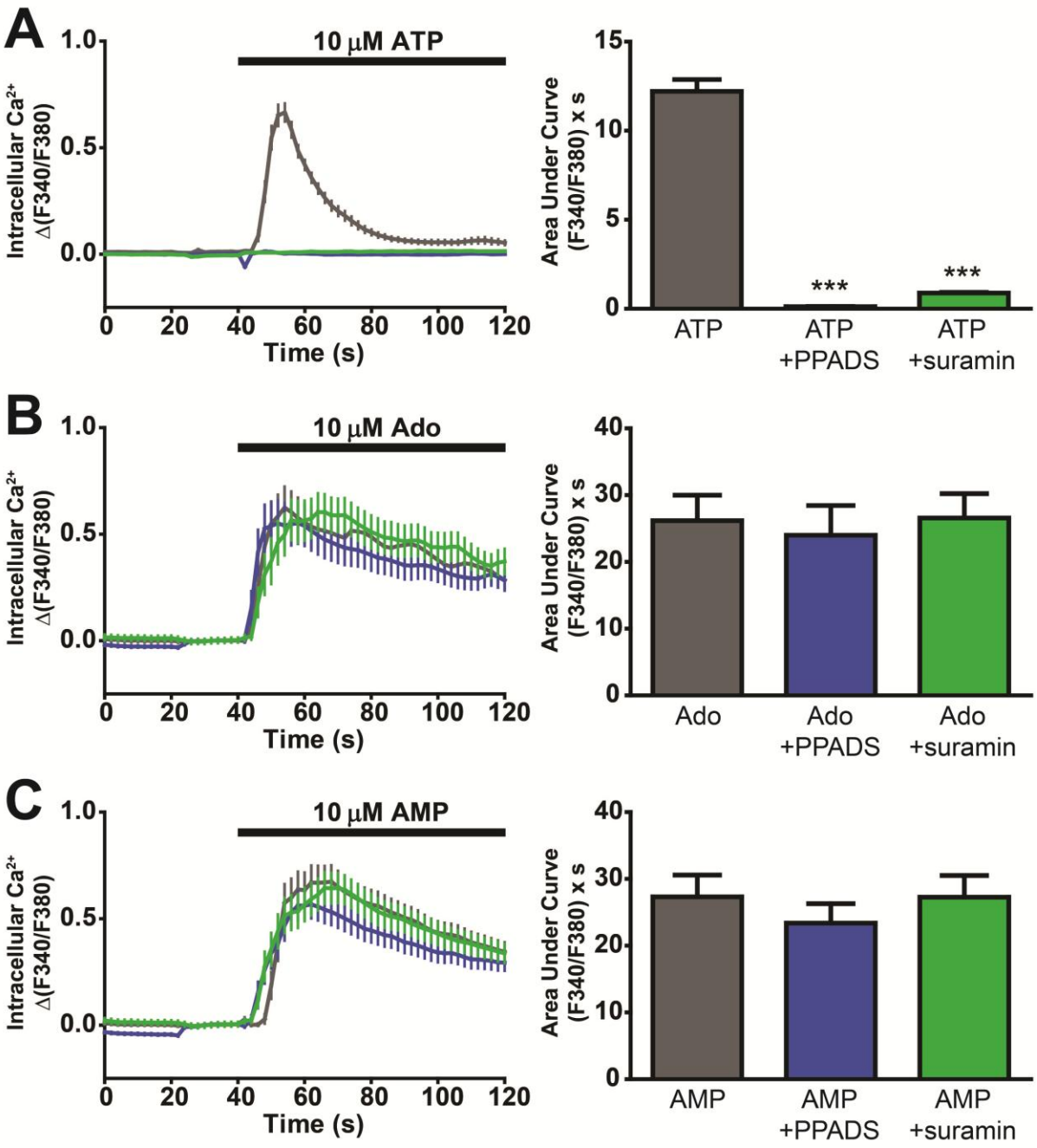
A
10 μM ATP
Intracellular Ca2+ Δ(F340/F380)
1.0
0.5
0.0
0
20
40
60
80
100
120
Time (s)
Area Under Curve (F340/F380) x s
15
10
5
0
***
***
ATP
ATP +PPADS
ATP +suramin
B
10 μM Ado
Intracellular Ca2+ Δ(F340/F380)
Time (s)
Area Under Curve (F340/F380) x s
40
30
20
10
0
Ado
Ado +PPADS
Ado +suramin
C
10 μM AMP
Intracellular Ca2+ Δ(F340/F380)
Time (s)
Area Under Curve (F340/F380) x s
AMP
AMP +PPADS
AMP +suramin

Figure 2.10. AMP activates hA_1R independent of P2Y receptor activity.

A) Calcium mobilization responses in untransfected HEK293 cells stimulated with 10 µM ATP in the absence or presence of P2Y receptor antagonists (PPADS or suramin). B and C) Calcium mobilization responses in HEK293 cells expressing hA_1R + Gqi following stimulation with (B) 10 µM adenosine or (C) 10 µM AMP, in the absence or presence of 100 µM PPADS or 100 µM suramin. Cells were incubated in 100 µM PPADS/suramin for 3 minutes prior to experiments. AUC measurements extended for 1 minute from agonist addition. Paired t tests were used to compare AUC data relative to agonist alone. ***, $p < 0.0005$. All data are the average of (A) one or (B, C) two experiments performed in duplicate. n = 21-74 cells per condition. All data, including calcium traces, are presented as means ± standard error.

Figure 2.11

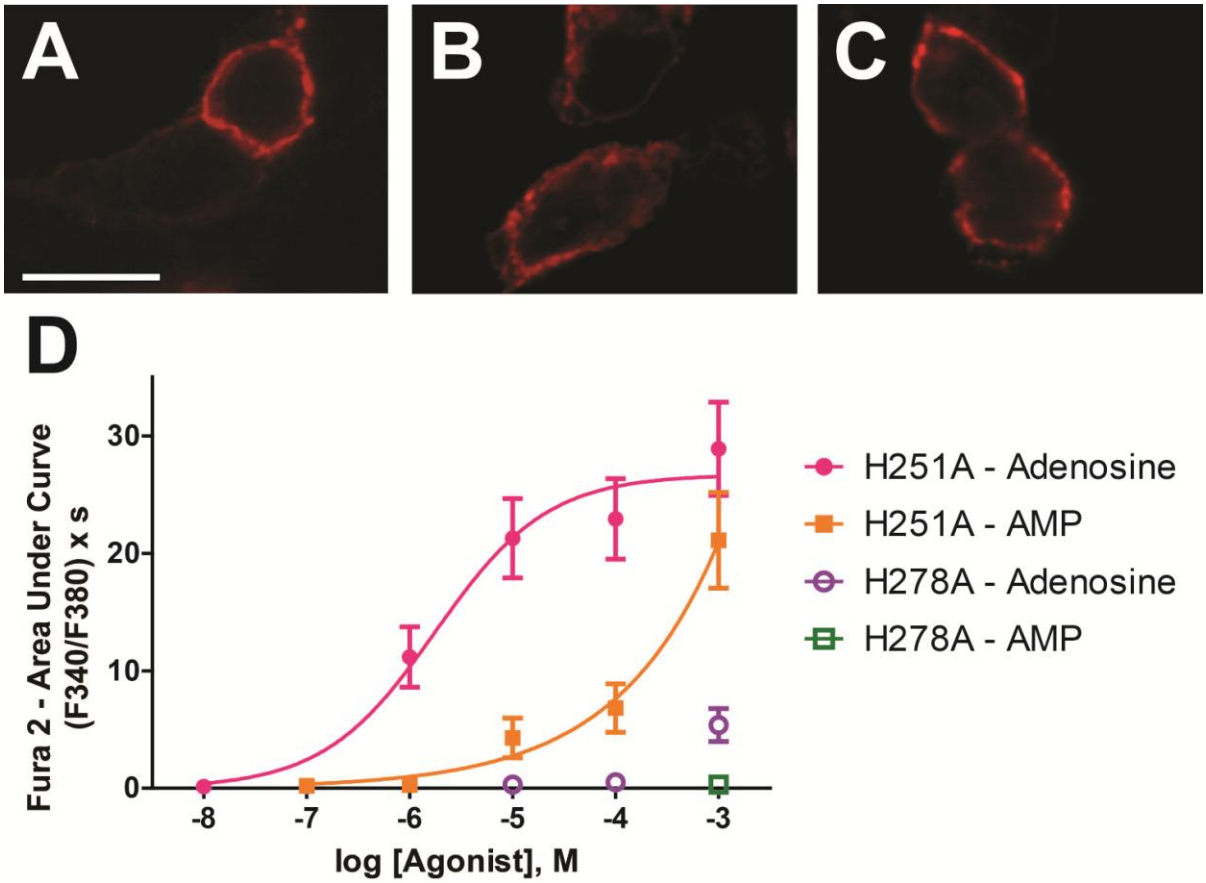
A
B
C
D
Fura 2 - Area Under Curve (F340/F380) x s
30
20
10
0
-8
-7
-6
-5
-4
-3
log [Agonist], M
H251A - Adenosine
H251A - AMP
H278A - Adenosine
H278A - AMP

Figure 2.11. Expression and activity of hA_1R point mutants.

A – C) Confocal images of HEK293 cells expressing (A) wild-type hA_1R, (B) hA_1R-H251A or (C) hA_1R- H278A and immunostained with anti-A_1R antibodies. Untransfected HEK293 cells in the same field of view were not immunostained, confirming antibody specificity. Scale bar = 10 µm. D) Calcium mobilization in HEK293 cells co-expressing indicated hA_1R mutant and Gqi then stimulated with increasing concentrations of the indicated compounds. For all conditions, cells were incubated with 10 µM αβ-met-ADP for 3 minutes and then were stimulated with agonist in the presence of 10 µM αβ-met-ADP. AUC measurements extended for 1 minute from agonist addition. All experiments performed in duplicate, except H278A – AMP, which was performed in triplicate. n = 17-49 cells per condition. All data are presented as means ± standard error.

DISCUSSION

Prior to our study, it was unknown if a receptor for AMP existed. An older study suggested AMP might act directly and indirectly on adenosine receptors (73); however, the investigators did not fully inhibit the multiple ectonucleotidases that are now known to hydrolyze AMP to adenosine (75,77,78). In addition, AMP has never been evaluated as an agonist with cloned adenosine receptors, possibly because all previous assays of adenosine receptor activation required relatively long incubation periods with agonist, causing uncertainty as to whether AMP or its hydrolysis product (adenosine) was the active compound.

Using a novel cell-based assay that allowed for real-time visualization of adenosine receptor activation, we found that AMP directly activated hA_1R, independent of hydrolysis. In support of this conclusion, we found that AMP activated hA_1R in HEK293 cells as effectively as adenosine, even after inhibition of the main ectonucleotidase in HEK293 cells. Furthermore, a non-hydrolyzable analog of AMP also activated hA_1R in heterologous cells and in primary neurons, demonstrating that activation was not due to hydrolysis to adenosine. Our data thus provide the first direct evidence that hA_1R is a receptor for the naturally occurring nucleotide AMP, and argue for reclassification of A_1R as an adenosine and nucleotide (AMP) receptor.

Inbe and colleagues previously reported that GPR80/GPR99 was a receptor for adenosine and AMP, although others could not reproduce this result (62-64). As suggested by Abbracchio and colleagues, GPR80/GPR99 may have been misidentified as a purinergic receptor because HEK293 cells (the cells used in the GPR80/GPR99 study and our present study) endogenously express P2Y receptors in addition to $A_{2A}R$ and $A_{2B}R$. Alternatively,

heteromeric interactions between GPR80/GPR99 and endogenous purinergic receptors could hypothetically impart GPR80/GPR99 with a novel pharmacological profile.

Neither of these hypothetical possibilities explains why AMP activated hA_1R in our assays. The HEK293 cells we used do contain A_2 receptors (as evidenced by stimulation of cAMP production in cells transfected only with GloSensor plasmid, Fig. 2.8B) and P2Y receptors (as evidenced by ATP-evoked, P2Y antagonist-sensitive calcium responses, Fig. 2.10A). However, our data with P2Y antagonists rule out the possibility that AMP signaled through P2Y receptors. In addition, point mutations in hA_1R shifted or eliminated responses to AMP, providing strong evidence that AMP signaled directly through hA_1R and not through any other receptor in HEK293 cells. AMP also directly stimulated hA_1R when expressed in a different mammalian cell line (COS7 cells; Fig. 2.5).

Our findings were also not an artifact of using a chimeric G protein to couple hA_1R to calcium mobilization. Indeed, we found that AMP (±αβ-met-ADP) and ACP activated hA_1R when coupled to endogenous G_i proteins using the GloSensor cAMP accumulation assay and that this effect could be blocked by G_i-specific disruption with pertussis toxin. Our findings were not an artifact of overexpressing A_1R, as ACP inhibited forskolin-induced cAMP accumulation in mouse cortical neurons that contain only native A_1R and downstream signaling components.

There is a large amount of structure-activity data with 5'-substituted adenosine analogs, all of which indicate that A_1R is tolerant of bulky and negatively charged groups at the 5'-position (96-98). This includes 5'-ester, 5'-carbamoyl, 5'-halogen and 5'-sulfide derivatives of adenosine analogs, many of which are low nanomolar agonists of A_1R (99-

102). Despite this extensive literature with unnatural analogs, it is surprising that the most biologically relevant substitution – a 5'-phosphate – has never, to our knowledge, been directly tested as an A_1R agonist.

Our data also revealed that a different adenosine receptor – $hA_{2B}R$ – is not activated by AMP or the non-hydrolyzable analog ACP. Instead, $hA_{2B}R$ was only activated indirectly, following hydrolysis to adenosine. These results shed light on seemingly conflicting reports of AMP acting directly as well as indirectly on adenosine receptors in some tissues but only indirectly via conversion to adenosine in other tissues (65,71-73,103,104). Our data indicate that it is important to determine which adenosine receptor is activated when AMP is used as the ligand. If $A_{2B}R$ is activated, the signaling effects of AMP should be indirect and fully dependent on ectonucleotidases. In contrast, if A_1R is activated, the signaling effects of AMP could be direct and indirect, with the level of direct activation dependent on AMP stability and ectonucleotidase levels.

We found that a non-hydrolyzable phosphonate analog of AMP could activate hA_1R. Interestingly, other ectonucleotidase-resistant phosphonate analogs of AMP reportedly activate P2X receptors and have cardioprotective activity *in vivo* (105,106). While it was suggested that the cardioprotective effects of these AMP analogs were due to P2X activation, P2X involvement was never directly tested *in vivo* with antagonists or knockout mice. Given that A_1R agonists also have cardioprotective effects (61), it is equally possible that the cardioprotective effects of these phosphonate analogs, and possibly AMP itself, are A_1R-mediated and not P2X-mediated.

Our findings also have implications for AMP-based prodrugs that were designed to be full agonists for $A_{2A}R$ only after hydrolysis by ectonucleotidases (107). Given our results and the extensive structure-activity data with substitutions at the 5'-position, these AMP prodrugs may display a complex pharmacology with direct A_1R activation combined with indirect, hydrolysis-dependent $A_{2A}R$ activation. Clearly, it will be important to rigorously evaluate the extent to which these and other AMP-based prodrugs activate A_1R independent of hydrolysis. This will require pharmacologically or genetically eliminating all of the AMP hydrolytic enzymes in a given tissue – a potentially daunting task given that numerous ectonucleotidases are present in complex tissues and are difficult to experimentally eliminate completely (79).

CHAPTER 3: FURTHER INVESTIGATION OF A_1R SIGNALING

INTRODUCTION

The results presented in Chapter 2 raise several significant questions regarding the function of adenosine receptors. Firstly, what causes the difference in AMP sensitivity between the A_1 and A_{2B} receptors? Agonist sensitivity of GPCRs is usually thought to be determined by the residues in the receptor's agonist binding site; that is, the residues that directly interact with the agonist in the final, activated conformation. However, as detailed in Chapter 2, these residues are essentially completely conserved between the human A_1 and A_{2B} receptors (and therefore cannot be responsible for the difference in AMP sensitivity). Thus, the molecular mechanism(s) that determine the AMP sensitivity of adenosine receptors remains unknown.

Secondly, what explains AMP's lack of *in vivo* antinociceptive activity? The initial experiments in Chapter 2 (Fig. 2.2) were originally undertaken in order to better understand the activity of the pain-relieving ectonucleotidases prostatic acid phosphatase (PAP) and NT5E. These enzymes reduce pain sensitivity when administered intrathecally (70,76) – or peripherally in the case of PAP (108) – by generating adenosine in situ. The substrate for both enzymes is AMP, which is present in the extracellular environment at much higher levels than adenosine (109). Furthermore, the effects of both PAP and NT5E are mediated by the A_1 adenosine receptor. Taken together with the results from Chapter 2, this brings to light an apparent paradox: if AMP and adenosine are equipotent A_1R agonists (Fig. 2.6), why

does conversion of one into the other have any A_1R-mediated effect at all? Nevertheless, direct intrathecal injection of adenosine generates transient antinociceptive effects but injection of AMP does not (Dutton and Zylka, unpublished data), indicating that there is indeed a difference between AMP and adenosine *in vivo*.

Lastly, there is great interest in the development of A_1 adenosine receptor agonists as pharmaceuticals. In recent years there have been numerous A_1 agonists in clinical trials for conditions as diverse as cardiac arrhythmia, angina, diabetes, and neuropathic pain (98). However, none of these compounds are based on an AMP scaffold. Furthermore, many promising A_1 agonists have encountered difficulties in clinical trials due to severe cardiovascular side effects and loss of efficacy due to A_1 receptor desensitization (98). Thus, the therapeutic potential of AMP-derived A_1R agonists (and whether they will be subject to these problems) is worthy of further investigation.

Here, we set out to answer the above questions regarding adenosine receptor activity, primarily by adapting the calcium mobilization assay used extensively in chapter 2. We found that the difference in AMP sensitivity between the human A_1 and A_{2B} receptors is at least partially determined by the sequence of the second extracellular loop, which likely affects the ability of AMP to access the agonist binding pocket by influencing the electrical charge on the extracellular face of the receptor. Additionally, we found that although AMP and adenosine are equally potent and equally efficacious hA_1R agonists through the $G\alpha_i$-coupled pathway, they exhibit dramatically different efficacies at hA_1R through the $G\alpha_q$-coupled pathway. This difference, or differential activation of other downstream effectors, is likely responsible for the discrepancy between AMP- and adenosine-evoked effects in vivo. Finally, we found that several AMP analogues are also potent hA_1R agonists, and that one of

these compounds does indeed have significant A_1R-mediated antinociceptive activity in mice. Furthermore, this compound lacks the characteristic cardiovascular side effects caused by many adenosine receptor agonists, indicating that there may be therapeutic applications for AMP-derived drugs in the treatment of pain.

MATERIALS AND METHODS

Molecular Biology

The human $G\alpha_q$ expression construct was a gift from Dr. Bryan Roth. $A_1R/A_{2B}R$ loop-replacement chimeras were generated by traditional PCR-based mutagenesis and were sequence verified. All other expression constructs were described previously (110). ACP, **3a**, and **3d** were synthesized as described previously (110,111).

Calcium Imaging

All calcium mobilization experiments and the data analysis thereof were performed as described previously (110).

Telemetry

Data Sciences International ETA-F20 transmitters were implanted as follows: A 2 cm midline abdominal incision was made in anesthetized mice. The transmitter was placed intra-abdominally on top of the intestines, parallel with the long axis of the body and the two leads pointing caudally. A large (14 gauge) needle was used to pass through the abdominal muscles on either side of the incision. The leads were passed through the lumen of the needle, one on each side and the needle was withdrawn. The leads were placed (positive by

the xiphoid and negative on the right pectoral) and anchored in place. The abdomen was closed with absorbable sutures and the skin with non-absorbable sutures.

Note: Figures 3.3 and 3.4, and the methods and results sections referring to them, are adapted from Korboukh et al (111) and constitute my personal contributions to that study.

RESULTS

Adenosine receptor sensitivity to AMP is partially determined by extracellular loop 2

We first set out to determine why the hA_1 receptor is sensitive to AMP but the hA_{2B} receptor is not, despite the fact that the residues in their respective binding pockets are nearly identical (11). Although the amino acid sequences of the transmembrane helices are highly conserved between hA_1R and $hA_{2B}R$, the sequences of the extracellular loops (ELs) diverge significantly (Fig. 3.1A). In fact, the net charge of the solvent-exposed extracellular faces of hA_1R and $hA_{2B}R$ is very different, due to the composition of these loops (Fig. 3.1B). Furthermore, we previously found that negative charge was important in the activation of hA_1R by AMP (110). We therefore hypothesized that the relative AMP sensitivities of the hA_1 and hA_{2B} receptors may be determined by their extracellular charge.

In order to test this hypothesis, we created A_1/A_{2B} chimeric receptors in which EL1, EL2, or ELs 1 and 2 from hA_1R were replaced with the equivalent loops from $hA_{2B}R$. We focused on ELs 1 and 2 because a homology model based on the crystal structure of the human A_{2A} receptor (11) predicts that these loops are located in much closer proximity to the agonist binding pocket than either EL3 or the N terminus (not shown). Furthermore, the net charge in EL3 does not vary between hA_1R and $hA_{2B}R$ (Fig. 3.1B), suggesting that mutagenesis of this loop is likely to have little effect. We then co-transfected the A_1/A_{2B} chimeras together with Gqi into HEK293 cells and measured calcium mobilization after stimulation with multiple concentrations of AMP. We performed these experiments in the presence of 10 μM αβ-met-ADP, to block the hydrolysis of AMP into adenosine.

We found that AMP potency and efficacy were very similar between WT hA_1R (Fig. 3.1C, *pink*; EC_{50} = 1.11 µM, E_{max} = 27.0) and the EL1 chimera (Fig. 3.1C, *orange*; EC_{50} = 1.25 µM, E_{max} = 22.8), suggesting that EL1 does not play a significant role in determining the AMP sensitivity of hA_1R and $hA_{2B}R$. However, AMP potency and efficacy were both drastically reduced in the EL2 chimera (Fig. 3.1C, *olive*; EC_{50} = 65.3 µM, E_{max} = 10.8), indicating that EL2 is a regulator of AMP sensitivity. The EL1,2 chimera (Fig. 3.1C, *green*; EC_{50} = 28.3 µM; E_{max} = 9.6) responded similarly to the EL2 chimera, again suggesting that EL1 is not involved in AMP sensitivity. As expected, we did not observe a calcium response after stimulating cells expressing WT $hA_{2B}R$ with any concentration of AMP (Fig. 3.1C, *blue*). The potency and efficacy of adenosine was similar at WT hA_1R and each of the chimeras (data not shown), indicating that modification of EL2 does not affect general receptor function. There are likely other determinants of adenosine receptor AMP sensitivity, as the loss of AMP sensitivity in the EL2 and EL1,2 chimeras was not complete. However, our data strongly suggest that the composition of EL2 is an important determinant of AMP sensitivity in hA_1R and $hA_{2B}R$, likely by influencing the electrostatic charge immediately outside the agonist binding pocket.

Figure 3.1

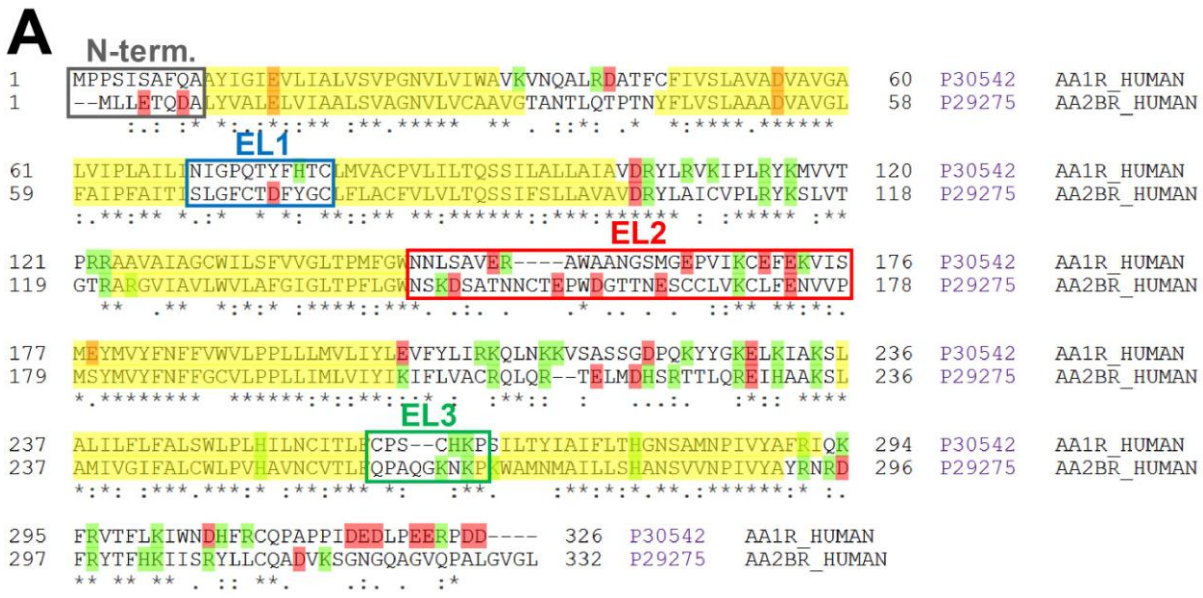

B

	N-term.	EL1	EL2	EL3	Total
hA_1R	0	+1	-1	+2	+2
$hA_{2B}R$	-2	-1	-3	+2	-4
Δ Charge	2	2	2	0	6

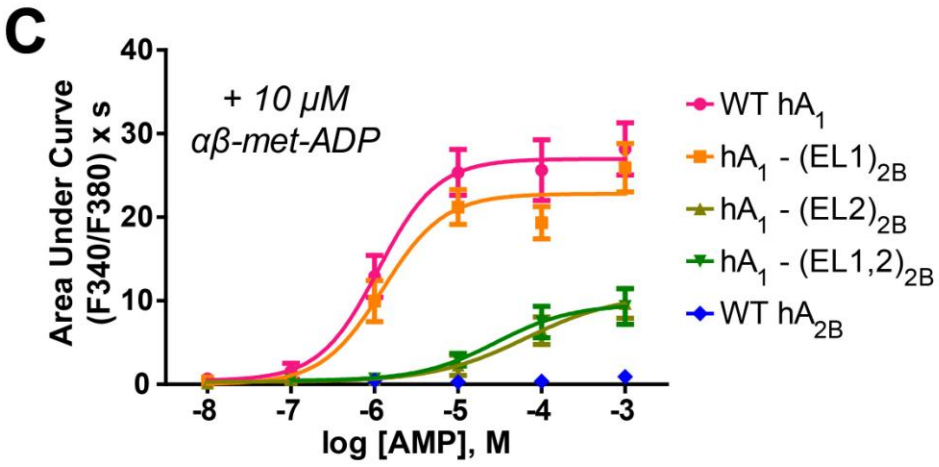

Figure 3.1. Adenosine receptor sensitivity to AMP is partially determined by extracellular loop 2.

A) Amino acid sequence alignment of hA_1R and $hA_{2B}R$. *Yellow*, transmembrane domain. *Red*, negatively charged residue. *Green*, positively charged residue. *, identical residues in hA_1R and $hA_{2B}R$. :, similar residues in hA_1R and $hA_{2B}R$. *Grey box*, N-terminus. *Blue box*, extracellular loop 1. *Red box*, extracellular loop 2. *Green box*, extracellular loop 3. B) Comparison of net charge in the extracellular regions of hA_1R and $hA_{2B}R$. C) Calcium mobilization in HEK293 cells expressing the indicated A_1/A_{2B} chimeras + Gqi and stimulated with AMP. WT hA_1: EC_{50} = 1.11 μM; E_{max} = 27.0. hA_1-$(EL1)_{2B}$: EC_{50} = 1.25 μM; E_{max} = 22.8. hA_1-$(EL2)_{2B}$: EC_{50} = 65.3 μM; E_{max} = 10.8. hA_1-$(EL1,2)_{2B}$: EC_{50} = 28.3 μM; E_{max} = 9.6. For all conditions, cells were incubated with 10 μM αβ-met-ADP for 3 minutes and then stimulated in the presence of 10 μM αβ-met-ADP. AUC measurements extended for 1 minute from AMP addition. n = 11-43 cells per condition. All data are presented as mean ± standard error.

AMP and adenosine differentially activate $G\alpha_q$ through the A_1 adenosine receptor

Administration of prostatic acid phosphatase (PAP) causes A_1R-mediated antinociceptive effects by hydrolyzing AMP to adenosine in situ (76). Additionally, intrathecal injection of adenosine causes short-lived antinociceptive effects, whereas intrathecal injection of AMP does not (Dutton and Zylka, unpublished data). These results appear to conflict with our evidence that adenosine and AMP are equipotent A_1R agonists (Fig. 2.6). However, although primarily coupled to $G\alpha_i$, hA_1R is a 'promiscuous' GPCR, meaning that it can couple to multiple G proteins, including $G\alpha_s$, and $G\alpha_q$ (112). In fact, an adenosine analog with a bulky substituent at the 5' position (similar to 5'-AMP) causes selective activation of $G\alpha_i$ over $G\alpha_q$ by A_1R (112). Furthermore, PAP's antinociceptive effects are mediated by the depletion of PIP_2 (113), a pathway downstream of $G\alpha_q$. Thus, we hypothesized that differential activation of $G\alpha_q$ downstream of A_1R may explain AMP's lack of antinociceptive activity, despite its A_1 agonist activity.

To examine hA_1R activation of $G\alpha_q$, we repeated our adenosine and AMP calcium mobilization experiments, replacing the chimeric G protein Gqi with wild-type human $G\alpha_q$. We found that in cells expressing hA_1R + $G\alpha_q$, stimulation with 1 mM AMP (Fig. 3.2 A,B; *blue*) evoked a much smaller calcium response compared to stimulation with 1 mM adenosine (Fig. 3.2 A,B; *red*). This is a striking difference from the assay employing Gqi, in which adenosine and AMP evoked identical responses (Fig. 2.2). Since $G\alpha_q$ is ubiquitously expressed, and should be present in HEK293 cells without overexpression, we also performed the experiment without transfecting $G\alpha_q$. In cells expressing only hA_1R, stimulation with 1mM adenosine (Fig. 3.2 A,B; *green*) evoked a very small calcium

response, and stimulation with 1 mM AMP (Fig. 3.2 A,B; *orange*) evoked no response at all, consistent with a much lower level of $G\alpha_q$ expression.

We then examined the relative potency and efficacy of adenosine and AMP through $G\alpha_q$ by repeating our dose-response experiments in the same fashion. We found that in cells expressing $hA_1R + G\alpha_q$ adenosine (Fig. 3.2C, *red*; EC_{50} = 8.97 µM, E_{max} = 18.0) had moderately reduced potency and efficacy compared to cells expressing hA_1R + Gqi (compare Fig. 3.2C to Fig. 2.6), consistent with preferential coupling of hA_1R to $G\alpha_i$. Moreover, the efficacy of AMP (Fig. 3.2C, *blue*; EC_{50} = 7.69 µM; E_{max} = 7.90) was far lower than that of adenosine in cells expressing $hA_1R + G\alpha_q$, although the potencies of adenosine and AMP were similar. Again, this is a very different result from the assay employing Gqi, in which both the potencies and efficacies of adenosine and AMP were essentially identical (Fig. 2.6). We did not observe significant calcium mobilization in cells expressing $hA_1R + G\alpha_q$ after stimulation with 1 mM ACP (Fig. 3.2C, *black*), consistent with ACP's low efficacy compared with AMP. Taken together, these data suggest that adenosine and AMP may still have different effects in vivo – despite being equally potent and equally efficacious A_1R agonists through $G\alpha_i$ – via differential activation of other downstream signaling pathways, including $G\alpha_q$.

Figure 3.2

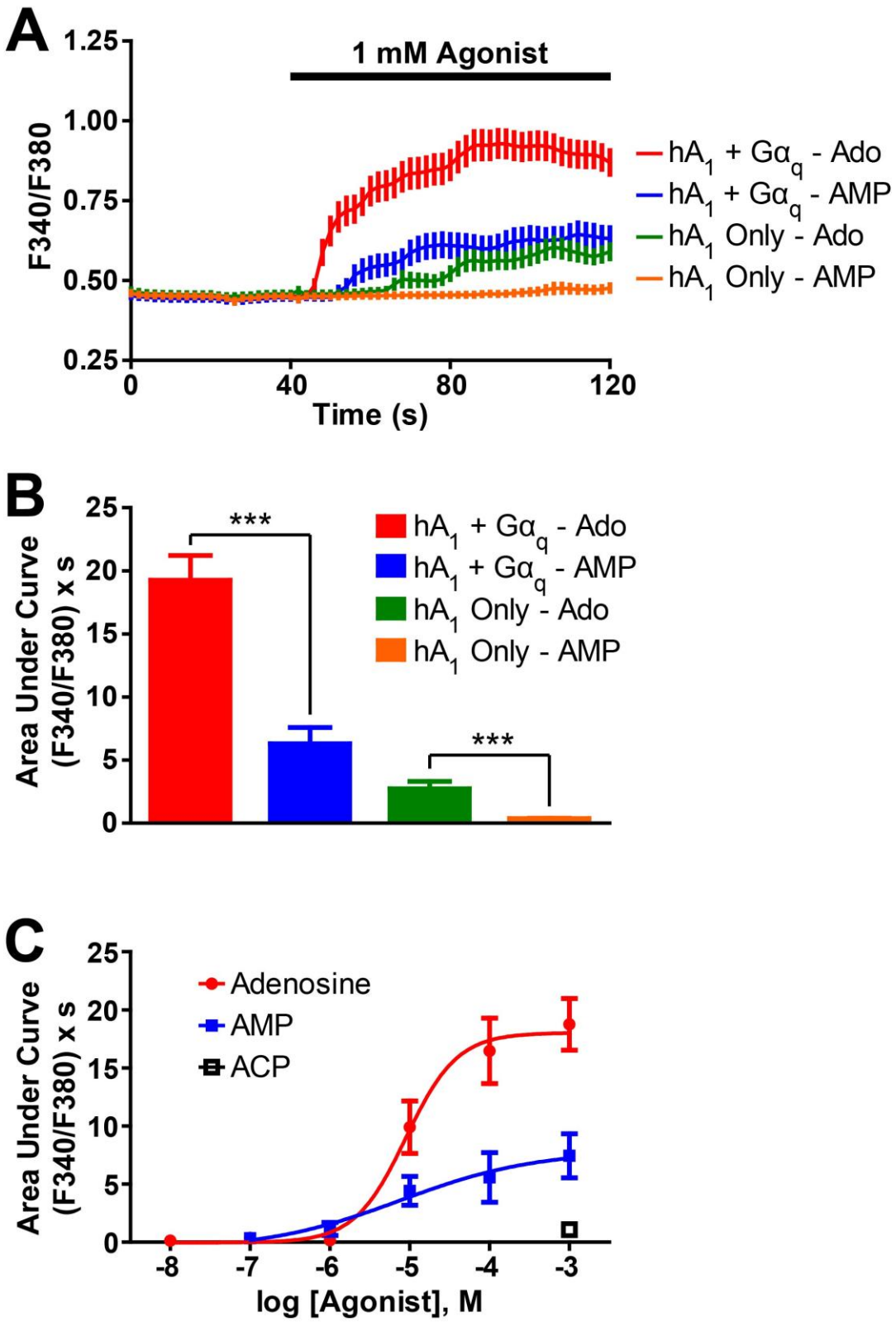
A
1 mM Agonist
F340/F380
1.25
1.00
0.75
0.50
0.25
0
40
80
120
Time (s)
hA1 + Gαq - Ado
hA1 + Gαq - AMP
hA1 Only - Ado
hA1 Only - AMP
B
Area Under Curve (F340/F380) x s
25
20
15
10
5
0
***
***
hA1 + Gαq - Ado
hA1 + Gαq - AMP
hA1 Only - Ado
hA1 Only - AMP
C
Area Under Curve (F340/F380) x s
25
20
15
10
5
0
Adenosine
AMP
ACP
-8
-7
-6
-5
-4
-3
log [Agonist], M

Figure 3.2. Adenosine and AMP have similar potencies but very different efficacies when stimulating hA_1R activation of $G\alpha_q$.

Calcium mobilization in HEK293 cells expressing hA_1R. A) Real-time calcium mobilization profiles in cells expressing $hA_1R + G\alpha_q$ or hA_1R alone and stimulated with 1 mM adenosine or AMP. n = 54-75 cells per condition. B) AUC quantification of calcium mobilization. C) Adenosine and AMP dose responses in cells expressing $hA_1R + G\alpha_q$. Adenosine: EC_{50} = 8.97 µM; E_{max} = 18.0. AMP: EC_{50} = 7.69 µM; E_{max} = 7.90. n = 14-53 cells per condition. AUC measurements extended for 1 minute from agonist addition. ***, $p < 0.0005$. All data are presented as mean ± standard error.

AMP analogues are potent A_1R agonists

In order to investigate whether compounds similar to AMP have A_1R agonist activity and/or antinociceptive activity, we synthesized a series of AMP analogues containing an N^6-cyclopentyl group, which is known to confer A_1R subtype selectivity (114). Nearly all of these compounds were potent agonists of hA_1R in a cAMP accumulation assay identical to the one presented in Figure 2.7 (111). We then selected compounds **3a** (Fig. 3.3A, a representative phosphate ester) and **3d** (Fig. 3.3B, a representative phosphate) and tested them in the hA_1R + Gqi calcium mobilization assay. The E_{max} of **3a** and **3d** were normalized to the E_{max} of adenosine in this assay. Both **3a** (Fig. 3.3C, *pink*) and **3d** (Fig. 3.3C, *orange*) were potent agonists of hA_1R with EC_{50} values of 0.52 μM and 0.021 μM, respectively. Furthermore, the E_{max} of **3a** and **3d** were similar to that of adenosine, indicating that **3a** and **3d** are full agonists at hA_1R. Therefore, using two distinct and complementary assay platforms, we confirmed that compounds **3a** and **3d** directly activate A_1R-mediated signaling.

Figure 3.3

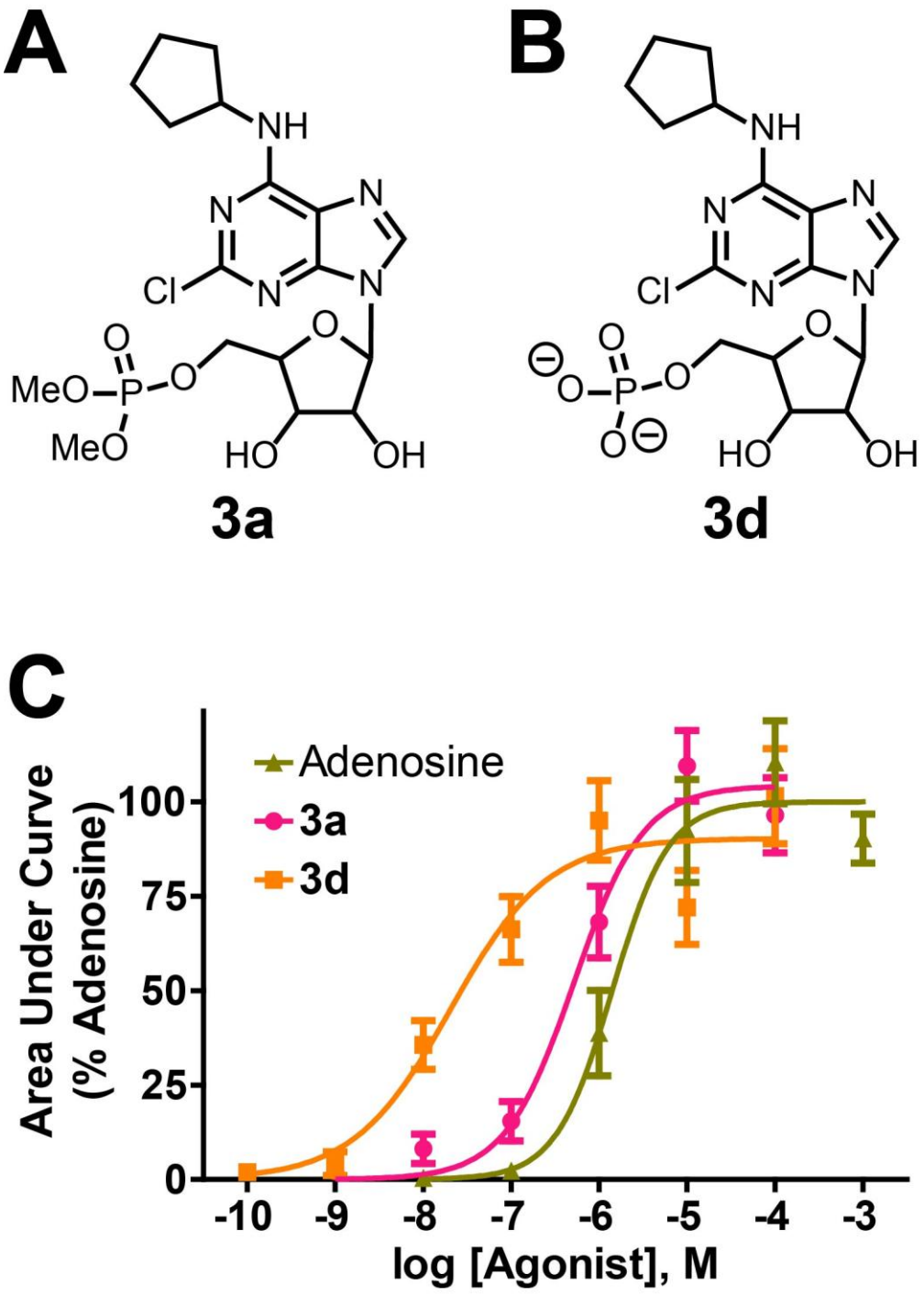
A
NH
N
N
Cl
N
N
O
MeO
P
O
MeO
HO
OH
3a
B
NH
N
N
Cl
N
N
O
O
P
O
O
HO
OH
3d
C
Area Under Curve
(% Adenosine)
100
75
50
25
0
Adenosine
3a
3d
-10
-9
-8
-7
-6
-5
-4
-3
log [Agonist], M

Figure 3.3. Compounds 3a and 3d are full agonists of human A_1R in a calcium mobilization assay.

A and B) Chemical structures of (A) **3a** and (B) **3d** at physiological pH. C) Calcium mobilization in HEK293 cells expressing hA_1R + Gqi and stimulated with the indicated compounds. **3a**: EC_{50} = 0.52 μM; and **3d**: EC_{50} = 0.021 μM. Adenosine (EC_{50} = 1.41 μM) was used as a positive control. AUC measurements extended for 1 minute from agonist addition. n = 27-50 cells per condition. All data are presented as mean ± standard error.

An AMP analogue has antinociceptive activity and lacks cardiovascular side effects in mice

Further experiments with our series of AMP analogues revealed that compound **3a** has potent A_1R-mediated antinociceptive effects in mice when administered orally or by intrathecal injection (111). However, clinical applications of the currently available A_1R agonists are hampered by their cardiovascular side effects (98). To determine if compound **3a** affected cardiovascular function, we monitored heart rate and body temperature in wild-type and $A_1R^{-/-}$ mice following oral administration (CPA was administered as a positive control). At the highest dose tested, a 5000 nmol/kg (2.39 mg/kg) single dose by oral administration, compound **3a** had no to negligible effects on heart rate and body temperature in wild-type and $A_1R^{-/-}$ mice (Fig. 3.4 A,C). On the other hand, CPA elicited a statistically significant decrease in heart rate and body temperature which lasted for 4 to 6 hours in wild-type mice (Fig. 3.4 B,D), but not in $A_1R^{-/-}$ mice. CPA caused a modest increase in heart rate in $A_1R^{-/-}$ mice, possibly reflecting known off-target activation of stimulatory A_2 receptors (100,115). Collectively, our results indicate that our novel A_1R agonist **3a** has potent antinociceptive effects but minimal to no cardiovascular side effects when administered orally at a high 5000 nmol/kg dose. In contrast, the same high dose of CPA has antinociceptive effects and significant cardiovascular side effects. These data suggest that **3a** has a large therapeutic window, and uniquely lacks cardiovascular side-effects that are associated with other A_1R agonists like CPA.

Figure 3.4

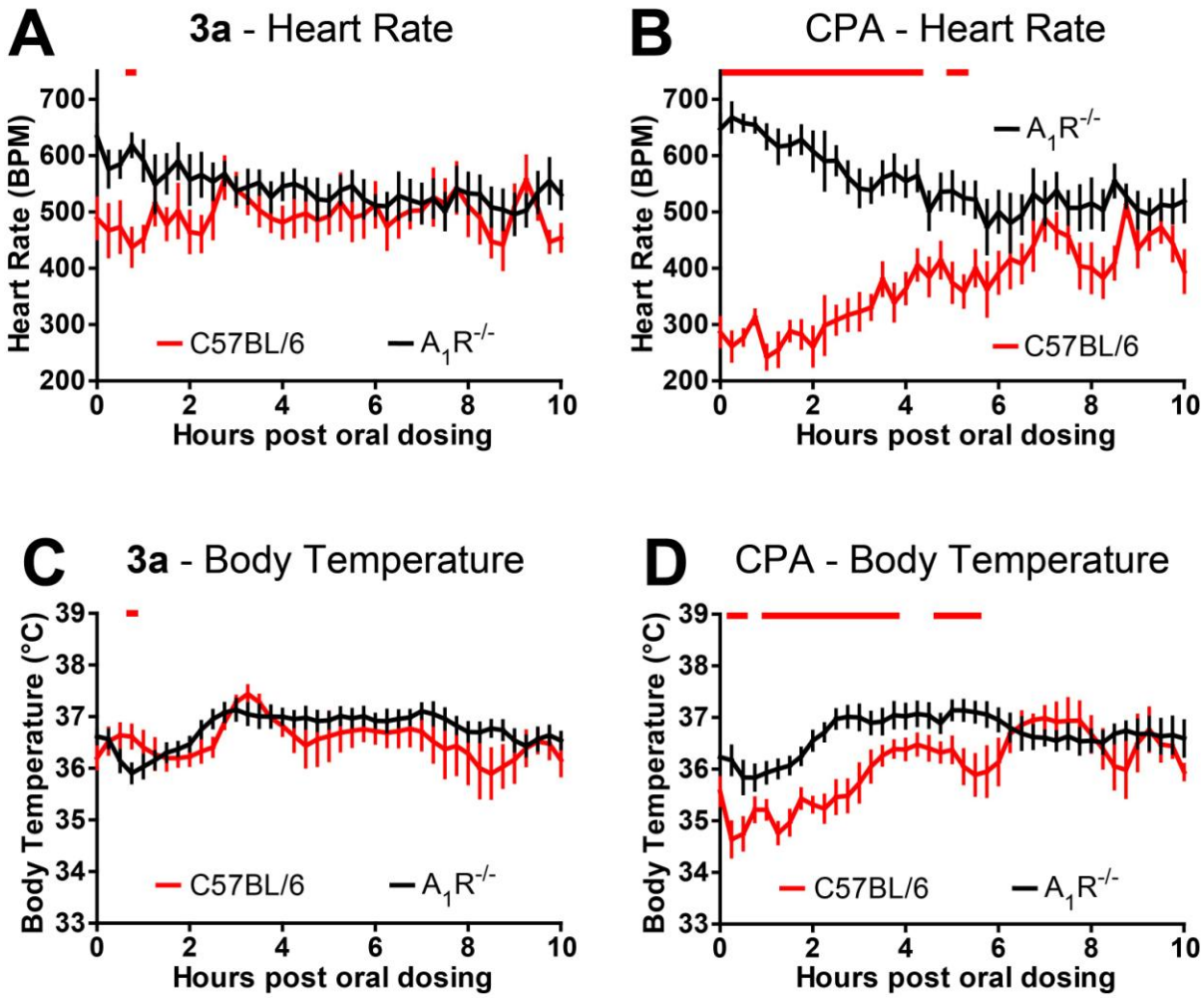
A
3a - Heart Rate
Heart Rate (BPM)
700
600
500
400
300
200
C57BL/6
A1R-/-
0
2
4
6
8
10
Hours post oral dosing
B
CPA - Heart Rate
Heart Rate (BPM)
A1R-/-
C57BL/6
Hours post oral dosing
C
3a - Body Temperature
Body Temperature (°C)
39
38
37
36
35
34
33
C57BL/6
A1R-/-
Hours post oral dosing
D
CPA - Body Temperature
Body Temperature (°C)
C57BL/6
A1R-/-
Hours post oral dosing

Figure 3.4. Compound 3a does not have long-lasting effects on heart rate or body temperature while CPA causes a significant decrease in heart rate and body temperature in wild-type mice.

A and C) Effects of **3a** on (A) heart rate and (C) body temperature in wild-type (*red*) and $A_1R^{-/-}$ (*black*) mice. B and D) Effects of CPA on (B) heart rate and (D) body temperature in wild-type (*red*) and $A_1R^{-/-}$ (*black*) mice. Compounds were orally administered at 5000 nmol/kg immediately before telemetry recording began. n = 8 C57BL/6 male mice per group for $A_1R^{-/-}$ body temperature measurements, 6 male mice per group for all other conditions.

DISCUSSION

We found that that the difference in AMP sensitivity between hA_1R and $hA_{2B}R$ is partially determined by the composition of extracellular loop 2, as replacement of EL2 in hA_1R with the EL2 from $hA_{2B}R$ caused a dramatic drop in both AMP potency and efficacy (Fig. 3.1C). Differences in ligand binding interactions are unlikely to mediate this effect, as no hA_1R-$hA_{2B}R$ divergent residues in EL2 interact with AMP while it is in the hA_1R binding pocket (based on our hA_1R homology model, derived from the crystal structure of $hA_{2A}R$). Rather, this effect is likely due to electrostatic repulsion, as the EL2 of $hA_{2B}R$ is more negatively charged than that of hA_1R (Fig. 3.1B), and AMP is a negatively charged ligand. Interestingly, replacement of EL1 instead of or in addition to EL2 had no effect on AMP potency or efficacy (Fig. 3.1C), despite the fact that EL1 and EL2 have the same net charge difference between hA_1R and $hA_{2B}R$ (Fig. 3.1B). This suggests that extracellular loop position is also critical in influencing AMP sensitivity. In our hA_1R homology model EL2 is located immediately outside of the agonist binding pocket (in fact, a conserved phenylalanine residue in EL2 forms a π-stacking interaction with the purine moiety of adenosine (11)), while the other extracellular portions of hA_1R are located farther away. We therefore propose that the negatively charged EL2 of $hA_{2B}R$ acts as a 'gatekeeper', restricting the access of anionic ligands (such as AMP) to the binding pocket, but allowing neutral ligands (such as adenosine) to pass freely.

Notably, the composition of EL2 is not responsible for the entire difference in AMP sensitivity between hA_1R and $hA_{2B}R$, as the EL2 and EL1,2 chimeric receptors retain some level of activity in response to AMP stimulation (Fig. 3.1C). The origin of this remaining AMP sensitivity is not known. One possibility is that the remaining sensitivity is determined

by the composition of the N-terminus, which was not mutated in our study. However, there is reason to believe that this is not the case. As mentioned above, in our hA_1R homology model, EL2 is located immediately outside the agonist binding pocket. Among the remaining extracellular portions of hA_1R, EL3 is located the closest to the binding pocket, EL1 is located at an intermediate distance, and the N-terminus is located at the greatest distance. Since mutation of EL1 had no effect on AMP sensitivity, it is unlikely that mutation of the N-terminus, which has the same net charge difference as EL1 (Fig. 3.1B) but is located farther from the agonist binding pocket, would have any significant effect. In a similar fashion, the composition of EL3 is likely not relevant, as although it is located relatively close to the agonist binding pocket, it is well-conserved and possesses an identical net charge in both hA_1R and $hA_{2B}R$ (Fig. 3.1B).

The other possibility is that AMP sensitivity is also partly due to differences in G protein coupling between A_1R and $A_{2B}R$. A_1R primarily couples to $G\alpha_i$, whereas $A_{2B}R$ primarily couples to $G\alpha_s$, although coupling to additional $G\alpha$ subunits has been described for both receptors (112,116-118). The characteristic G protein-coupling interfaces of hA_1R and $hA_{2B}R$ are determined by the sequences of the intracellular loops, which are divergent between the two receptors (Fig. 3.1A). Furthermore, AMP binds to the hA_1R binding pocket through an interaction with histidine 251, whereas adenosine does not (Fig. 2.11D). This unique binding interaction implies that the A_1 receptor adopts a distinct conformation upon the binding of each ligand. It is therefore possible that binding of AMP in the hA_1R binding pocket causes a conformational shift which is sufficient to cause full activation of $G\alpha_i$, but that this same conformational shift in $hA_{2B}R$ causes no or limited activation of $G\alpha_s$. Further investigation of this potential mechanism is warranted, but would entail mutagenesis of the

hA_1R intracellular loops. This would by definition change the coupling properties of the receptor, and likely necessitate the development of new downstream assays to measure receptor activity.

The recently-discovered phenomenon by which a single agonist, binding to a single GPCR, preferentially activates some downstream signaling pathways over others is known as functional selectivity (35,119). Although the concept was first recognized less than 10 years ago, the potential implications of functional selectivity on drug discovery has quickly led to a significant body of work on the subject. As such, functionally selective ligands have now been identified for multiple GPCRs (120-125), including the A_1 and A_3 adenosine receptors (112,126). However, the vast majority of such studies have focused on synthetic agonists, as opposed to biological signaling molecules.

Here, we have shown that the physiologically relevant nucleotide AMP is a functionally selective agonist at the human A_1 receptor. AMP is a full agonist (i.e. its maximal response is equivalent to that of adenosine) of $G\alpha_i$-coupled signaling through hA_1R (Fig. 2.6), but only a partial agonist (i.e. a saturating agonist concentration elicits a smaller response than a saturating concentration of adenosine) of $G\alpha_q$-coupled signaling through the same receptor (Fig. 3.2). This is not dependent on overexpression of $G\alpha_q$, as we also observed greater adenosine-evoked responses using endogenously expressed G proteins (Fig. 3.2 A,B; *green*). In fact, at endogenous levels of $G\alpha_q$ expression, AMP may not stimulate $G\alpha_q$-coupled signaling through hA_1R at all (Fig. 3.2 A,B; *orange*).

This effect is not caused by a deficiency in AMP binding to hA_1R, as AMP has comparable potency to adenosine, even via pathways for which it is only a partial agonist

(Fig. 3.2C). Rather, this effect is caused by deficient signal transduction between the intracellular face of hA_1R and its associated G protein. As discussed above, AMP and adenosine binding to hA_1R generates two unique receptor conformations, as AMP forms a unique interaction with at least one residue in the hA_1R binding pocket (Fig 2.11D). Our data indicate that the AMP-induced conformation strongly promotes activation of $G\alpha_i$, but only weakly promotes activation of $G\alpha_q$. In support of this mechanism, another hA_1R agonist with a bulky 5' substituent – the binding of which is therefore likely to cause a similar receptor conformation to that caused by the binding of AMP – also causes preferential activation of $G\alpha_i$ (112).

It is important to note that while adenosine is assumed to be a universal full agonist at A_1R, this may not necessarily be the case. There are other pathways activated downstream of A_1R through which adenosine and AMP have not been compared, including $G\alpha_s$-coupled and β-arrestin mediated signaling. It is possible that AMP is a more efficacious A_1R agonist than adenosine through another downstream effector. Indeed, the discovery of functional selectivity has largely made obsolete the simple concept of a 'full agonist', and our results underscore the necessity of measuring multiple pathways downstream of GPCR activation in order to obtain a more complete understanding of a given compound's true agonist activity.

We found that compound **3a** (Fig. 3.3A) has potent antinociceptive activity in mice when delivered by intrathecal injection (111), while AMP (Fig. 2.4A) does not. Although the basis for this difference in activity is not known, the structures of the two compounds are very similar. In fact, there are only three structural modifications between AMP and **3a** that could be responsible: **3a** is a dimethyl ester, rather than a charged phosphate, and it contains both a 2-chloro and an N^6-cyclopentyl group attached to the adenine moiety. It is unlikely

that the addition of the methyl groups – which eliminates both negative charges from the 5'-phosphate group – is responsible for **3a**'s activity, as elimination of even one negative charge from the 5'-phosphate (in the compound ACP, Fig. 2.4B), had a deleterious effect on efficacy at hA_1R (Fig. 2.6). Indeed, compound **3d** (Fig. 3.3B), which lacks these methyl groups, also has antinociceptive activity in mice (Coleman and Zylka, unpublished data).

The other set of modifications made to AMP to yield compound **3a** are the addition of 2-chloro and N^6-cyclopentyl groups. These groups were derived from the compound CCPA, an exceptionally potent (Fig. 2.6) and highly selective A_1R agonist (114). As the pain-relieving effects of adenosine agonists are A_1R-mediated (98), these 'CCPA-like' groups were added to some of our AMP analogues in an attempt to enhance A_1R activity (111). This effort was successful, as the 'CCPA-like' compounds **3a** and **3d** both displayed higher potency at hA_1R than adenosine in the calcium mobilization assay (Fig. 3.3C). Of these two substituents, the 2-chloro group appears to be less important, as another AMP analogue similar to **3a** but lacking the 2-chloro group also had antinociceptive activity via intrathecal injection (Coleman and Zylka, unpublished data). Thus, it appears that the N^6-cyclopentyl ring is the critical structural component conveying *in vivo* antinociceptive activity to the AMP scaffold.

Furthermore, we found that oral administration of compound **3a** (Fig. 3.4 A,C) did not cause the cardiovascular side effects characteristic of A_1R agonists (Fig. 3.4 B,D; CPA used as representative A_1R agonist). This difference in side effect profile was unexpected, as depression of heart rate and body temperature is A_1R-mediated (Fig. 3.4 B,D; compare wild-type C57BL/6, *red*, to $A_1R^{-/-}$, *black*), and **3a** is a potent A_1R agonist (Fig 3.3C) (111). Interestingly, intracerebroventricular injection of an A_1R agonist was recently shown to

severely depress heart rate and body temperature in rats (127), suggesting that the cardiovascular effects of A_1R agonists are at least partially mediated by the central nervous system (CNS). Since **3a** was administered orally in this experiment, this raises the possibility that **3a** may lack cardiovascular side effects because it cannot cross the blood-brain barrier and access the CNS. However, A_1R agonists also have direct inhibitory effects on the heart itself. Thus, the lack of cardiovascular effects may be caused by differential signaling downstream of A_1R, as **3a** has only been evaluated in $G\alpha_i$-coupled assays of A_1R activity.

The other problem that has plagued A_1R agonists in the clinic – the rapid development of tolerance due to A_1 receptor desensitization (98) – has not been evaluated using AMP-derived agonists. GPCR desensitization is largely mediated by β-arrestin signaling (128), which is activated in a distinct fashion from G protein-mediated signaling (21). Once again, this suggests that differential activation of multiple downstream signaling pathways may be critical in determining if AMP-derived A_1R agonists realize their therapeutic potential. The ideal A_1R-mediated pain therapeutic will need to be CNS-impermeable – to avoid cardiovascular side effects as much as possible, although specific activation of antinociceptive A_1 receptors over those in the heart may prove to be an impossible task, at least with systemic drug administration – and functionally selective towards G protein signaling over β-arrestin signaling, to avoid the development of tolerance. Thus, whether focusing on **3a**, other AMP analogues, or structurally unrelated A_1R agonists, additional work is needed to determine if these compounds are CNS-penetrant and to fully characterize their A_1R agonist activity.

CHAPTER 4: OVEREXPRESSION OF DIACYLGLYCEROL KINASE ETA PROLONGS GPCR SIGNALING

INTRODUCTION

Diacylglycerol kinases (DGKs) are a large family of enzymes that catalyze the phosphorylation of the membrane lipid diacylglycerol (DAG) to phosphatidic acid (PA) (129,130). Both DAG and PA are important second messengers and regulate diverse proteins and pathways, including protein kinase C (PKC) (30,131), ion channels (132), endocannabinoid production (133), and phosphatidylinositide synthesis (134). Thus, by affecting the levels of DAG and PA, DGKs are well positioned to regulate diverse intracellular signaling pathways (135).

In recent years, a number of studies have identified genetic associations between *DGKH* and bipolar disorder (BPD) (136-141). *DGKH* is the gene that encodes diacylglycerol kinase eta (DGKη). Moreover, Moya and colleagues found that DGKη mRNA was expressed at higher levels in post-mortem tissue samples from patients with BPD than unaffected controls (142). DGKη is a Type II DGK isoform with two known splice variants (143-145), and was recently implicated in lung cancer (146). However, how alterations in DGKη levels might affect cellular functions or contribute to BPD pathogenesis is currently unknown.

Dysregulation of G protein-coupled receptor (GPCR) activity is involved in the pathology of many psychiatric disorders, including BPD (147). Indeed, tissues from BPD patients exhibit changes in GPCR (148) and G protein subunit (149,150) expression, enhanced receptor-G protein coupling (151), and decreased expression of a GPCR-regulating kinase (150). Furthermore, therapeutic concentrations of lithium and valproate, common treatments of BPD, inhibit G protein activation after GPCR stimulation in cell membranes (152) and platelets from bipolar patients (153).

Given that DGKη is expressed at higher levels in BPD patients and has the potential to affect GPCR signaling, we sought to determine if overexpression of DGKη affected GPCR signaling in HEK293 cells, a model cell line with well-characterized GPCR signaling cascades (154). Here, we found that overexpression of DGKη dramatically prolonged the duration of calcium responses after stimulating endogenous $G\alpha_q$-coupled GPCRs. This DGKη-mediated effect was dependent on DGKη catalytic activity and was abolished after depleting multiple PKC isoforms. Taken together, our data indicate that DGKη prolongs GPCR signaling by attenuating PKC activity and suggest this occurs by attenuating PKC-dependent receptor desensitization.

MATERIALS AND METHODS

Materials

Carbamoylcholine chloride (carbachol, C4382), D-sorbitol (S1876), n-butanol (B7906), ethylenediaminetetraacetic acid (EDTA, EDS), phenylmethanesulfonyl fluoride (PMSF, P7626), sodium fluoride (201154), DL-dithiothreitol (DTT, D0632), sodium deoxycholate (D6750), adenosine 5'-triphosphate disodium salt (ATP, A7699), HEPES sodium salt (H7006), glycerol (G7893), sodium pyrophosphate (P8135), Dulbecco's phosphate buffered saline (PBS, D8537), and fatty acid-free BSA (A6003) were purchased from Sigma-Aldrich. Concentrated hydrochloric acid (A144SI), Tris hydrochloride (Tris-HCl, BP153), sodium chloride (NaCl, BP358), magnesium chloride hexahydrate ($MgCl_2$, BP214), Triton X-100 (BP151), Tween 20 (BP337), and D-glucose (D16) were purchased from Fisher Scientific. Nonidet P40 substitute was acquired from USB Corporation (NP40, 19628). [γ-^{32}P]-labeled ATP (6000 Ci/mmol, 150 mCi/ml) was obtained from Perkin Elmer (NEG035C005MC).

Molecular Biology

A full-length clone of mouse DGKη isoform 1 was generated by PCR amplification using cDNA from C57BL/6 mouse neurons as a template (bases 1-3471 from GenBank accession #NM_001081336.1) (143). The initial clone was found to be unstable due to high GC content at the 5' end of the DGKη coding sequence. To remedy this problem, the first 70 bases of the DGKη coding sequence were modified to decrease GC content while preserving the wild-type (WT) DGKη amino acid sequence (native sequence: ATGGCCGGGG

CCGGCAGCCA GCACCACCCT CAGGGCGTCG CGGGAGGAGC GGTCGCTGGG GCCAGCGCGG; modified sequence: ATGGCAGGAG CAGGAAGTCA GCATCATCCT CAGGGAGTTG CAGGAGGAGC AGTTGCAGGA GCAACTGCAG). The resulting construct was stable and was used to generate all subsequent constructs. DGKη truncation constructs were generated by PCR amplification. The G389D point mutant was generated by traditional PCR-based mutagenesis. Full-length DGKη and all DGKη constructs were inserted into the multiple cloning site of pcDNA 3.1(+) downstream of monomeric RFP lacking a stop codon, to create fusion constructs with N-terminal RFP tags. A DGKη-646Δ fusion construct with an N-terminal Venus tag was generated in the same fashion. All constructs contained a Kozak consensus sequence and were sequence verified.

Cell Culture

HEK293 cells were grown in Dulbecco's modified Eagle's medium (DMEM; Gibco, 11995) containing 10% fetal bovine serum, 100 U/ml penicillin, and 100 µg/ml streptomycin at 37°C and 5% CO_2. Cells were plated on polylysine-coated glass-bottom dishes (MatTek, P35G-0-10-C) for calcium imaging, polylysine-coated glass coverslips (Brain Research Laboratories, 2222) for immunostaining, and polylysine-coated 6-well plates (Corning, 3516) for all other experiments. Twenty-four hours after plating, cells were transfected with Lipofectamine/Plus (Invitrogen) in serum-free DMEM according to the manufacturer's instructions. Each plate/well was transfected with 500 ng of each DNA construct, and the total amount of DNA per transfection was normalized to 1 µg with empty vector. After 4 hours, the transfection medium was replaced with fresh growth medium. To deplete PKC

isoforms, cells were treated overnight with 300 nM phorbol 12-myristate 13-acetate (PMA; Sigma, P8139) in growth medium (155). All experiments except those measuring ERK phosphorylation were performed 24 hours after transfection. For experiments measuring ERK phosphorylation, 24 hours after transfection, the growth medium was replaced with serum-free DMEM and cultured for an additional 24 hours.

Calcium Imaging

Calcium imaging was performed as described previously (110). Briefly, HEK293 cells expressing various DGKη constructs and controls were washed twice in HBSS assay buffer (Invitrogen #14025, supplemented with 9 mM HEPES, 11 mM D-glucose, and 0.1% fatty acid-free BSA, pH 7.3) and loaded with 2 μM Fura-2 AM (Invitrogen, F-1221) in 0.02% Pluronic F-127 (Invitrogen, P3000-MP) in assay buffer for 1 hour at room temperature. Cells were then washed three times in assay buffer, incubated at room temperature for 30 minutes, and imaged on a Nikon Eclipse Ti microscope. A Sutter DG-4 light source and Andor Clara CCD camera were used to image calcium responses. 500-ms excitation at 340 nm and 250-ms excitation at 380 nm was used for all experiments. Fura-2 emission was measured at 510 nm.

Fresh assay buffer was added prior to each experiment. After 40 seconds of baseline imaging, the assay buffer was aspirated and agonist solution was added. All solutions were aspirated and pipetted manually. For experiments involving overnight treatment with PMA, 300 nM PMA was present in all loading and wash solutions. Only cells that expressed visible RFP fluorescence, had low baseline Fura-2 ratios (< 0.6), and responded to agonist

stimulation (Fura-2 ratio > 0.8 at any time after agonist addition) were analyzed. For experiments using cells transfected with RFP-DGKη-Δ645 and Venus-DGKη-646Δ, only cells expressing both visible RFP fluorescence and visible Venus fluorescence were analyzed. Real-time response profiles and area under curve (AUC) values were generated as described previously (110). To control for day-to-day variation in calcium responses, control cells expressing RFP alone were tested as part of each experiment. AUC values were then normalized such that RFP alone was set at a value of 1.

Confocal Microscopy

HEK293 cells expressing RFP-DGKη were washed twice in HBSS assay buffer and imaged using a Yokogawa CSU-10 spinning disc confocal scanner mounted on a Nikon TE2000 microscope. An Argon/Krypton laser light source and a Hamamatsu Orca-ER camera were used to image RFP-tagged DGKη. After approximately 1 minute of baseline imaging, assay buffer was replaced with buffer containing 10 μM carbachol or 500 mM sorbitol, and imaging continued for an additional 15 minutes. Solutions were removed and added by manual pipetting.

Immunostaining

HEK293 cells expressing RFP were incubated in PBS alone or 300 nM PMA in PBS for 10 minutes at 37°C then fixed in ice-cold 4% paraformaldehyde (Fisher, T353) for 15 minutes. After incubating in 0.5% Triton X-100 in PBS for 15 minutes, coverslips were

blocked for 30 minutes in blocking solution [0.1% Triton X-100 and 5% normal goat serum (Invitrogen, PCN5000) in PBS] then incubated with Rabbit anti-PKCδ primary antibody (Santa Cruz Biotechnology, sc-937) in blocking solution overnight at 4°C. Cells were then washed with 10% goat serum in PBS for 30 minutes and incubated in Alexa Fluor 488-conjugated Goat anti-Rabbit secondary antibody (Invitrogen, A11008) and DRAQ5 nuclear dye (Cell Signaling, 4084S) in blocking solution for 1 hour at room temperature. Cells were washed three times (5 minutes/wash) with PBS between each step. Coverslips were mounted onto microscope slides (Fisher, 12-550-143) with Fluoro-Gel (Electron Microscopy Sciences, 17985-10) and stored at 4°C until imaging. Slides were imaged the following day on a Zeiss LSM 510 microscope, with Multiline Argon and Helium-Neon laser light sources and a 63x objective.

Phospho-ERK Western Blotting

HEK293 cells expressing RFP alone or RFP-DGKη were cultured overnight in serum-free growth medium, then incubated with agonist (or vehicle) in serum-free growth medium for 5 minutes at 37°C. Cells were then quickly washed with ice-cold PBS, and phosphoprotein lysis buffer was added [20 mM HEPES pH 7.4, 150 mM NaCl, 10 mM EDTA, 3 mM sodium pyrophosphate, 1% Triton X-100, 1x Complete Mini protease inhibitor cocktail (Roche, 11 836 153 001), 1x Phosphatase Inhibitor Cocktail 2 (Sigma, P5726)]. After buffer addition, cells were frozen at -80°C and left overnight. The lysed cells were thawed on ice and collected, and the lysates were clarified by centrifugation at 10,000g for

15 minutes at 4°C. Protein content of the clarified lysates was measured using a BCA assay kit (Thermo, 23227) according to the manufacturer's instructions.

A portion (20 µg) of each lysate was heated at 94°C for 5 minutes with an appropriate amount of 4x Laemmli sample buffer, and separated by SDS-PAGE on a 4-15% gradient gel (Bio-Rad, 456-1083) at 100 V for 1 hour. Proteins were transferred to a PVDF membrane (Bio-Rad, 162-0174) at 100 V for 70 minutes on ice, and blocked with 5% nonfat milk (Bio-Rad, 170-6404) in TBST (100 mM Tris-HCl pH 7.5, 165 mM NaCl, 0.1% Tween 20) for 1 hour at room temperature. Blots were then incubated with Rabbit anti-phospho-ERK (Cell Signaling, 4370S) or anti-total-ERK (Cell Signaling, 4695S) primary antibodies in 5% BSA (Sigma, A3912) in TBST overnight at 4°C. The following day, blots were washed three times (5 minutes/wash) with TBST and incubated with IRDye800-conjugated Donkey anti-Rabbit secondary antibody (LI-COR, 926-32213) in 5% nonfat milk/TBST for 1.5 hours at room temperature. Blots were then washed three times (5 minutes/wash) with TBST and imaged on a LI-COR Odyssey CLx infrared imaging system. Phospho-ERK and total-ERK blots were imaged simultaneously under identical conditions. Band intensity was quantified using ImageJ image analysis software (National Institutes of Health).

Co-immunoprecipitation

HEK293 cells expressing tagged DGKη truncation constructs or fluorescent tags alone were washed twice with ice-cold PBS and scraped into glycerol-Co-IP buffer containing 50 mM HEPES pH 7.4, 250 mM NaCl, 2 mM EDTA, 10% (v/v) glycerol, 0.5% (v/v) NP40, 1x protease inhibitor cocktail, and 1x phosphatase inhibitor cocktail. Cellular

debris was removed by centrifugation at 10,000g for 10 minutes at 4°C and input aliquots of the clarified lysate were set aside. The remaining lysate was then incubated with Chicken anti-GFP primary antibody (Aves Labs, GFP-1020) or normal Chicken IgY control (Santa Cruz, sc-2718) for 3 hours at 4°C with gentle mixing. Agarose beads coupled to Goat anti-Chicken IgY (Aves, P-1010) were then added to each sample and incubated for 1 hour at 4°C. The beads were washed four times (5 minutes/wash) with ice-cold glycerol Co-IP buffer, and bound proteins were eluted from the beads by incubation with Laemmli sample buffer for 15 minutes at 37°C. Input and IP fractions were then separated by SDS-PAGE, transferred to PVDF membrane, and blotted as described above, using Rabbit anti-RFP primary antibody (Invitrogen, R10367). After imaging, blots were re-probed with Rabbit anti-GFP primary antibody (Invitrogen, A11122) to determine the specificity of the precipitation. Samples containing RFP alone were heated for 5 minutes at 94°C before SDS-PAGE; samples containing RFP-DGKη constructs were not heated, because we found that DGKη protein and DGKη truncation constructs were undetectable on western blots when heated at 94°C.

In-vitro Kinase Assay

The DGK in vitro kinase assay was adapted from previous studies (156,157). HEK293 cells expressing RFP-tagged DGKη (WT or truncation constructs) or RFP alone were washed twice with ice cold PBS and scraped into lysis buffer (50 mM Tris-HCl pH 7.5, 150 mM NaCl, 1 mM EDTA, 1 mM PMSF, 1x protease inhibitor cocktail, 1x phosphatase

inhibitor cocktail). Cells were disrupted by brief sonication on ice, and debris was collected by centrifugation at 10,000g for 10 minutes at 4°C. Clarified lysates were kept on ice.

The final reaction mixture contained 50 mM Tris-HCl pH 7.4, 100 mM NaCl, 20 mM NaF, 10 mM $MgCl_2$, 1 mM DTT, 1 mM EDTA, 1 mM sodium deoxycholate, 0.5 mM DAG (8:0, 12:0, or 18:1), 1 mM [γ-^{32}P]ATP (50 µCi/rxn), and lysate; reaction volume was 50 µl. A calculated amount of 1,2-dioctanoyl-glycerol (8:0 DAG), 1,2-dilauroyl-glycerol (12:0 DAG), or 1,2-dioleoyl-glycerol (18:1 DAG) in chloroform (Avanti Polar Lipids; 800800C, 800812C, and 800811C respectively) was deposited in a glass tube under a stream of dry nitrogen gas. The DAG was then resuspended in an appropriate amount of 5x kinase buffer (250 mM Tris-HCl pH 7.4, 500 mM NaCl, 100 mM NaF, 50 mM $MgCl_2$, 5 mM DTT, 5 mM EDTA) and 10 mM sodium deoxycholate by brief bath sonication. 15 µl of the DAG suspension was added to a tube containing 20 µl of water, followed by 5 µl of 10 mM [γ-^{32}P]ATP. The reaction was initiated by adding 10 µl of lysate, incubated for 3 minutes at 30°C, and then stopped by adding 25 µl of 12 N HCl followed by 750 µl of water saturated with n-butanol. Lipids were extracted from the reaction mixture by adding 500 µl of n-butanol, mixing thoroughly, and separating by centrifugation at 1,000g for 5 minutes. 450 µl of the organic phase was washed with 500 µl of n-butanol-saturated water and separated by centrifugation, with care taken not to disturb the aqueous phase. 350 µl of this organic phase was then washed again in the same fashion. Finally, 250 µl of the washed organic phase was transferred to a scintillation vial containing 2 ml of ScintiSafe Econo 2 (Fisher, SX21-5) scintillation fluid, mixed gently, and counted on a LKB Wallac Rackbeta 1209 liquid scintillation counter.

For experiments comparing different DGKη truncation constructs, 15 µl of each lysate sample used in the in-vitro kinase assay was analyzed by western blotting with Rabbit anti-RFP antibody as described above, and the band intensity was quantified. The DGKη activity data were corrected for differences in expression, and normalized such that RFP alone was set at a value of 0, and wild-type DGKη was set at a value of 1.

RESULTS

Mouse DGKη phosphorylates multiple DAG substrates

First, we set out to evaluate whether mouse DGKη isoform 1 was catalytically active (Fig. 4.1A shows domain structure of isoform 1). To accomplish this, we transfected HEK293 cells with RFP-tagged DGKη or RFP only (control) expression constructs. One day later, we prepared cell lysates, incubated these lysates with purified DAG substrates and [γ-^{32}P]ATP, then monitored ^{32}P-labeled phosphatadic acid (PA) formation (Fig. 4.1B). This in vitro assay was previously used to monitor DGK activity (156,157). We found that kinase reactions containing RFP-DGKη produced significantly more ^{32}P-PA than reactions containing RFP alone (Fig. 4.1C) when 500 μM dioctanoyl (8:0), dilauroyl (12:0), or dioleoyl (18:1) glycerol was used as substrate. Given that mouse DGKη could phosphorylate multiple DAG substrates, and that 18:1 DAG was previously used to characterize human DGKη and other DGK isoforms (143), we elected to use 18:1 DAG for subsequent experiments. The K_m of DGKη for 18:1 DAG was 18.4 μM (Fig. 4.1D), justifying our use of a saturating 500 μM DAG concentration for subsequent in vitro kinase reactions.

DGKη prolongs intracellular calcium mobilization after GPCR stimulation

Since DGKη is expressed at higher levels in patients with bipolar disorder (142), we next sought to determine if overexpression of DGKη affects endogenous GPCR signaling. We focused our research on HEK293 cells because they endogenously express the M_3 muscarinic acetylcholine receptor, a $G\alpha_q$-coupled GPCR that mobilizes intracellular calcium following stimulation with carbachol (154). Moreover, M_3 receptor desensitization and

downstream signaling pathways have been extensively studied (154,158-162). After stimulating with 10 μM carbachol, we found that the calcium mobilization response was dramatically prolonged in HEK293 cells expressing RFP-DGKη compared to RFP alone (Fig. 4.1E). Based on quantifying the area under the curve (AUC), the carbachol-evoked calcium response in RFP-DGKη-expressing cells was 80% greater than in cells expressing RFP alone ($p < 0.0005$). The N-terminal RFP tag did not affect DGKη activity, as untagged DGKη, HA-DGKη, and DGKη-mCherry also prolonged carbachol-evoked calcium responses (data not shown; we identified cells with untagged or HA-tagged DGKη by co-transfecting with Venus, a yellow fluorescent protein).

We next investigated whether DGKη could prolong calcium mobilization downstream of other $G\alpha_q$-coupled GPCRs. To accomplish this, we stimulated HEK293 cells with 10 μM ATP, which elicits intracellular calcium mobilization by activating endogenous P2Y receptors (110). We found that HEK293 cells expressing RFP-DGKη exhibited dramatically prolonged ATP-evoked calcium responses compared to cells expressing RFP alone (Fig. 4.1F). When quantified by AUC, ATP-evoked calcium responses in RFP-DGKη-expressing cells were 81% greater than responses in cells expressing RFP alone ($p < 0.005$). These data indicate that overexpression of DGKη can enhance calcium responses downstream of two different GPCRs. Since calcium mobilization was more pronounced (longer duration) following endogenous M_3 receptor activation, we focused the remainder of our experiments on DGKη modulation of M_3 receptor activation.

Figure 4.1

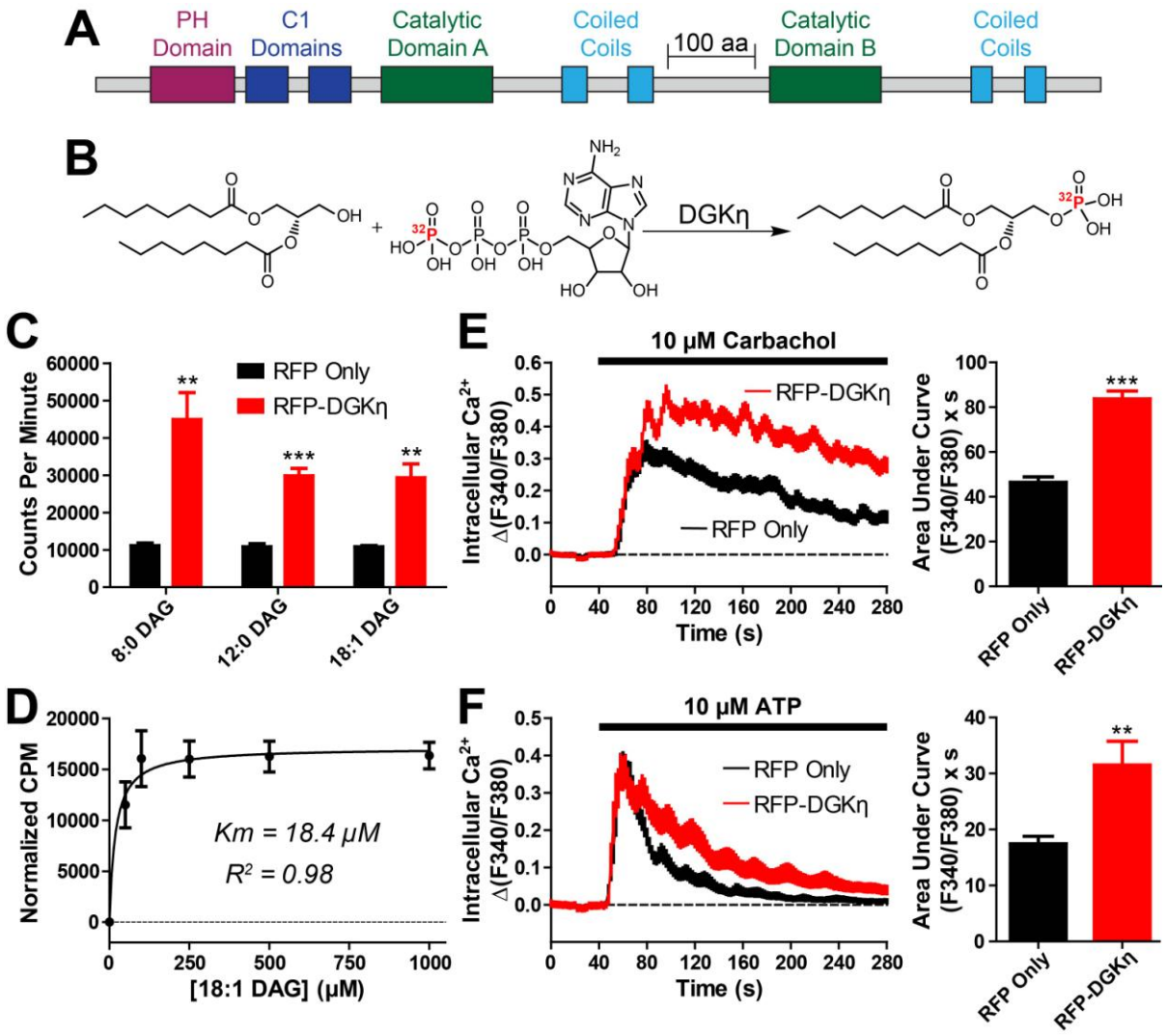
A
PH Domain
C1 Domains
Catalytic Domain A
Coiled Coils
100 aa
Catalytic Domain B
Coiled Coils
B
DGKη
C
Counts Per Minute
RFP Only
RFP-DGKη
8:0 DAG
12:0 DAG
18:1 DAG
D
Normalized CPM
Km = 18.4 μM
R² = 0.98
[18:1 DAG] (μM)
E
10 μM Carbachol
Intracellular Ca2+ Δ(F340/F380)
Time (s)
Area Under Curve (F340/F380) x s
F
10 μM ATP

Figure 4.1. Mouse DGKη is catalytically active and prolongs GPCR signaling.

A) Domain architecture of DGKη. PH = Pleckstrin Homology. C1 = PKC homology domain 1. aa = amino acid. B) Schematic of the reaction forming ^{32}P-labeled PA from DAG and radiolabeled ATP. C) Full-length mouse RFP-DGKη is catalytically active. Lysates from HEK293 cells expressing (*black*) RFP alone or (*red*) RFP-DGKη were incubated with the indicated DAG substrates, each at 500 μM. D) ^{32}P-PA production from reactions containing the indicated concentrations of 18:1 DAG, catalyzed by lysates from HEK293 cells expressing RFP-DGKη. Data were normalized to the signal in the absence of DAG substrate and fit to a Michaelis-Menton curve. E and F) Calcium mobilization in HEK293 cells expressing (*black*) RFP alone or (*red*) RFP-DGKη after stimulation with (E) 10 μM carbachol or (F) 10 μM ATP. AUC measurements extended for 4 minutes from agonist addition. Data in C and D are the average of two experiments performed in duplicate. Data in E and F are the average of three independent experiments; n = 41-104 cells per condition. Paired t tests were used to compare data. **, $p < 0.005$; ***, $p < 0.0005$. All data, including calcium traces, are presented as means ± standard error.

DGKη catalytic activity is required to prolong carbachol-evoked calcium mobilization

DGKη, like all type II DGK isoforms, possesses a split catalytic domain (130). To determine if DGKη catalytic activity was required to prolong carbachol-evoked calcium mobilization, we generated two DGKη deletion constructs, DGKη-Δ645 and DGKη-646Δ, each containing one half of the catalytic domain (Fig. 4.2A). We also generated DGKη-G389D, containing a point mutation that is predicted to abolish ATP binding based on homology to other DGK proteins (163). We found that DGKη-Δ645, DGKη-646Δ and DGKη-G389D were expressed (Fig. 4.3, Fig. 4.2E) but were catalytically inactive, as they generated no more ^{32}P-PA than lysates containing RFP alone (Fig. 4.2B). In contrast, lysates from cells co-expressing DGKη-Δ645 and DGKη-646Δ displayed specific activity approximately 32% of that of wild-type (WT) RFP-DGKη (Fig. 4.2B), suggesting the two halves directly interact. Indeed, we found that RFP-DGKη-Δ645 co-immunoprecipitated with Venus-DGKη-646Δ (Fig. 4.2C). This interaction was specific to DGKη-Δ645 and DGKη-646Δ and did not involve the fluorescent tags or non-specific binding to the immunoprecipitation beads, as evidenced by controls showing no interaction when either construct was replaced with a fluorescent protein alone or when the anti-GFP antibody was replaced with an IgY control (Fig. 4.2C).

Additionally, none of these catalytically dead constructs (DGKη-Δ645, DGKη-646Δ or DGKη-G389D) prolonged calcium mobilization after carbachol stimulation (Fig. 4.2D). Cells expressing DGKη-646Δ alone appeared unhealthy and displayed a slight reduction in calcium mobilization. In contrast, co-expression of each half of DGKη (RFP-tagged DGKη-Δ645 and Venus-tagged DGKη-646Δ) increased calcium mobilization by 62% (based on

AUC measurement, Fig. 4.2D). Our data clearly indicate that DGKη catalytic activity is required to prolong carbachol-evoked calcium mobilization.

We also tested the catalytic activity of several DGKη truncation mutants lacking structural domains (Fig. 4.4A). We found that the PH domain and C-terminal tail negatively regulated DGKη catalytic activity and that the C1 domains were required for catalytic activity (Fig. 4.4 B,D). Furthermore, catalytic activity closely correlated with the ability to prolong carbachol-evoked calcium mobilization (Fig. 4.4C).

We next analyzed calcium mobilization AUC data on a cell-by-cell basis, to determine if the expression level of DGKη correlated with how effectively DGKη prolonged calcium mobilization responses. Notably, there was no relationship between the level of DGKη expression and the extent of calcium mobilization in cells expressing WT DGKη or kinase-dead DGKη-G389D (Fig. 4.2E). There was also no significant difference in the expression level of WT DGKη and DGKη-G389D across individual cells. Similarly, no correlation between DGKη expression and calcium mobilization was observed for any of the DGKη truncation constructs (Figs. 4.3 & 4.4; data not shown). Taken together, these data suggest that the amount of DGKη required to maximally prolong carbachol-evoked calcium mobilization is very small, perhaps because only a small amount of DAG substrate is generated upon M_3 receptor activation. In support of this possibility, we did not detect an increase in DAG levels after activating the endogenous M_3 receptor with carbachol (with a sensitive DAG biosensor—Upward DAG2, data not shown) (164).

Figure 4.2

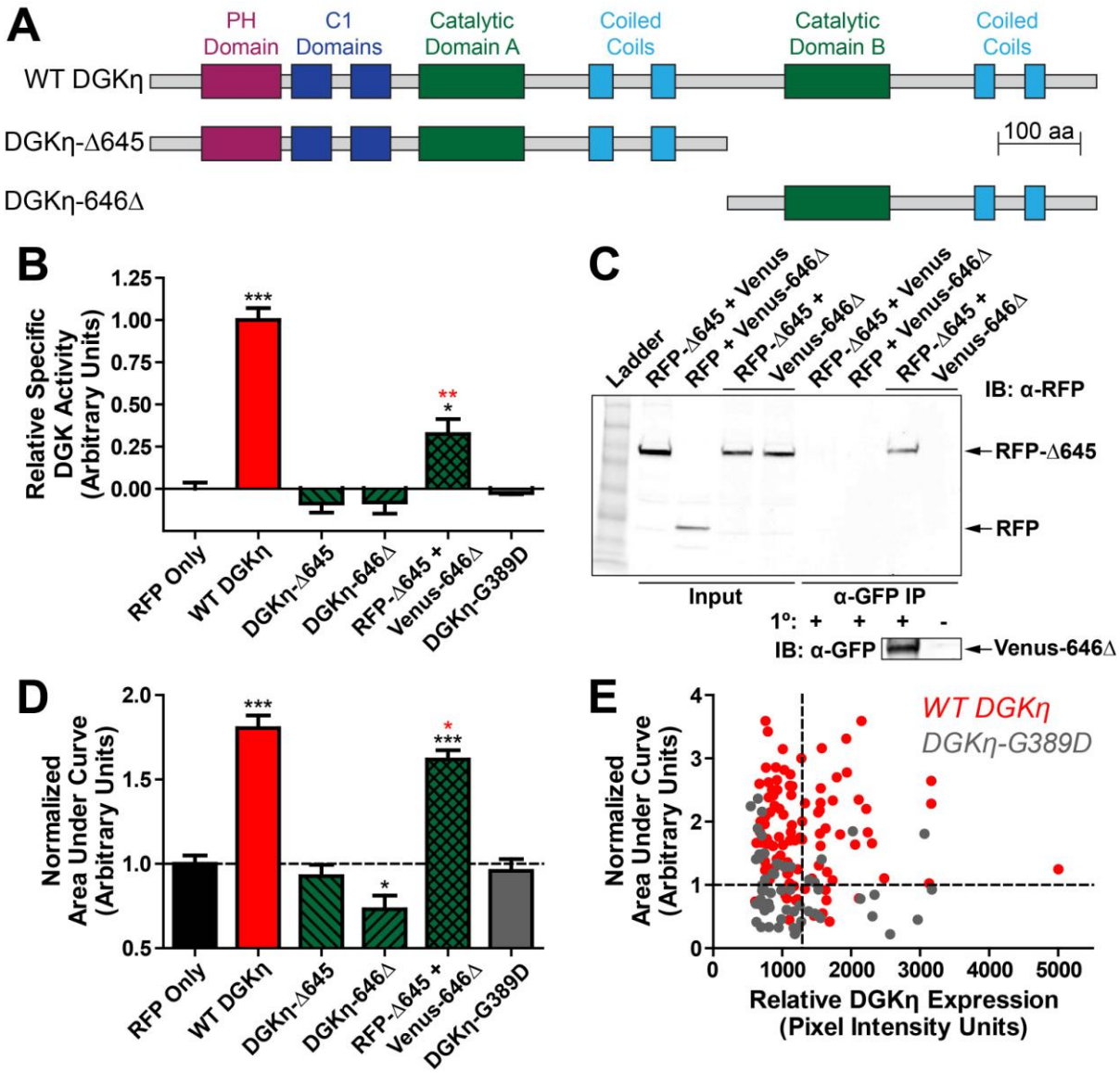
A
PH Domain
C1 Domains
Catalytic Domain A
Coiled Coils
Catalytic Domain B
Coiled Coils
WT DGKη
DGKη-Δ645
DGKη-646Δ
100 aa
B
Relative Specific DGK Activity (Arbitrary Units)
1.25
1.00
0.75
0.50
0.25
0.00
***
**
*
RFP Only
WT DGKη
DGKη-Δ645
DGKη-646Δ
RFP-Δ645 + Venus-646Δ
DGKη-G389D
C
Ladder
RFP-Δ645 + Venus
RFP + Venus-646Δ
RFP-Δ645 + Venus-646Δ
IB: α-RFP
RFP-Δ645
RFP
Input
α-GFP IP
1°: + + + -
IB: α-GFP
Venus-646Δ
D
Normalized Area Under Curve (Arbitrary Units)
2.0
1.5
1.0
0.5
***
*
***
*
E
Normalized Area Under Curve (Arbitrary Units)
WT DGKη
DGKη-G389D
0
1000
2000
3000
4000
5000
Relative DGKη Expression (Pixel Intensity Units)

Figure 4.2. DGKη catalytic activity is required to prolong GPCR signaling.

A) Structure of the DGKη truncation constructs used. DGKη-G389D contains a point mutation in catalytic domain A (not shown). All DGKη constructs were N-terminally tagged with RFP unless otherwise noted. B) Production of ^{32}P-PA in reactions containing lysates from HEK293 cells expressing the indicated DGKη constructs, using 500 μM 18:1 DAG as substrate. Data were normalized to DGKη expression, which was assessed by western blotting against RFP, then normalized so that RFP alone = 0 and WT DGKη = 1. Data are the average of two experiments performed in duplicate. C) N- and C-terminal halves of DGKη interact. Lysates from HEK293 cells expressing RFP-tagged DGKη-Δ645 and Venus-tagged DGKη-646Δ or fluorescent protein controls were immunoprecipitated using an anti-GFP antibody or an IgY control. Input and precipitated fractions were then run on SDS-PAGE and blotted using an anti-RFP antibody. The blot was later re-probed with an anti-GFP antibody to verify the specificity of the immunoprecipitation. D) AUC measurements of calcium mobilization in HEK293 cells expressing the indicated DGKη constructs after stimulation with 10 μM carbachol, normalized such that RFP alone = 1. AUC data for the RFP and WT DGKη conditions is also presented, in non-normalized form, in Fig. 4.1E. Data are the average of three to six independent experiments. n = 58-162 cells per condition, except DGKη-646Δ, where n = 23. E) Scatter plot comparing calcium mobilization AUC measurements to DGKη expression levels in individual HEK293 cells expressing (*red*) WT DGKη or (*gray*) DGKη-G389D. Horizontal dashed line indicates average level of calcium mobilization in HEK293 cells expressing RFP alone. Vertical dashed line indicates average expression level of WT DGKη. Paired t tests were used to compare data. *Black asterisks* indicate a statistically significant difference when compared

with RFP alone. *Red asterisks* indicate a statistically significant difference when compared to WT DGKη. *, $p < 0.05$; **, $p < 0.005$; ***, $p < 0.0005$. All data are presented as means ± standard error.

Figure 4.3

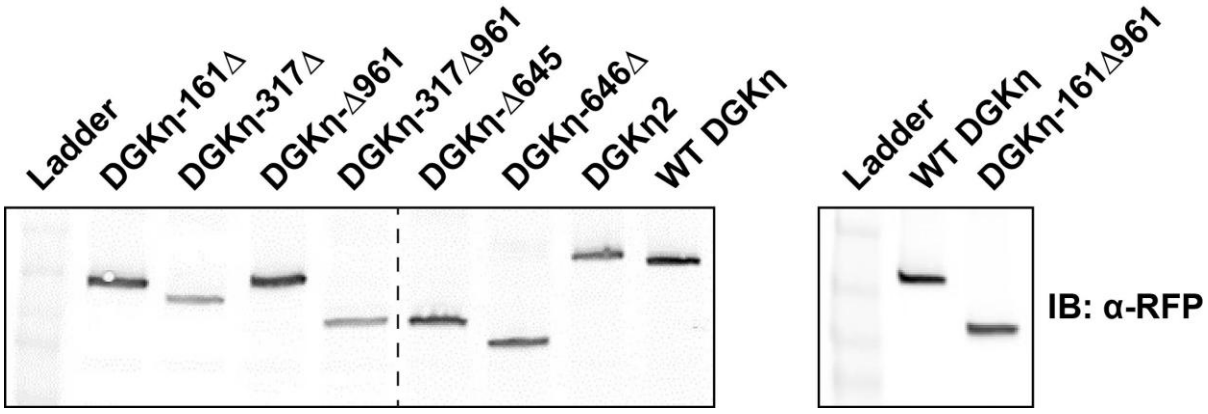
Ladder
DGKη-161Δ
DGKη-317Δ
DGKη-Δ961
DGKη-317Δ961
DGKη-Δ645
DGKη-646Δ
DGKη2
WT DGKη
Ladder
WT DGKη
DGKη-161Δ961
IB: α-RFP

Figure 4.3. Expression of DGKη truncation constructs in HEK293 cells.

HEK293 cells expressing the indicated DGKη constructs were lysed and western blotted using an anti-RFP antibody. All DGKη constructs were N-terminally tagged with RFP.

Figure 4.4

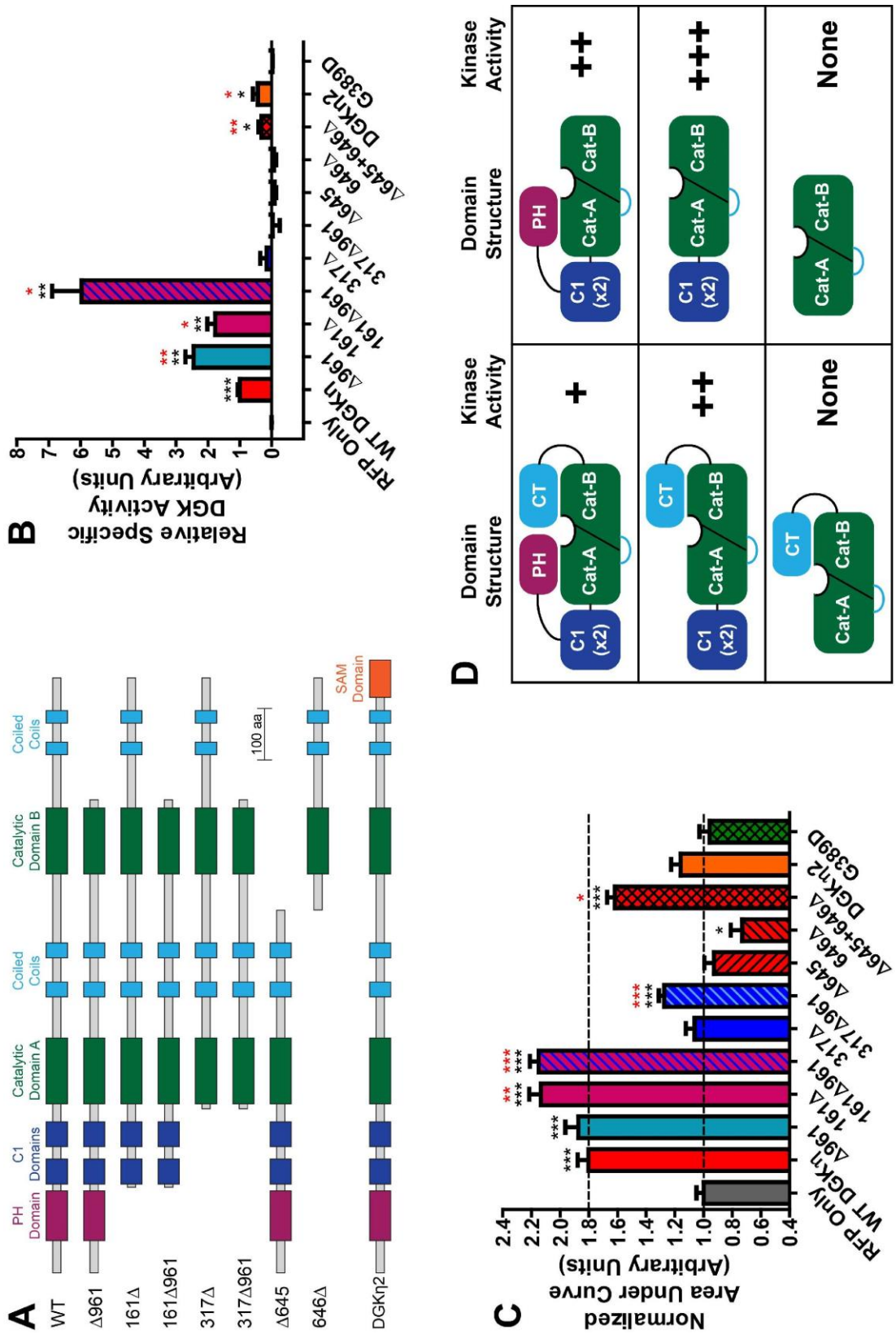
A
PH Domain
C1 Domains
Catalytic Domain A
Coiled Coils
Catalytic Domain B
Coiled Coils
SAM Domain
100 aa
WT
Δ961
161Δ
161Δ961
317Δ
317Δ961
Δ645
646Δ
DGKη2
B
Relative Specific DGK Activity (Arbitrary Units)
RFP Only
WT DGKη1
Δ961
161Δ
161Δ961
317Δ
317Δ961
Δ645
646Δ
Δ645+646Δ
DGKη2 G389D
C
Normalized Area Under Curve (Arbitrary Units)
D
Domain Structure
Kinase Activity
PH
C1 (x2)
Cat-A
Cat-B
CT
+
++
+++
None

Figure 4.4. Catalytic activity and signaling effects of DGKη truncation constructs.

A) Domain architecture of the indicated DGKη constructs. All constructs are N-terminally tagged with RFP. Δ645, 646Δ, and G389D constructs are discussed in Figure 4.2. B) Production of ^{32}P-PA in reactions with the indicated DGKη constructs, using 500 μM 18:1 DAG as substrate. Data were normalized to DGKη expression, which was assessed by western blotting against RFP, then normalized so that RFP alone = 0 and WT DGKη = 1. Data are the average of two experiments performed in duplicate. In the enzymatic assay, the PH domain and the C-terminal tail of DGKη appear to have negative regulatory activity, as truncation of either domain led to increased specific activity. The construct lacking both domains, 161Δ961, has a specific activity 6-fold higher than WT DGKη. Both constructs lacking C1 domains were inactive. As observed previously, the long splice isoform DGKη2 had decreased catalytic activity relative to DGKη1 (143). C) AUC measurements of calcium mobilization in HEK293 cells expressing the indicated DGKη constructs after stimulation with 10 μM carbachol, normalized such that RFP alone = 1. Data were not normalized to expression, as there was no relationship between expression and signaling effect for any of the DGKη constructs (data not shown, and see Fig. 4.2E). Data are the average of three to six independent experiments. n = 75-209 cells per condition. In the signaling assay, truncation of the PH domain also resulted in a small increase in activity. However, truncation of the C-terminal tail had no effect on activity in DGKη constructs with C1 domains. The 317Δ construct lacking C1 domains was inactive, but truncating the C-terminal tail from this construct restored some degree of signaling activity. DGKη2 had a very low level of activity, statistically indistinguishable from RFP alone ($p = 0.057$). D) Speculative model of DGKη regulatory domain function; based on data from in vitro

enzymatic assays. CT = C terminal tail. Truncation of the PH domain or the C-terminal tail increases specific activity, suggesting that these domains inhibit the catalytic activity of DGKη, perhaps by restricting access of DAG and/or ATP to the DGKη active site (although not completely, as WT DGKη retains activity). Inhibition by the PH domain and C terminal tail appear to be independent, as truncation of both domains increases catalytic activity in an additive manner. The C1 domains are required for activity in this assay, as loss of the C1 domains results in a complete loss of catalytic activity. The SAM domain (not shown in Panel D, present only in DGKη2) also negatively regulates DGKη activity, possibly by enhancing inhibition by the C terminal tail. Paired t tests were used to compare data. *Black asterisks*, statistically significant difference when compared with RFP alone. *Red asterisks*, statistically significant difference when compared to WT DGKη. *, $p < 0.05$; **, $p < 0.005$; ***, $p < 0.0005$. All data are presented as means ± standard error.

DGKη does not affect ER calcium loading or store-operated calcium entry

Next, to determine if DGKη prolonged calcium responses by affecting intracellular calcium stores, we treated RFP-DGKη-expressing cells and RFP-expressing controls with thapsagargin, a non-competitive sarco/endoplasmic reticulum calcium ATPase (SERCA) inhibitor that causes release of intracellular calcium stores into the cytosol (165,166). Calcium release was not significantly different between cells expressing RFP alone and RFP-DGKη (Fig. 4.5A), indicating that DGKη has no effect on the loading of intracellular calcium stores.

When intracellular calcium stores become depleted, calcium-sensing proteins trigger the opening of calcium channels in the plasma membrane, allowing the entry of extracellular calcium, a process known as store-operated calcium entry (167,168). To determine if DGKη prolonged calcium mobilization by affecting this process, we stimulated cells with carbachol in the absence of extracellular calcium (to abolish calcium entry through store-operated channels). In the absence of extracellular calcium, carbachol-evoked calcium mobilization was reduced, particularly in the later stages of the response (compare Fig. 4.5B to Fig. 4.1E). However, overexpression of DGKη still prolonged the calcium response by 77% (based on AUC measurements) when compared to RFP alone. This effect was nearly identical to the 80% AUC increase in the presence of extracellular calcium. Thus, these data indicate that DGKη prolongs the carbachol-evoked calcium response via a mechanism that is independent of store-operated calcium entry.

Figure 4.5

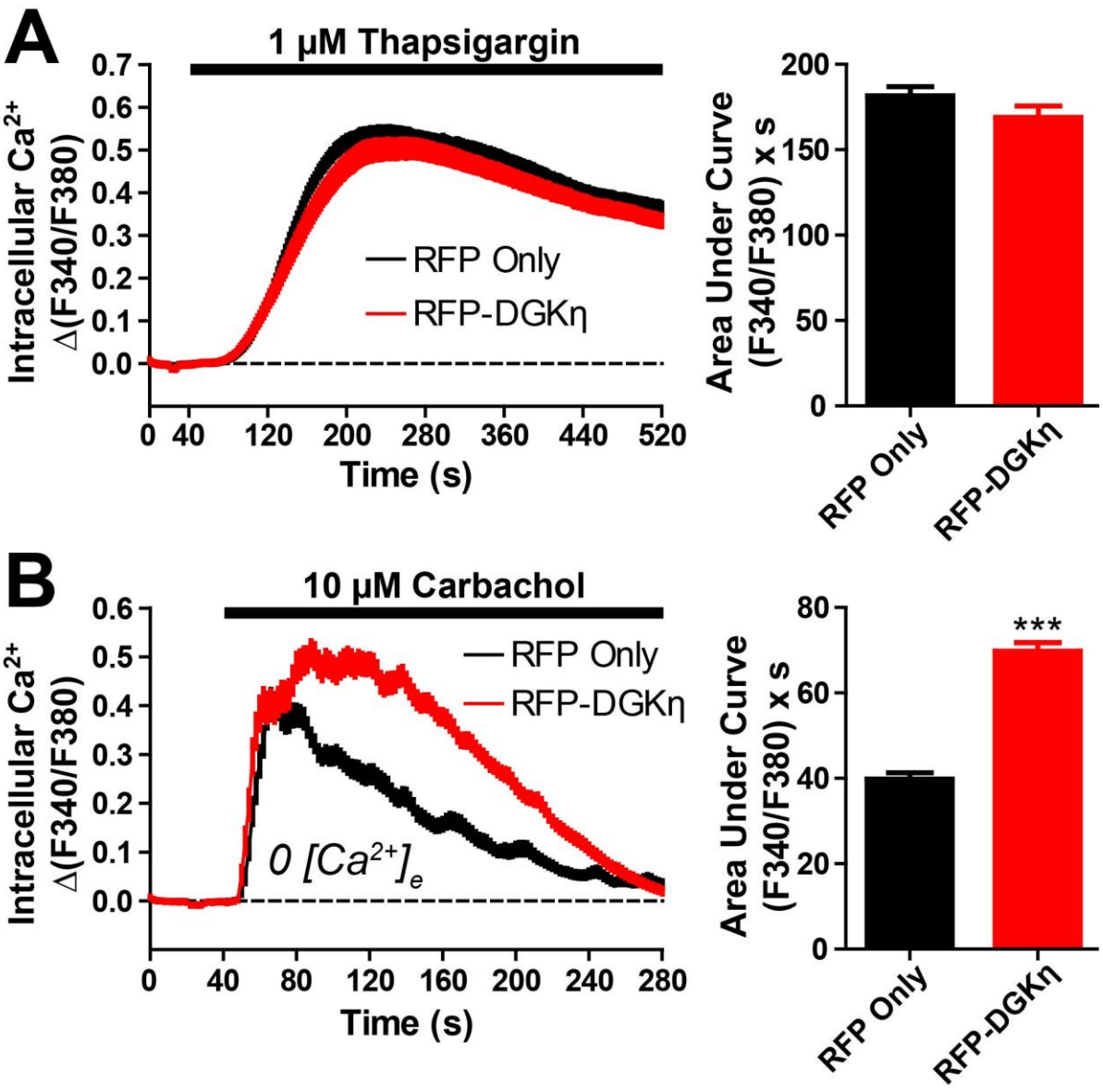
A
1 μM Thapsigargin
Intracellular Ca2+
Δ(F340/F380)
0.7
0.6
0.5
0.4
0.3
0.2
0.1
0.0
RFP Only
RFP-DGKη
0 40 120 200 280 360 440 520
Time (s)
Area Under Curve
(F340/F380) x s
200
150
100
50
0
RFP Only
RFP-DGKη
B
10 μM Carbachol
Intracellular Ca2+
Δ(F340/F380)
0.6
0.5
0.4
0.3
0.2
0.1
0.0
RFP Only
RFP-DGKη
0 [Ca2+]e
0 40 80 120 160 200 240 280
Time (s)
Area Under Curve
(F340/F380) x s
80
60
40
20
0
***
RFP Only
RFP-DGKη

Figure 4.5. DGKη does not affect intracellular calcium stores.

Calcium mobilization in HEK293 cells expressing (*black*) RFP alone or (*red*) RFP-DGKη after (A) stimulation with 1 μM thapsigargin or (B) stimulation with 10 μM carbachol in the absence of extracellular calcium. AUC measurements extended 8 minutes (A) or 4 minutes (B) after stimulation. Paired t tests were used to compare AUC data. ***, $p < 0.0005$. Data are the average of two (A) or five (B) independent experiments. n = 69-190 cells per condition. All data, including calcium traces, are presented as means ± standard error.

DGKη does not translocate after GPCR stimulation

Human DGKη localizes to the cytosol under baseline conditions and translocates to endosomes after osmotic shock (143,169). However, whether DGKη translocates to the plasma membrane, where DAG is located, following GPCR stimulation is unknown. Using live cell confocal imaging, we found that mouse DGKη is localized throughout the cytoplasm in unstimulated cells and did not translocate to the plasma membrane or any other subcellular compartment after stimulation with 10 μM carbachol (Fig. 4.6A). This experiment was conducted under conditions that were identical to those used in the carbachol-evoked calcium mobilization assay, suggesting that the prolonged effects of DGKη on GPCR signaling require little if any translocation of DGKη to the plasma membrane. Furthermore, we were unable to detect translocation of DGKη when cells were stimulated with 10 μM or 100 μM carbachol at 37°C (data not shown). Our inability to detect DGKη translocation was not a technical limitation, as our mouse DGKη construct rapidly translocated to endosomes after osmotic shock (Fig. 4.6B), as previously shown using human DGKη (143,169).

DGKη prolongs GPCR signaling via attenuating PKC activation

DAG is a canonical activator of conventional and novel isoforms of PKC (30). Additionally, PKC is directly and indirectly involved in the phosphorylation and subsequent desensitization of GPCRs (44,170,171). Therefore, we hypothesized that DGKη could prolong GPCR signaling by metabolizing DAG and hence reducing PKC activation. To test this hypothesis, we used the phorbol ester PMA, which potently activates PKC (172). First, we confirmed that acute treatment with 300 nM PMA could activate PKCδ in HEK293 cells,

as evidenced by rapid (within 2 minutes) translocation of PKCδ to the plasma membrane (Fig. 4.7A). We then measured calcium mobilization after stimulating RFP- and RFP-DGKη-expressing cells with 300 nM PMA followed immediately by 10 μM carbachol. Stimulation with 300 nM PMA profoundly accelerated the return of carbachol-evoked calcium mobilization to baseline (Fig. 4.7B, compare to Fig. 4.1E). Furthermore, the carbachol-evoked calcium responses were identical in cells expressing RFP alone and RFP-DGKη when PKC was acutely activated with 300 nM PMA (Fig. 4.7B). In contrast, stimulation of RFP-expressing cells with 300 nM PMA alone did not evoke a calcium response (Fig. 4.7B). Taken together, these data indicate that PKC activation blunts GPCR signaling in HEK293 cells and occludes the effect of DGKη.

We next took advantage of the fact that overnight stimulation with PMA is reported to lead to the near complete depletion of all PKC isoforms that are expressed in HEK293 cells (155) except one (PKCδ was not tested in this reference). We examined PKCδ and found that it was also significantly depleted by overnight stimulation with 300 nM PMA (Fig. 4.7C). Furthermore, after culturing HEK293 cells overnight in 300 nM PMA, stimulation with 10 μM carbachol elicited identical calcium responses in cells expressing RFP alone and RFP-DGKη (Fig. 4.7D). This was not due to a lack of DGKη, as there was no decrease in RFP-DGKη expression in cells cultured in 300 nM PMA compared to cells cultured in DMEM alone (data not shown). Instead, these data indicate that DGKη potentiates GPCR signaling via PKC, likely by reducing the levels of a PKC activator (DAG) and attenuating PKC activity.

Figure 4.6

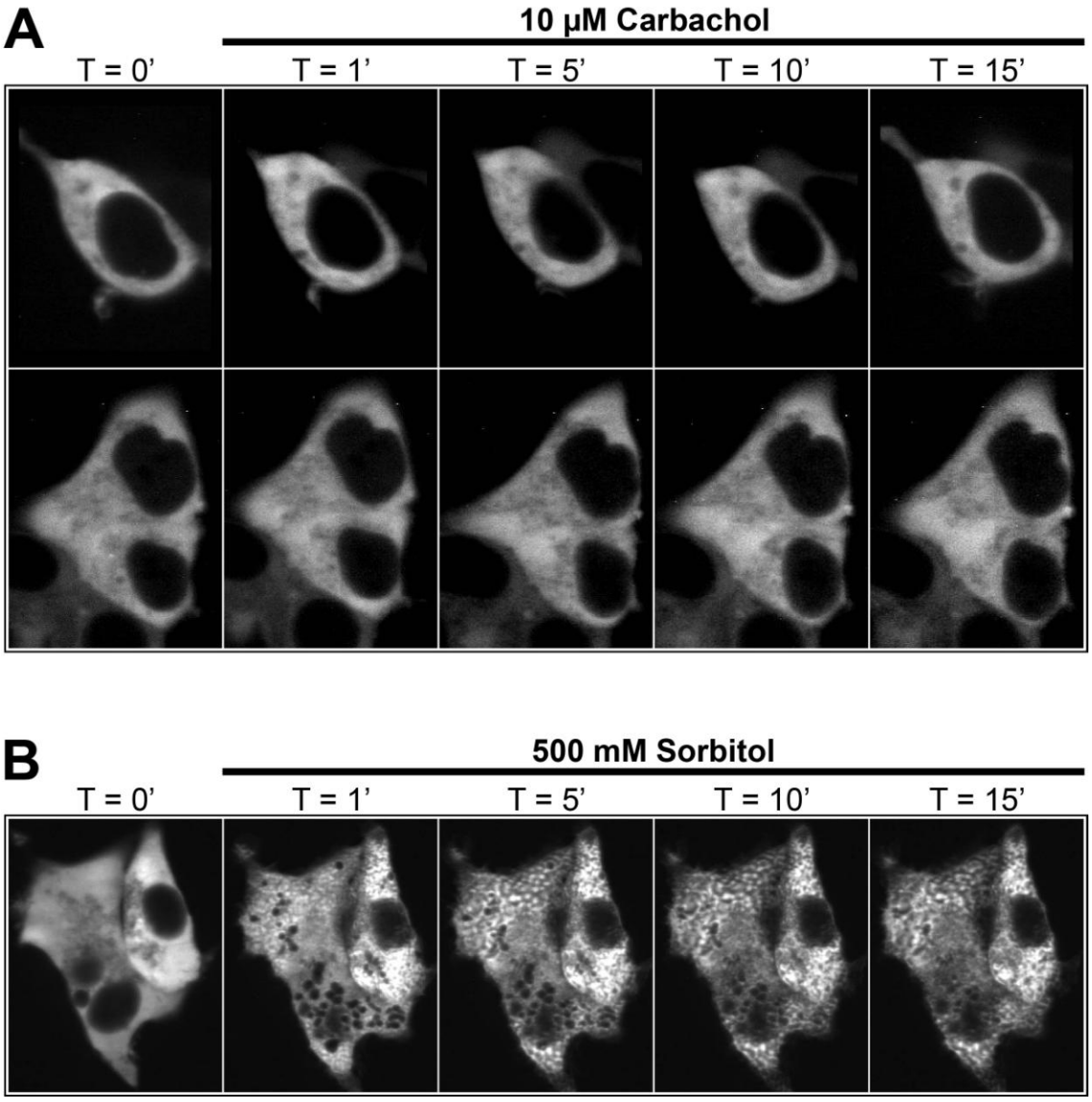
A
10 μM Carbachol
T = 0'
T = 1'
T = 5'
T = 10'
T = 15'
B
500 mM Sorbitol
T = 0'
T = 1'
T = 5'
T = 10'
T = 15'

Figure 4.6. DGKη does not translocate within cells after GPCR stimulation.

Confocal images of live HEK293 cells expressing RFP-DGKη after stimulation with (A) 10 μM carbachol or (B) 500 mM sorbitol for the indicated times. Cell culture and imaging conditions were identical to those used in calcium mobilization experiments. Panel (A) shows cells from independent experiments.

Figure 4.7

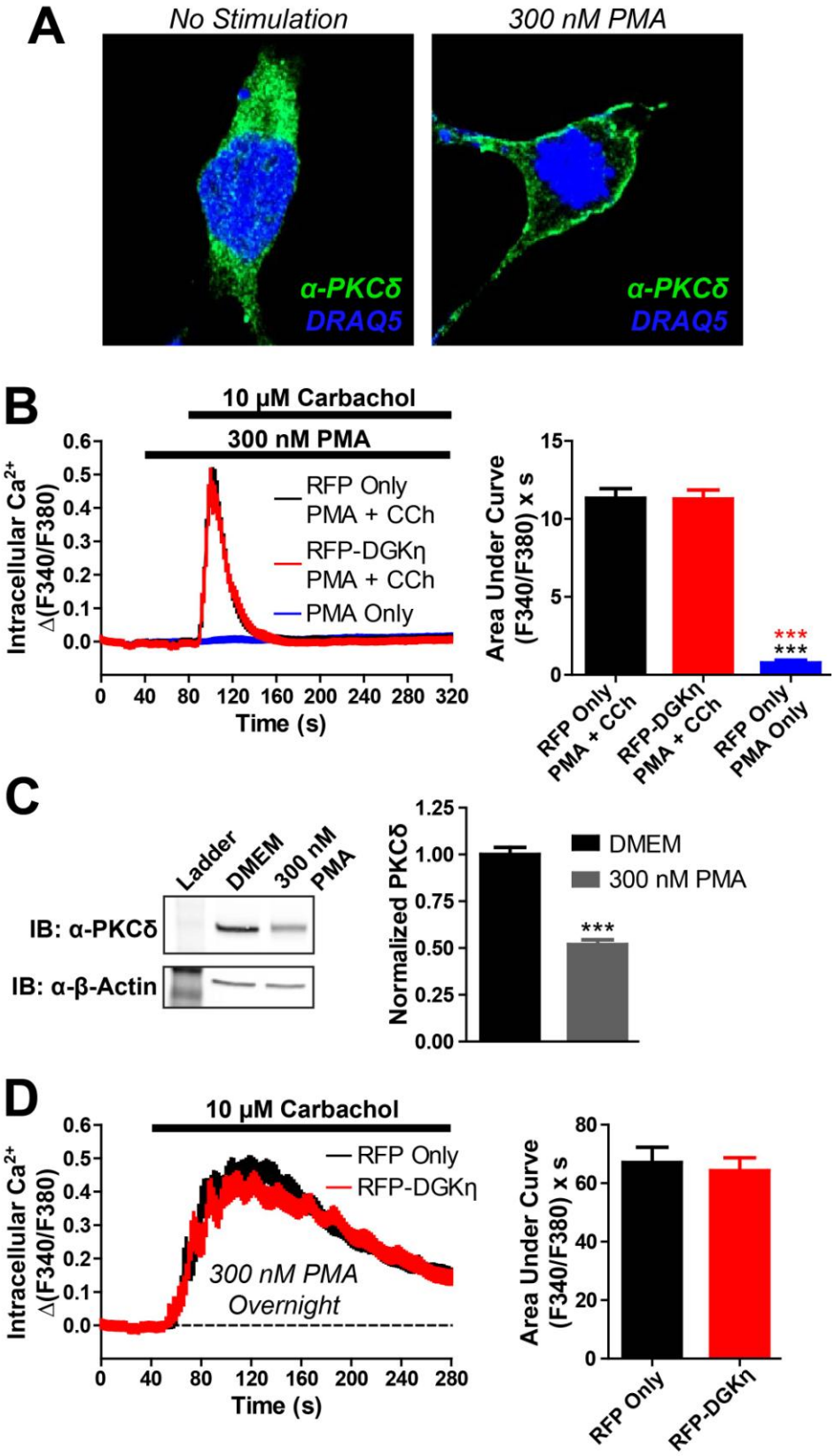
A
No Stimulation
300 nM PMA
α-PKCδ
DRAQ5
α-PKCδ
DRAQ5
B
10 μM Carbachol
300 nM PMA
Intracellular Ca2+ Δ(F340/F380)
RFP Only PMA + CCh
RFP-DGKη PMA + CCh
PMA Only
Time (s)
Area Under Curve (F340/F380) x s
***
***
RFP Only PMA + CCh
RFP-DGKη PMA + CCh
RFP Only PMA Only
C
Ladder
DMEM
300 nM PMA
IB: α-PKCδ
IB: α-β-Actin
Normalized PKCδ
DMEM
300 nM PMA
***
D
10 μM Carbachol
Intracellular Ca2+ Δ(F340/F380)
RFP Only
RFP-DGKη
300 nM PMA Overnight
Time (s)
Area Under Curve (F340/F380) x s
RFP Only
RFP-DGKη

Figure 4.7. DGKη prolongs GPCR signaling via PKC.

A) PKCδ translocation following PMA stimulation. Confocal images of HEK293 cells after treatment with (*left*) vehicle or (*right*) 300 nM PMA for 2 minutes. Cells were fixed, immunostained with an anti-PKCδ antibody (*green*), and counterstained with DRAQ5 nuclear dye (*blue*). B) Calcium mobilization in HEK293 cells expressing RFP alone or RFP-DGKη after stimulation with (*black, red*) 300 nM PMA followed by 10 μM carbachol, or (*blue*) 300 nM PMA alone. AUC measurements extended 80 seconds from final agonist addition. Data are the average of two (PMA alone) or three (PMA + carbachol) independent experiments. n = 49-83 cells per condition. C) HEK293 cells were cultured overnight in growth medium ± 300 nM PMA to deplete PKC isoforms. Cells were lysed and 20 μg of protein from each lysate was run on SDS-PAGE and blotted using anti-PKCδ and anti-β-actin antibodies. (*Right*) Band intensities were quantified using ImageJ. Data are the average of three independent experiments. Overnight PMA treatment was previously shown to deplete all other PKC isoforms in HEK293 cells (155). D) Calcium mobilization in HEK293 cells expressing (*black*) RFP alone or (*red*) RFP-DGKη, after overnight culture in media containing 300 nM PMA. Cells were stimulated with 10 μM carbachol. AUC measurements extended 4 minutes from agonist addition. Data are the average of four (RFP-DGKη) or five (RFP alone) independent experiments. n = 28-35 cells per condition. Paired t tests were used to compare all data. ***, $p < 0.0005$. All data, including calcium traces, are presented as means ± standard error.

DGKη reduces baseline and GPCR agonist-evoked ERK phosphorylation

Carbachol-evoked phosphorylation of ERK is mediated by PKCδ in HEK293 cells (154). Thus, we next evaluated the extent to which overexpression of DGKη affected ERK phosphorylation. We treated HEK293 cells expressing RFP or RFP-DGKη with vehicle, 10 μM carbachol, or 300 nM PMA for 5 minutes, lysed the cells, and then ran western blots using a phospho-specific anti-ERK primary antibody (Fig. 4.8A). After treatment with vehicle or 10 μM carbachol, RFP-DGKη cell lysates contained less phospho-ERK than lysates from RFP alone cell lysates (Fig. 4.8B). The DGKη-evoked decrease in ERK phosphorylation was modest (approximately 20%), but statistically significant ($p < 0.05$), both at baseline and after carbachol stimulation. This likely reflects the fact that not every cell was transfected with RFP-DGKη. In contrast, after direct stimulation of PKC with 300 nM PMA, which bypasses the need for DAG to activate PKC, there was no difference in ERK phosphorylation between lysates from cells expressing RFP alone and RFP-DGKη (Fig. 4.8B). Taken together, these data indicate that overexpression of DGKη reduces ERK phosphorylation.

Figure 4.8

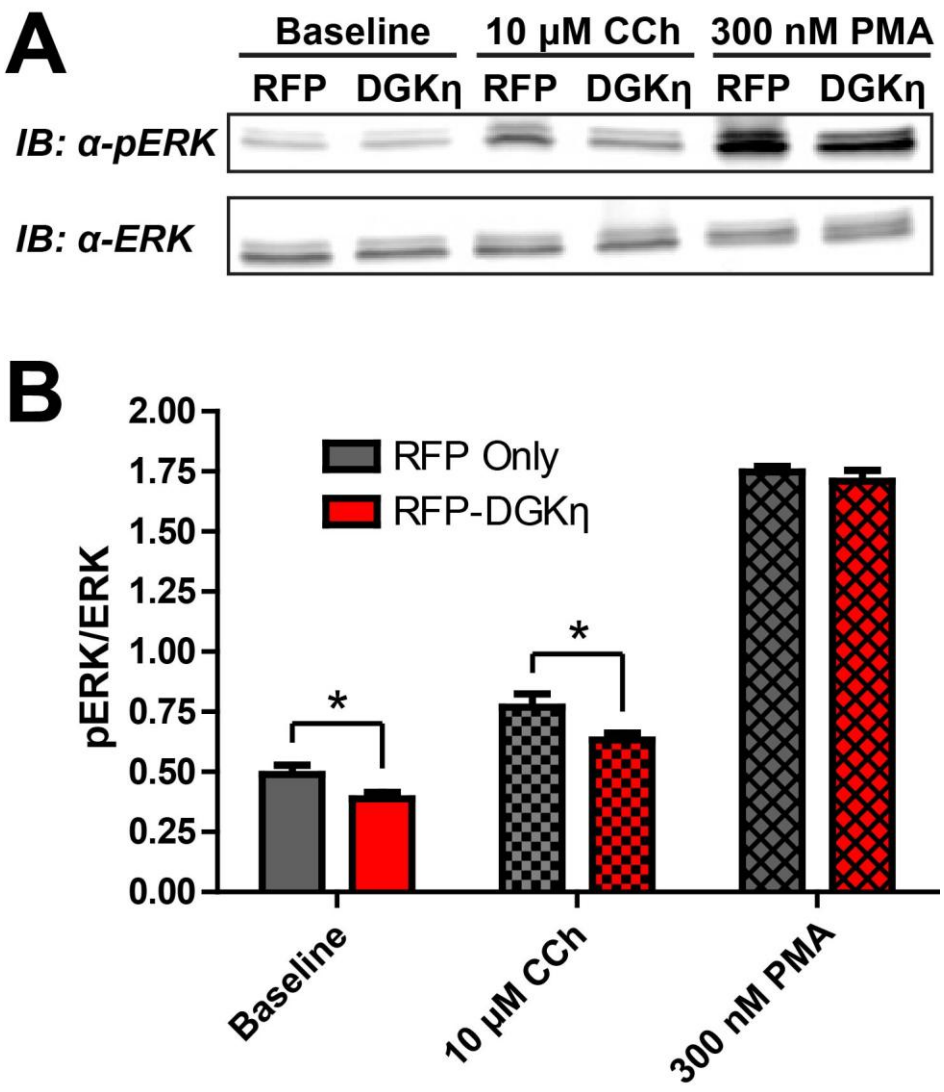
A
Baseline
10 μM CCh
300 nM PMA
RFP
DGKη
RFP
DGKη
RFP
DGKη
IB: α-pERK
IB: α-ERK
B
pERK/ERK
2.00
1.75
1.50
1.25
1.00
0.75
0.50
0.25
0.00
RFP Only
RFP-DGKη
*
*
Baseline
10 μM CCh
300 nM PMA

Figure 4.8. DGKη reduces baseline and GPCR agonist-evoked phosphorylation of ERK.

A) After serum-starvation (no serum) for 24 hours, HEK293 cells expressing RFP or RFP-DGKη were treated with vehicle, 10 μM carbachol, or 300 nM PMA for 5 minutes then were lysed. 20 μg of protein from each lysate was run on SDS-PAGE and blotted using anti-phospho ERK and anti-ERK antibodies. B) Band intensities were quantified using ImageJ and pERK/ERK ratios were calculated. Paired t tests were used to compare data. *, $p < 0.05$. Data are the average of four experiments performed in duplicate. All data are presented as means ± standard error.

Figure 4.9

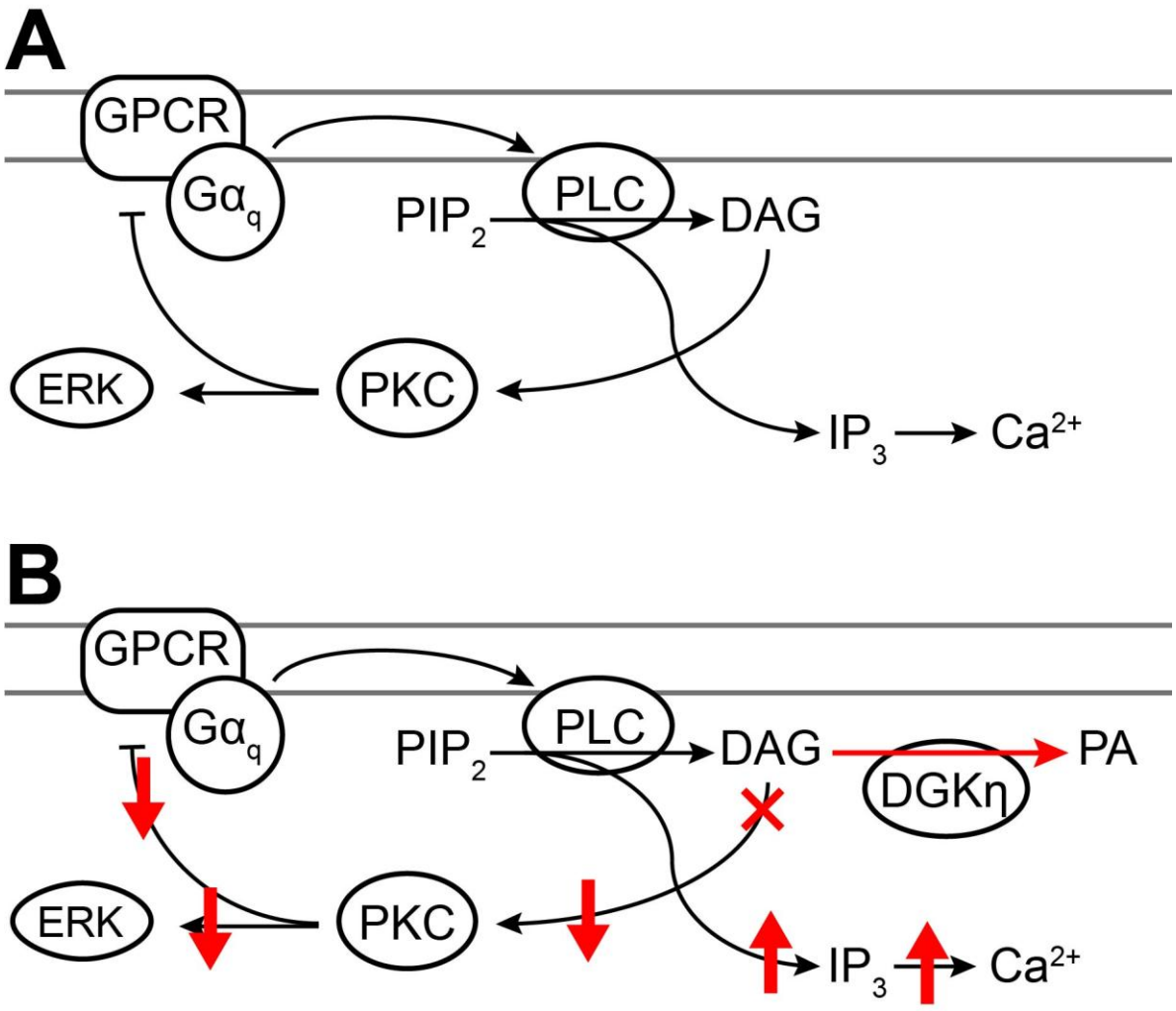
A
GPCR
Gαq
PIP2
PLC
DAG
ERK
PKC
IP3
Ca2+
B
GPCR
Gαq
PIP2
PLC
DAG
DGKη
PA
ERK
PKC
IP3
Ca2+

Figure 4.9. Model showing how DGKη prolongs $G\alpha_q$-coupled GPCR signaling.

A) Activation of $G\alpha_q$-coupled GPCRs leads to the stimulation of PLC-catalyzed hydrolysis of PIP_2 and the release of IP_3 and DAG. IP_3 activates IP_3 receptors on the endoplasmic reticulum, resulting in the release of intracellular calcium stores. Concurrently, DAG activates conventional and novel isoforms of PKC, leading to the phosphorylation of ERK by MAP kinase cascades. Additionally, PKC activity leads to the phosphorylation of activated GPCRs, resulting in receptor desensitization and the attenuation of GPCR signaling. B) After receptor activation, overexpressed DGKη reduces the pool of free DAG by converting it into PA, thus suppressing the activation of PKC. Decreased PKC activity leads to reduced phosphorylation of ERK. As previously shown (173-176), reduced PKC activity attenuates GPCR desensitization. This leads to prolonged IP_3 and intracellular calcium release following receptor activation.

DISCUSSION

Collectively, our data suggest a model for how DGKη prolongs GPCR signaling (Fig. 4.9). Stimulation of $G\alpha_q$-coupled GPCRs leads to the activation of phospholipase C (PLC) and the hydrolysis of phosphatidylinositol 4,5-bisphosphate (PIP_2) into inositol 1,4,5-triphosphate (IP_3) and DAG. IP_3 subsequently induces the release of endoplasmic reticulum calcium stores, raising the cytosolic concentration of Ca^{2+}. In cells without DGKη activity (Fig. 4.9A), DAG activates PKC, leading to the phosphorylation and desensitization of the activated GPCR, followed by termination of GPCR signaling (170,173,174). Activated PKC also signals through other downstream pathways, including MAPK cascades which culminate in ERK phosphorylation. However, in cells overexpressing DGKη, DAG is phosphorylated to PA, leading to a decreased level of PKC activation (Fig. 4.9B, *red*). This causes a decrease in the rate of GPCR phosphorylation and desensitization, resulting in prolonged GPCR signaling (as evidenced by sustained intracellular calcium release). Reduced PKC activity also leads to reduced activation of MAPK cascades, resulting in decreased phosphorylation of ERK.

We focused on PKCδ because it is highly expressed (177) and mediates ERK phosphorylation (154) in HEK293 cells, and because it preferentially activates GRK2, a regulator of GPCR signaling (171). Moreover, PKCδ is a Ca^{2+}-insensitive isoform of PKC (30), and thus would not be affected by prolonged calcium responses.

During activation, PKC isoforms translocate to the plasma membrane (178), and are autophosphorylated at multiple amino acid residues (179,180). We attempted to measure PKC activation directly via: 1) PKCδ immunostaining (Fig. 4.7A), 2) membrane/cytosol fractionation and PKCδ western blotting (181), 3) anti-phospho-PKCδ western blotting

(182), 4) anti-pan-phospho-PKC western blotting (183), and 5) a FRET biosensor of PKC activity (184). Unfortunately, we did not observe endogenous PKC activation with any of these techniques after stimulation of endogenous receptors with carbachol, and were therefore unable to measure the effect of DGKη on endogenous PKC activity. This did not reflect technical limitations, as we did observe endogenous PKCδ activation after direct stimulation with PMA (Fig. 4.7A). Instead, our inability to directly measure endogenous PKC activity suggests very little PKC is activated when endogenous receptors are stimulated. Indeed, previous studies that measured PKC activity employed overexpressed receptors (181,183). It is well-documented that overexpressed receptors activate signaling pathways at non-physiological (excessive) levels relative to endogenous receptor activation (185). This is precisely why we used endogenous M_3 receptors and a sub-EC_{50} concentration of carbachol (154) in our signaling experiments, to probe potential negative and positive modulation at physiological levels of GPCR activation.

Alternatively, it is possible that 10 μM carbachol selectively stimulates the strong activation of a single PKC isoform other than PKCδ, which does not phosphorylate either itself or the PKC biosensor. However, it is far more likely that stimulation of endogenous M_3 receptors in HEK293 cells simply results in a very low level of DAG release and PKC activation. Indeed, only a minimal level of DGKη expression results in the full DGKη-mediated signaling effect (Fig. 4.2E), consistent with a very small amount of available substrate. Nevertheless, modulation of PKC activity clearly mediates the effect of DGKη on GPCR signaling, as both activation (Fig. 4.7B) and depletion (Fig. 4.7D) of PKC blocks overexpressed DGKη from prolonging endogenous M_3 receptor activation. Furthermore,

after signal amplification downstream of PKC by the Raf-MEK-ERK cascade, activation by 10 μM carbachol and suppression by DGKη were observed (Fig. 4.8B).

It is well-established that PKC activation leads to desensitization of GPCRs (170,173,174). Based on this literature, we propose that overexpression of DGKη prolongs GPCR signaling by attenuating PKC-mediated phosphorylation and desensitization of GPCRs (Fig. 4.9). Such a mechanism should have a greater effect on the duration of calcium responses than the intensity, as we observed (Fig. 4.1 E,F). Likewise, cholinergic stimulation of cells expressing a phosphorylation-deficient M_3 receptor resulted in prolonged calcium mobilization compared to cells expressing wild-type M_3 receptor (186), strongly resembling the effect of overexpressed DGKη on the M_3 receptor. Although PKC directly phosphorylates some GPCRs (44,170), phosphorylation of the M_3 receptor in HEK293 cells is likely indirect, through the activation of G protein-coupled receptor kinases (GRKs). In HEK293 cells, M_3 receptor activity is regulated by GRKs 2, 3, and 6 (154), at least one of which is activated by PKC (171,187,188). Interestingly, GRK3 is also genetically linked to BPD (150), suggesting that dysregulation of GPCR signaling is important in the pathology of BPD.

Like DGKη, other DGK isoforms regulate PKC and receptor signaling. For example, disruption of the gene encoding DGKδ leads to DAG accumulation, enhanced PKC activity and EGFR phosphorylation (189), culminating in a PKC-dependent increase in EGFR ubiquitination and degradation (190). DGKs also regulate inter-receptor desensitization pathways, as DGKθ attenuates bradykinin-evoked, PKC-mediated phosphorylation of EGFR, a phosphorylation event that is linked to EGFR desensitization (191). Interestingly, EGFR is a receptor tyrosine kinase, indicating that regulation of receptor signaling by DGKs is not

limited to GPCRs. Together with our study, it is clear that multiple members of the DGK enzyme family regulate PKC activity and receptor signaling.

Lastly, there are several connections between DGKη-regulated signaling pathways and BPD. Patients with BPD show increased levels of PKC activity compared to unaffected controls, which can be inhibited by the mood stabilizers lithium and valproate (153,192-194). In fact, there is clinical interest in PKC inhibitors as treatments for BPD (195-199). Based on our current study, increased DGKη activity should reduce PKC activity, suggesting that increased DGKη expression does not contribute to BPD simply by regulating global PKC activity. The DGKη product PA is also a critical intermediate in the phosphatidylinositol cycle, another proposed therapeutic target of lithium (200-202). Interestingly, three polymorphisms in the DGKη gene which are linked to BPD are not correlated with responsiveness to lithium therapy (203), although this does not rule out lithium-sensitive pathways in the role of DGKη in BPD. Future studies are needed to delineate precisely how DGKη activity is altered in BPD patients and how alterations in DGKη levels affect PKC and GPCR signaling in neurons and in animal models of BPD.

CHAPTER 5: CONCLUSIONS AND FUTURE DIRECTIONS

Perhaps the most fundamental result to come out of my graduate work is the discovery that the physiologically relevant nucleotide AMP is an adenosine A_1 receptor agonist (see Chapter 2). AMP was previously known to have some signaling activity, primarily via stimulation of AMP-activated protein kinase, an important intracellular regulator of energy homeostasis (204). However, prior to my work, an extracellular receptor for AMP was not believed to exist. Indeed, AMP was thought of as the sole silent intermediate in an extracellular hydrolysis pathway in which both the upstream (ATP and ADP, which activate P2X and P2Y receptors) and downstream elements (adenosine, which activates adenosine receptors) had active signaling roles (75). The fact that AMP activates the A_1 receptor independent of hydrolysis to adenosine, considering the biological ubiquity of AMP, necessitates a fundamental reevaluation of A_1R-mediated signaling.

For example, one area in which AMP activity through the A_1 receptor may be important is in the regulation of sleep and hibernation. Circulating AMP concentration varies in a circadian fashion and is elevated in mice exposed to continuous darkness (82). Intraperitoneal injection of AMP also induces a hypothermic state similar to torpor, although there is some disagreement as to whether this state reflects true torpor (205). Strikingly, intraventricular injection of a selective A_1R agonist induces torpor and injection of an A_1R antagonist reverses spontaneous torpor in the arctic ground squirrel, a hibernating mammal (206). Furthermore, central administration of a selective A_1R agonist induces a similar

torpor-like state in rats (127), a non-hibernating mammal. These studies indicate that both circulating AMP levels and A_1R activity in the CNS are very important in mediating hypothermic metabolic states during torpor or hibernation. Thus, it is possible that AMP signaling through A_1R may play a role in this metabolic regulation.

Clearly, future studies are needed to delineate the biological functions of AMP and adenosine signaling through the A_1 receptor. However, there is reason to believe that such studies may be very difficult to perform. In vivo signaling environments are significantly more complex than the highly controlled systems used to evaluate adenosine receptor signaling in Chapter 2. Multiple, redundant enzymes which hydrolyze AMP to adenosine exist in vivo, including three (PAP, NT5E, and tissue-nonspecific alkaline phosphatase) in the dorsal root ganglia alone (207), which will hamper the use of genetic approaches. Likewise, a lack of known inhibitors for all such enzymes, as well as bioavailability/delivery concerns will limit the effectiveness of pharmacological inhibition strategies. Thus, even using a combination of genetic and pharmacological approaches the complete elimination of AMP hydrolysis in a biologically relevant setting may prove to be an impossible task. Indeed, due to the ubiquity of both AMP and adenosine, even accurately evaluating the degree to which enzymatic hydrolysis of AMP has been abolished would be very difficult. Furthermore, extracellular adenosine is primarily generated via AMP hydrolysis (75), and also activates A_{2A}, A_{2B} and A_3 receptors, so even with the complete elimination of extracellular AMP hydrolysis, changes in $A_{2A}R$-, $A_{2B}R$-, and A_3R-mediated signaling due to decreases in adenosine would complicate the analysis of A_1R signaling.

Nevertheless, clever experimental design may allow the biological signaling roles of adenosine and AMP to be teased apart. For example, one promising experiment entails the

creation of a knockin mouse expressing an AMP-insensitive A_1 receptor in place of wild-type A_1R. Specifically, this mouse would express a receptor in which the residue homologous to histidine 251 is mutated to alanine, as in Figure 2.11. Despite the A_1 receptor's ubiquitous expression and importance in regulation of the cardiovascular system, A_1R knockout mice are completely viable and have been used for various behavioral studies (70,76,108,109). Thus, it is likely that a knockin mouse expressing a mutated A_1 receptor would survive as well. The A_1 receptors expressed by this mouse should be resistant to activation by AMP, but should retain wild-type sensitivity towards adenosine (Fig. 2.11). Therefore, these mice should exhibit a systemic lack of extracellular AMP signaling, but unaffected adenosine signaling. Phenotypic analysis of these mice – evaluation of sleep behavior/circadian rhythms, cardiovascular function, or nociceptive behavior, for example – and comparison to wild-type mice should lead to a better understanding of the biological roles of AMP signaling through the A_1 receptor.

During my graduate work, I also discovered that AMP preferentially activates $G\alpha_i$ over $G\alpha_q$ through A_1R (Fig. 2.6, Fig. 3.2), one of the first known instances of functional selectivity by an endogenous signaling molecule. Functional selectivity has been heavily studied in recent years, with a particular focus on the potential of functionally selective compounds in drug design (35,119). Nevertheless, very little work has been done to examine functional selectivity in the context of endogenous signaling. The physiological trace amine N,N-dimethyltryptamine (DMT) stimulates calcium mobilization downstream of the 5-HT_{2A} serotonin receptor with an efficacy approximately 25% of that of serotonin itself (208). However, this may not be functional selectivity per se, as the efficacies of serotonin and DMT at 5-$HT_{2A}R$ have not been compared via other downstream signaling pathways (i.e.

DMT could simply be a universally low-efficacy agonist). Furthermore, DMT is only present in vivo in very small amounts, so the biological relevance of this activity is suspect. Additionally, discrepancies in the efficacy of the endogenous cannabinoid receptor agonist anandamide have been observed by different groups when measuring different downstream signaling pathways (209), but these differences have not been rigorously confirmed in a single laboratory. In contrast to these studies, AMP is known to be present in vivo in significant quantities (with concentrations regulated by light exposure and food consumption), and the differential efficacy of AMP was measured in two very similar signaling assays under identical conditions. These results suggest that functional selectivity may have an important role in endogenous GPCR signaling.

A confounding problem in the investigation of the endogenous role of GPCR functional selectivity is the limited number of GPCRs that are known to have more than one physiological ligand. This complicates the analysis of functional selectivity by preventing comparisons between endogenous ligands, thus necessitating the use of synthetic ligands to define 'full agonist' activity (which may or may not be accurate, particularly if only a few synthetic agonists have been developed for a given receptor). For example, the 5-HT_{1A}, 5-HT_{2A}, and 5-HT_{2C} serotonin receptors are activated by both serotonin and DMT, a closely related compound (210,211). However, as mentioned above, DMT is present at very low levels in most biological systems and thus has little relevance as an endogenous signaling molecule. Additionally, some P2Y receptors (notably $P2Y_2$) are sensitive to both adenine and uridine nucleotides (212), and the CB_1 and CB_2 cannabinoid receptors are activated by multiple endocannabinoid ligands, including anandamide and 2-arachidonoyl glycerol (213).

Lastly, the metabotropic glutamate receptor mGluR4 is sensitive to the protein metabolite phosphoserine as well as glutamate (214).

Nevertheless, the vast majority of GPCRs are either orphan receptors with no known ligand, or have exactly one known endogenous ligand. To a great extent, the lack of known receptors with multiple biological ligands is simply due to a lack of investigation. Despite the existence of many ligands which activate multiple receptors, it is largely assumed that each receptor is activated by a single ligand. By this logic, if one biological ligand has been identified for a given receptor, there is no need to search for others. Indeed, I assumed that this was true regarding the A_1 receptor, until my serendipitous discovery that a second ligand did indeed exist.

High-throughput screening to identify ligands of orphan GPCRs has now been taking place for nearly two decades (215,216). My discovery of a second endogenous A_1R ligand, together with the studies discussed above, suggest that these screening efforts should be expanded considerably. Notably, all of the agonist pairs (or families, in the case of the endocannabinoids) identified thus far that activate a single GPCR are chemically very similar, suggesting that the most profitable way to search for additional GPCR ligands is among biological compounds closely related to the known ligand. Thus, any such structurally related candidate molecules should also be screened against GPCRs with known endogenous ligands, as part of or in addition to current orphan GPCR screening efforts. Furthermore, for the growing number of GPCRs at which multiple endogenous ligands have been identified, the functional selectivity of each ligand should be systematically evaluated using assays which measure as many downstream signaling pathways as possible.

GPCRs are an absolutely fundamental part of eukaryotic cellular signaling. Indeed, it is hard to overstate their importance in modern drug discovery and pharmacology: over 30% of currently marketed small-molecule drugs target GPCRs (2). However, that is not to say that GPCR pharmacology is without its challenges. Biological regulation of GPCR-activating ligands is incredibly complex, and blanket stimulation or inhibition of GPCRs in vivo often has undesirable effects by interfering with endogenous signaling patterns. This is especially true of GPCRs whose endogenous ligands are critical neurotransmitters or signaling molecules. For example, serotonin receptor agonists have psychedelic effects and are of limited medical use, whereas serotonin reuptake inhibitors – which enhance available levels of serotonin after endogenous release, but have no activity at serotonin receptors themselves – have immense therapeutic value as antidepressants. This problem can largely be addressed by drugs that do not activate or inhibit GPCRs, but adjust the signaling caused by endogenous ligands; that is to say, GPCR modulators.

One possibility is the development of drugs that directly modulate GPCR signaling by binding to a secondary (allosteric) binding site on the receptor. Allosteric modulator binding alters receptor conformation in such a way that does not cause downstream signaling alone, but affects (either positively or negatively) the degree of downstream signaling that occurs when the receptor is activated by a true agonist. The most well-known example of a drug class that has this mechanism is the anxiolytic/sedative benzodiazepines, which function as positive allosteric modulators of the $GABA_A$ receptor (217). The phenomenon is also very important in physiological signaling, as the inhibitory neurotransmitter glycine is also a positive allosteric modulator of NMDA-type glutamate receptors (218). However, most of the work on allosteric modulators thus far has focused on ion channels (219), although there

have been recent advances in the development of allosteric GPCR modulators (220). Notably, many ion channels have large extracellular domains with a great deal of exposed surface area, and altering ion channel pore size offers a simple mechanism for signal modulation. Conversely, the vast majority of GPCRs (all except the small class C subfamily) have very small extracellular domains (221) and the nature of the conformational changes that would have the desired modulatory effects is very poorly understood, which may limit the development of allosteric GPCR modulators.

Thus, there is also great promise in targeting other proteins which regulate GPCR signaling for drug discovery. As with direct GPCR modulators, this strategy may avoid the side effects that accompany direct activation or inhibition of GPCRs. Furthermore, this strategy would allow for the modulation of multiple GPCRs simultaneously. It is recognized that nonselective GPCR-targeting drugs (both agonists and antagonists) have been significantly more effective in the clinic than highly selective ones, particularly for psychological indications (222). These drugs have been dubbed 'magic shotguns' (as opposed to more selective 'magic bullets'), and drugs targeting GPCR modulators should benefit from a similar breadth of function. Indeed, the receptor selectivity of drugs targeting GPCR modulators should be determined more by the tissue and cellular distribution of the modulators themselves, and not by GPCR family or structural similarity. This may aid in the treatment of diseases in which dysregulated GPCR signaling is localized to a particular target tissue, but is not limited to a single receptor.

Fortunately for such drug discovery efforts, there are multiple protein families which are critical in the regulation of GPCRs, including most notably the G protein-coupled receptor kinase (GRK) family (223) and the arrestin family (224). The regulator of G protein

signaling (RGS) family is also important in the regulation of GPCR signaling, although RGS proteins do not modulate GPCRs themselves. Instead, they enhance the GTPase activity of the associated Gα subunits, attenuating G protein signaling after GPCR activation (225). My graduate work has added DGKη, a seemingly unrelated lipid kinase, to this list of GPCR-modulating enzymes, and other DGK isoforms may have similar activity. Indeed, drug discovery targeting members of any or all of these protein families may prove fruitful in the future. However, arrestins and RGS proteins act solely via protein-protein interactions, and do not possess enzymatic activity. This necessitates the development of protein-protein interaction inhibitors in order to affect arrestin or RGS function, which will make the discovery of effective compounds more difficult. Thus, the catalytically active GRK and DGK families are likely to provide more attractive targets, particularly using current ligand discovery strategies.

More specifically, since DGKη catalytic activity positively modulates GPCR signaling (Fig. 4.2), DGKη inhibitors may have therapeutic potential, particularly for the treatment of bipolar disorder, where increased DGKη expression is already implicated (142). However, pharmacological inhibition of DGKη may selectively affect only certain DGKη-mediated signaling pathways. DGKη is a very large protein with multiple and varied interaction domains (PH, C1, coiled-coil, and SAM), and DGKη enhances ERK signaling downstream of EGFR activation via a scaffolding mechanism unrelated to catalytic activity (226). In fact, modulation of EGFR activity by DGKη may be important in lung cancer, as DGKη depletion (as distinct from inhibition) reduced the growth of lung cancer cells and improved the efficacy of an EGFR inhibitor (146). Pharmacological inhibition of DGKη will most likely only affect the catalytic activity of DGKη, and not affect its scaffolding

functions. Thus, therapeutic DGKη inhibitors will be better suited towards pathologies where the catalysis-dependant modulation of GPCR signaling is likely to be important (such as bipolar disorder), than diseases in which the catalysis-independent modulation of EGFR signaling is likely to be important (such as cancer).

Among protein families whose members regulate GPCR signaling, the DGK family is very diverse, containing ten unique isoforms with highly divergent expression profiles, some of which have multiple splicing variants (130). In contrast, the arrestin family contains only two non-visual isoforms, which are both widely expressed, and the GRK family contains five non-visual isoforms, three of which are widely expressed. Therefore, the DGK family may prove to be an exceptionally good target for the development of GPCR-regulating therapeutics, as the existence of so many isoforms with dramatically different expression profiles lessens the chance that a specific inhibitor of a single DGK isoform will either have broad systemic side effects due to global DGK inhibition, or will prove ineffective due to enzymatic compensation by other DGK isoforms in the target tissue. On the other hand, the existence of so many DGK isoforms may make the identification of a truly isoform-selective DGK inhibitor more difficult. Regardless, GPCR-modulating enzymes in general, and the DGK family in particular, constitute a target class with a great deal of untapped potential for drug discovery in the future.

REFERENCES

1. Millar, R. P., and Newton, C. L. The year in G protein-coupled receptor research. *Mol Endocrinol* **24**, 261-274

2. Hopkins, A. L., and Groom, C. R. (2002) The druggable genome. *Nat Rev Drug Discov* **1**, 727-730

3. Palczewski, K., Kumasaka, T., Hori, T., Behnke, C. A., Motoshima, H., Fox, B. A., Le Trong, I., Teller, D. C., Okada, T., Stenkamp, R. E., Yamamoto, M., and Miyano, M. (2000) Crystal structure of rhodopsin: A G protein-coupled receptor. *Science* **289**, 739-745

4. Salom, D., Lodowski, D. T., Stenkamp, R. E., Le Trong, I., Golczak, M., Jastrzebska, B., Harris, T., Ballesteros, J. A., and Palczewski, K. (2006) Crystal structure of a photoactivated deprotonated intermediate of rhodopsin. *Proc Natl Acad Sci U S A* **103**, 16123-16128

5. Okada, T., Sugihara, M., Bondar, A. N., Elstner, M., Entel, P., and Buss, V. (2004) The retinal conformation and its environment in rhodopsin in light of a new 2.2 A crystal structure. *J Mol Biol* **342**, 571-583

6. Rasmussen, S. G., Choi, H. J., Rosenbaum, D. M., Kobilka, T. S., Thian, F. S., Edwards, P. C., Burghammer, M., Ratnala, V. R., Sanishvili, R., Fischetti, R. F., Schertler, G. F., Weis, W. I., and Kobilka, B. K. (2007) Crystal structure of the human beta2 adrenergic G-protein-coupled receptor. *Nature* **450**, 383-387

7. Rosenbaum, D. M., Cherezov, V., Hanson, M. A., Rasmussen, S. G., Thian, F. S., Kobilka, T. S., Choi, H. J., Yao, X. J., Weis, W. I., Stevens, R. C., and Kobilka, B. K. (2007) GPCR engineering yields high-resolution structural insights into beta2-adrenergic receptor function. *Science* **318**, 1266-1273

8. Rasmussen, S. G., DeVree, B. T., Zou, Y., Kruse, A. C., Chung, K. Y., Kobilka, T. S., Thian, F. S., Chae, P. S., Pardon, E., Calinski, D., Mathiesen, J. M., Shah, S. T., Lyons, J. A., Caffrey, M., Gellman, S. H., Steyaert, J., Skiniotis, G., Weis, W. I., Sunahara, R. K., and Kobilka, B. K. Crystal structure of the beta2 adrenergic receptor-Gs protein complex. *Nature* **477**, 549-555

9. Jaakola, V. P., Griffith, M. T., Hanson, M. A., Cherezov, V., Chien, E. Y., Lane, J. R., Ijzerman, A. P., and Stevens, R. C. (2008) The 2.6 angstrom crystal structure of a human A2A adenosine receptor bound to an antagonist. *Science* **322**, 1211-1217

10. Xu, F., Wu, H., Katritch, V., Han, G. W., Jacobson, K. A., Gao, Z. G., Cherezov, V., and Stevens, R. C. (2011) Structure of an agonist-bound human A2A adenosine receptor. *Science* **332**, 322-327

11. Lebon, G., Warne, T., Edwards, P. C., Bennett, K., Langmead, C. J., Leslie, A. G., and Tate, C. G. (2011) Agonist-bound adenosine A2A receptor structures reveal common features of GPCR activation. *Nature* **474**, 521-525

12. Reeves, P. J., Callewaert, N., Contreras, R., and Khorana, H. G. (2002) Structure and function in rhodopsin: high-level expression of rhodopsin with restricted and homogeneous N-glycosylation by a tetracycline-inducible N-acetylglucosaminyltransferase I-negative HEK293S stable mammalian cell line. *Proc Natl Acad Sci U S A* **99**, 13419-13424

13. Chini, B., and Parenti, M. (2009) G-protein-coupled receptors, cholesterol and palmitoylation: facts about fats. *J Mol Endocrinol* **42**, 371-379

14. Goddard, A. D., and Watts, A. Regulation of G protein-coupled receptors by palmitoylation and cholesterol. *BMC Biol* **10**, 27

15. Strader, C. D., Fong, T. M., Tota, M. R., Underwood, D., and Dixon, R. A. (1994) Structure and function of G protein-coupled receptors. *Annu Rev Biochem* **63**, 101-132

16. Conner, M., Hawtin, S. R., Simms, J., Wootten, D., Lawson, Z., Conner, A. C., Parslow, R. A., and Wheatley, M. (2007) Systematic analysis of the entire second extracellular loop of the V(1a) vasopressin receptor: key residues, conserved throughout a G-protein-coupled receptor family, identified. *J Biol Chem* **282**, 17405-17412

17. Rovati, G. E., Capra, V., and Neubig, R. R. (2007) The highly conserved DRY motif of class A G protein-coupled receptors: beyond the ground state. *Mol Pharmacol* **71**, 959-964

18. Chun, L., Zhang, W. H., and Liu, J. F. Structure and ligand recognition of class C GPCRs. *Acta Pharmacol Sin* **33**, 312-323

19. Hurley, J. B., Simon, M. I., Teplow, D. B., Robishaw, J. D., and Gilman, A. G. (1984) Homologies between signal transducing G proteins and ras gene products. *Science* **226**, 860-862

20. Wedegaertner, P. B., Wilson, P. T., and Bourne, H. R. (1995) Lipid modifications of trimeric G proteins. *J Biol Chem* **270**, 503-506

21. Liu, J. J., Horst, R., Katritch, V., Stevens, R. C., and Wuthrich, K. Biased signaling pathways in beta2-adrenergic receptor characterized by 19F-NMR. *Science* **335**, 1106-1110

22. Svoboda, P., Teisinger, J., Novotny, J., Bourova, L., Drmota, T., Hejnova, L., Moravcova, Z., Lisy, V., Rudajev, V., Stohr, J., Vokurkova, A., Svandova, I., and Durchankova, D. (2004) Biochemistry of transmembrane signaling mediated by trimeric G proteins. *Physiol Res* **53 Suppl 1**, S141-152

23. De Vries, L., Zheng, B., Fischer, T., Elenko, E., and Farquhar, M. G. (2000) The regulator of G protein signaling family. *Annu Rev Pharmacol Toxicol* **40**, 235-271

24. Downes, G. B., and Gautam, N. (1999) The G protein subunit gene families. *Genomics* **62**, 544-552

25. Jones, D. T., and Reed, R. R. (1989) Golf: an olfactory neuron specific-G protein involved in odorant signal transduction. *Science* **244**, 790-795

26. Lerea, C. L., Somers, D. E., Hurley, J. B., Klock, I. B., and Bunt-Milam, A. H. (1986) Identification of specific transducin alpha subunits in retinal rod and cone photoreceptors. *Science* **234**, 77-80

27. McLaughlin, S. K., McKinnon, P. J., and Margolskee, R. F. (1992) Gustducin is a taste-cell-specific G protein closely related to the transducins. *Nature* **357**, 563-569

28. Rozengurt, E. (2006) Taste receptors in the gastrointestinal tract. I. Bitter taste receptors and alpha-gustducin in the mammalian gut. *Am J Physiol Gastrointest Liver Physiol* **291**, G171-177

29. Fung, B. K., Hurley, J. B., and Stryer, L. (1981) Flow of information in the light-triggered cyclic nucleotide cascade of vision. *Proc Natl Acad Sci U S A* **78**, 152-156

30. Mellor, H., and Parker, P. J. (1998) The extended protein kinase C superfamily. *Biochem J* **332 (Pt 2)**, 281-292

31. Chin, D., and Means, A. R. (2000) Calmodulin: a prototypical calcium sensor. *Trends Cell Biol* **10**, 322-328

32. Siehler, S. (2009) Regulation of RhoGEF proteins by G12/13-coupled receptors. *Br J Pharmacol* **158**, 41-49

33. Conklin, B. R., Farfel, Z., Lustig, K. D., Julius, D., and Bourne, H. R. (1993) Substitution of three amino acids switches receptor specificity of Gq alpha to that of Gi alpha. *Nature* **363**, 274-276

34. Conklin, B. R., Herzmark, P., Ishida, S., Voyno-Yasenetskaya, T. A., Sun, Y., Farfel, Z., and Bourne, H. R. (1996) Carboxyl-terminal mutations of Gq alpha and Gs alpha that alter the fidelity of receptor activation. *Mol Pharmacol* **50**, 885-890

35. Urban, J. D., Clarke, W. P., von Zastrow, M., Nichols, D. E., Kobilka, B., Weinstein, H., Javitch, J. A., Roth, B. L., Christopoulos, A., Sexton, P. M., Miller, K. J., Spedding, M., and Mailman, R. B. (2007) Functional selectivity and classical concepts of quantitative pharmacology. *J Pharmacol Exp Ther* **320**, 1-13

36. Lee, S. P., So, C. H., Rashid, A. J., Varghese, G., Cheng, R., Lanca, A. J., O'Dowd, B. F., and George, S. R. (2004) Dopamine D1 and D2 receptor Co-activation

generates a novel phospholipase C-mediated calcium signal. *J Biol Chem* **279**, 35671-35678

37. Hurowitz, E. H., Melnyk, J. M., Chen, Y. J., Kouros-Mehr, H., Simon, M. I., and Shizuya, H. (2000) Genomic characterization of the human heterotrimeric G protein alpha, beta, and gamma subunit genes. *DNA Res* **7**, 111-120

38. Yan, K., Kalyanaraman, V., and Gautam, N. (1996) Differential ability to form the G protein betagamma complex among members of the beta and gamma subunit families. *J Biol Chem* **271**, 7141-7146

39. Dascal, N. (1997) Signalling via the G protein-activated K+ channels. *Cell Signal* **9**, 551-573

40. Boyer, J. L., Waldo, G. L., and Harden, T. K. (1992) Beta gamma-subunit activation of G-protein-regulated phospholipase C. *J Biol Chem* **267**, 25451-25456

41. Katz, A., Wu, D., and Simon, M. I. (1992) Subunits beta gamma of heterotrimeric G protein activate beta 2 isoform of phospholipase C. *Nature* **360**, 686-689

42. Kim, D., Lewis, D. L., Graziadei, L., Neer, E. J., Bar-Sagi, D., and Clapham, D. E. (1989) G-protein beta gamma-subunits activate the cardiac muscarinic K+-channel via phospholipase A2. *Nature* **337**, 557-560

43. Benovic, J. L., Pike, L. J., Cerione, R. A., Staniszewski, C., Yoshimasa, T., Codina, J., Caron, M. G., and Lefkowitz, R. J. (1985) Phosphorylation of the mammalian beta-adrenergic receptor by cyclic AMP-dependent protein kinase. Regulation of the rate of receptor phosphorylation and dephosphorylation by agonist occupancy and effects on coupling of the receptor to the stimulatory guanine nucleotide regulatory protein. *J Biol Chem* **260**, 7094-7101

44. Feng, B., Li, Z., and Wang, J. B. Protein kinase C-mediated phosphorylation of the mu-opioid receptor and its effects on receptor signaling. *Mol Pharmacol* **79**, 768-775

45. Benovic, J. L., Strasser, R. H., Caron, M. G., and Lefkowitz, R. J. (1986) Beta-adrenergic receptor kinase: identification of a novel protein kinase that phosphorylates the agonist-occupied form of the receptor. *Proc Natl Acad Sci U S A* **83**, 2797-2801

46. Penela, P., Ribas, C., and Mayor, F., Jr. (2003) Mechanisms of regulation of the expression and function of G protein-coupled receptor kinases. *Cell Signal* **15**, 973-981

47. Tobin, A. B. (2008) G-protein-coupled receptor phosphorylation: where, when and by whom. *Br J Pharmacol* **153 Suppl 1**, S167-176

48. Pitcher, J., Lohse, M. J., Codina, J., Caron, M. G., and Lefkowitz, R. J. (1992) Desensitization of the isolated beta 2-adrenergic receptor by beta-adrenergic receptor

kinase, cAMP-dependent protein kinase, and protein kinase C occurs via distinct molecular mechanisms. *Biochemistry* **31**, 3193-3197

49. Zamah, A. M., Delahunty, M., Luttrell, L. M., and Lefkowitz, R. J. (2002) Protein kinase A-mediated phosphorylation of the beta 2-adrenergic receptor regulates its coupling to Gs and Gi. Demonstration in a reconstituted system. *J Biol Chem* **277**, 31249-31256

50. Daaka, Y., Luttrell, L. M., and Lefkowitz, R. J. (1997) Switching of the coupling of the beta2-adrenergic receptor to different G proteins by protein kinase A. *Nature* **390**, 88-91

51. Friedman, J., Babu, B., and Clark, R. B. (2002) Beta(2)-adrenergic receptor lacking the cyclic AMP-dependent protein kinase consensus sites fully activates extracellular signal-regulated kinase 1/2 in human embryonic kidney 293 cells: lack of evidence for G(s)/G(i) switching. *Mol Pharmacol* **62**, 1094-1102

52. Lohse, M. J., Andexinger, S., Pitcher, J., Trukawinski, S., Codina, J., Faure, J. P., Caron, M. G., and Lefkowitz, R. J. (1992) Receptor-specific desensitization with purified proteins. Kinase dependence and receptor specificity of beta-arrestin and arrestin in the beta 2-adrenergic receptor and rhodopsin systems. *J Biol Chem* **267**, 8558-8564

53. Goodman, O. B., Jr., Krupnick, J. G., Santini, F., Gurevich, V. V., Penn, R. B., Gagnon, A. W., Keen, J. H., and Benovic, J. L. (1996) Beta-arrestin acts as a clathrin adaptor in endocytosis of the beta2-adrenergic receptor. *Nature* **383**, 447-450

54. Laporte, S. A., Oakley, R. H., Zhang, J., Holt, J. A., Ferguson, S. S., Caron, M. G., and Barak, L. S. (1999) The beta2-adrenergic receptor/betaarrestin complex recruits the clathrin adaptor AP-2 during endocytosis. *Proc Natl Acad Sci U S A* **96**, 3712-3717

55. Perry, S. J., Baillie, G. S., Kohout, T. A., McPhee, I., Magiera, M. M., Ang, K. L., Miller, W. E., McLean, A. J., Conti, M., Houslay, M. D., and Lefkowitz, R. J. (2002) Targeting of cyclic AMP degradation to beta 2-adrenergic receptors by beta-arrestins. *Science* **298**, 834-836

56. Nelson, C. D., Perry, S. J., Regier, D. S., Prescott, S. M., Topham, M. K., and Lefkowitz, R. J. (2007) Targeting of diacylglycerol degradation to M1 muscarinic receptors by beta-arrestins. *Science* **315**, 663-666

57. Luttrell, L. M., Roudabush, F. L., Choy, E. W., Miller, W. E., Field, M. E., Pierce, K. L., and Lefkowitz, R. J. (2001) Activation and targeting of extracellular signal-regulated kinases by beta-arrestin scaffolds. *Proc Natl Acad Sci U S A* **98**, 2449-2454

58. Milligan, G., and White, J. H. (2001) Protein-protein interactions at G-protein-coupled receptors. *Trends Pharmacol Sci* **22**, 513-518

59. Head, B. P., Patel, H. H., Roth, D. M., Murray, F., Swaney, J. S., Niesman, I. R., Farquhar, M. G., and Insel, P. A. (2006) Microtubules and actin microfilaments regulate lipid raft/caveolae localization of adenylyl cyclase signaling components. *J Biol Chem* **281**, 26391-26399

60. Burnstock, G. (2007) Physiology and pathophysiology of purinergic neurotransmission. *Physiol Rev* **87**, 659-797

61. Jacobson, K. A., and Gao, Z. G. (2006) Adenosine receptors as therapeutic targets. *Nat Rev Drug Discov* **5**, 247-264

62. Inbe, H., Watanabe, S., Miyawaki, M., Tanabe, E., and Encinas, J. A. (2004) Identification and characterization of a cell-surface receptor, P2Y15, for AMP and adenosine. *J Biol Chem* **279**, 19790-19799

63. Abbracchio, M. P., Burnstock, G., Boeynaems, J. M., Barnard, E. A., Boyer, J. L., Kennedy, C., Miras-Portugal, M. T., King, B. F., Gachet, C., Jacobson, K. A., and Weisman, G. A. (2005) The recently deorphanized GPR80 (GPR99) proposed to be the P2Y15 receptor is not a genuine P2Y receptor. *Trends Pharmacol Sci* **26**, 8-9

64. Qi, A. D., Harden, T. K., and Nicholas, R. A. (2004) GPR80/99, proposed to be the P2Y(15) receptor activated by adenosine and AMP, is not a P2Y receptor. *Purinergic Signal* **1**, 67-74

65. Bruns, R. F. (1980) Adenosine receptor activation by adenine nucleotides requires conversion of the nucleotides to adenosine. *Naunyn Schmiedebergs Arch Pharmacol* **315**, 5-13

66. Salter, M. W., and Henry, J. L. (1985) Effects of adenosine 5'-monophosphate and adenosine 5'-triphosphate on functionally identified units in the cat spinal dorsal horn. Evidence for a differential effect of adenosine 5'-triphosphate on nociceptive vs non-nociceptive units. *Neuroscience* **15**, 815-825

67. Dunwiddie, T. V., Diao, L., and Proctor, W. R. (1997) Adenine nucleotides undergo rapid, quantitative conversion to adenosine in the extracellular space in rat hippocampus. *J Neurosci* **17**, 7673-7682

68. Gao, N., Hu, H. Z., Liu, S., Gao, C., Xia, Y., and Wood, J. D. (2007) Stimulation of adenosine A1 and A2A receptors by AMP in the submucosal plexus of guinea pig small intestine. *Am J Physiol Gastrointest Liver Physiol* **292**, G492-500

69. Daniels, I. S., Zhang, J., O'Brien, W. G., 3rd, Tao, Z., Miki, T., Zhao, Z., Blackburn, M. R., and Lee, C. C. (2010) A role of erythrocytes in adenosine monophosphate initiation of hypometabolism in mammals. *J Biol Chem* **285**, 20716-20723

70. Sowa, N. A., Voss, M. K., and Zylka, M. J. (2010) Recombinant ecto-5'-nucleotidase (CD73) has long lasting antinociceptive effects that are dependent on adenosine A1 receptor activation. *Mol Pain* **6**, 20

71. Ragazzi, E., Wu, S. N., Shryock, J., and Belardinelli, L. (1991) Electrophysiological and receptor binding studies to assess activation of the cardiac adenosine receptor by adenine nucleotides. *Circ Res* **68**, 1035-1044

72. Patterson, S. L., Sluka, K. A., and Arnold, M. A. (2001) A novel transverse push-pull microprobe: in vitro characterization and in vivo demonstration of the enzymatic production of adenosine in the spinal cord dorsal horn. *J Neurochem* **76**, 234-246

73. Moody, C. J., Meghji, P., and Burnstock, G. (1984) Stimulation of P1-purinoceptors by ATP depends partly on its conversion to AMP and adenosine and partly on direct action. *Eur J Pharmacol* **97**, 47-54

74. Mustafa, S. J., Nadeem, A., Fan, M., Zhong, H., Belardinelli, L., and Zeng, D. (2007) Effect of a specific and selective A(2B) adenosine receptor antagonist on adenosine agonist AMP and allergen-induced airway responsiveness and cellular influx in a mouse model of asthma. *J Pharmacol Exp Ther* **320**, 1246-1251

75. Zylka, M. J. (2011) Pain-relieving prospects for adenosine receptors and ectonucleotidases. *Trends Mol Med* **17**, 188-196

76. Zylka, M. J., Sowa, N. A., Taylor-Blake, B., Twomey, M. A., Herrala, A., Voikar, V., and Vihko, P. (2008) Prostatic acid phosphatase is an ectonucleotidase and suppresses pain by generating adenosine. *Neuron* **60**, 111-122

77. Zimmermann, H. (2000) Extracellular metabolism of ATP and other nucleotides. *Naunyn Schmiedebergs Arch Pharmacol* **362**, 299-309

78. Ohkubo, S., Kimura, J., and Matsuoka, I. (2000) Ecto-alkaline phosphatase in NG108-15 cells : a key enzyme mediating P1 antagonist-sensitive ATP response. *Br J Pharmacol* **131**, 1667-1672

79. Street, S. E., Walsh, P. L., Sowa, N. A., Taylor-Blake, B., Guillot, T. S., Vihko, P., Wightman, R. M., and Zylka, M. J. (2011) PAP and NT5E inhibit nociceptive neurotransmission by rapidly hydrolyzing nucleotides to adenosine. *Mol Pain* **7**, 80

80. Arcuino, G., Lin, J. H., Takano, T., Liu, C., Jiang, L., Gao, Q., Kang, J., and Nedergaard, M. (2002) Intercellular calcium signaling mediated by point-source burst release of ATP. *Proc Natl Acad Sci U S A* **99**, 9840-9845

81. Halassa, M. M., Florian, C., Fellin, T., Munoz, J. R., Lee, S. Y., Abel, T., Haydon, P. G., and Frank, M. G. (2009) Astrocytic modulation of sleep homeostasis and cognitive consequences of sleep loss. *Neuron* **61**, 213-219

82. Zhang, J., Kaasik, K., Blackburn, M. R., and Lee, C. C. (2006) Constant darkness is a circadian metabolic signal in mammals. *Nature* **439**, 340-343

83. Dulla, C. G., Dobelis, P., Pearson, T., Frenguelli, B. G., Staley, K. J., and Masino, S. A. (2005) Adenosine and ATP link PCO2 to cortical excitability via pH. *Neuron* **48**, 1011-1023

84. Zhang, J. Y., Nawoschik, S., Kowal, D., Smith, D., Spangler, T., Ochalski, R., Schechter, L., and Dunlop, J. (2003) Characterization of the 5-HT6 receptor coupled to Ca2+ signaling using an enabling chimeric G-protein. *Eur J Pharmacol* **472**, 33-38

85. Coward, P., Chan, S. D., Wada, H. G., Humphries, G. M., and Conklin, B. R. (1999) Chimeric G proteins allow a high-throughput signaling assay of Gi-coupled receptors. *Anal Biochem* **270**, 242-248

86. Polleux, F., and Ghosh, A. (2002) The slice overlay assay: a versatile tool to study the influence of extracellular signals on neuronal development. *Sci STKE* **2002**, pl9

87. Cooper, J., Hill, S. J., and Alexander, S. P. (1997) An endogenous A2B adenosine receptor coupled to cyclic AMP generation in human embryonic kidney (HEK 293) cells. *Br J Pharmacol* **122**, 546-550

88. Naito, Y., and Lowenstein, J. M. (1985) 5'-Nucleotidase from rat heart membranes. Inhibition by adenine nucleotides and related compounds. *Biochem J* **226**, 645-651

89. Gerwins, P., Nordstedt, C., and Fredholm, B. B. (1990) Characterization of adenosine A1 receptors in intact DDT1 MF-2 smooth muscle cells. *Mol Pharmacol* **38**, 660-666

90. Schachter, J. B., Sromek, S. M., Nicholas, R. A., and Harden, T. K. (1997) HEK293 human embryonic kidney cells endogenously express the P2Y1 and P2Y2 receptors. *Neuropharmacology* **36**, 1181-1187

91. Nakata, H., Yoshioka, K., Kamiya, T., Tsuga, H., and Oyanagi, K. (2005) Functions of heteromeric association between adenosine and P2Y receptors. *J Mol Neurosci* **26**, 233-238

92. Yoshioka, K., Saitoh, O., and Nakata, H. (2001) Heteromeric association creates a P2Y-like adenosine receptor. *Proc Natl Acad Sci U S A* **98**, 7617-7622

93. Suzuki, T., Namba, K., Tsuga, H., and Nakata, H. (2006) Regulation of pharmacology by hetero-oligomerization between A1 adenosine receptor and P2Y2 receptor. *Biochem Biophys Res Commun* **351**, 559-565

94. Boyer, J. L., Siddiqi, S., Fischer, B., Romero-Avila, T., Jacobson, K. A., and Harden, T. K. (1996) Identification of potent P2Y-purinoceptor agonists that are derivatives of adenosine 5'-monophosphate. *Br J Pharmacol* **118**, 1959-1964

95. Olah, M. E., Ren, H., Ostrowski, J., Jacobson, K. A., and Stiles, G. L. (1992) Cloning, expression, and characterization of the unique bovine A1 adenosine receptor. Studies on the ligand binding site by site-directed mutagenesis. *J Biol Chem* **267**, 10764-10770

96. Schenone, S., Brullo, C., Musumeci, F., Bruno, O., and Botta, M. (2010) A1 receptors ligands: past, present and future trends. *Curr Top Med Chem* **10**, 878-901

97. Fredholm, B. B., AP, I. J., Jacobson, K. A., Klotz, K. N., and Linden, J. (2001) International Union of Pharmacology. XXV. Nomenclature and classification of adenosine receptors. *Pharmacol Rev* **53**, 527-552

98. Elzein, E., and Zablocki, J. (2008) A1 adenosine receptor agonists and their potential therapeutic applications. *Expert Opin Investig Drugs* **17**, 1901-1910

99. Ashton, T. D., Baker, S. P., Hutchinson, S. A., and Scammells, P. J. (2008) N6-substituted C5'-modified adenosines as A1 adenosine receptor agonists. *Bioorg Med Chem* **16**, 1861-1873

100. Cappellacci, L., Franchetti, P., Vita, P., Petrelli, R., Lavecchia, A., Costa, B., Spinetti, F., Martini, C., Klotz, K. N., and Grifantini, M. (2008) 5'-Carbamoyl derivatives of 2'-C-methyl-purine nucleosides as selective A1 adenosine receptor agonists: affinity, efficacy, and selectivity for A1 receptor from different species. *Bioorg Med Chem* **16**, 336-353

101. Dalpiaz, A., Scatturin, A., Menegatti, E., Bortolotti, F., Pavan, B., Biondi, C., Durini, E., and Manfredini, S. (2001) Synthesis and study of 5'-ester prodrugs of N6-cyclopentyladenosine, a selective A1 receptor agonist. *Pharm Res* **18**, 531-536

102. Maillard, M. C., Nikodijevic, O., LaNoue, K. F., Berkich, D., Ji, X. D., Bartus, R., and Jacobson, K. A. (1994) Adenosine receptor prodrugs: synthesis and biological activity of derivatives of potent, A1-selective agonists. *J Pharm Sci* **83**, 46-53

103. Lee, K. S., Schubert, P., Emmert, H., and Kreutzberg, G. W. (1981) Effect of adenosine versus adenine nucleotides on evoked potentials in a rat hippocampal slice preparation. *Neurosci Lett* **23**, 309-314

104. Pirotton, S., and Boeynaems, J. M. (1993) Evidence that ATP, ADP and AMP are not ligands of the striatal adenosine A2A receptors. *Eur J Pharmacol* **241**, 55-61

105. Zhou, S. Y., Mamdani, M., Qanud, K., Shen, J. B., Pappano, A. J., Kumar, T. S., Jacobson, K. A., Hintze, T., Recchia, F. A., and Liang, B. T. (2010) Treatment of heart failure by a methanocarba derivative of adenosine monophosphate: implication for a role of cardiac purinergic P2X receptors. *J Pharmacol Exp Ther* **333**, 920-928

106. Kumar, T. S., Zhou, S. Y., Joshi, B. V., Balasubramanian, R., Yang, T., Liang, B. T., and Jacobson, K. A. (2010) Structure-activity relationship of (N)-Methanocarba phosphonate analogues of 5'-AMP as cardioprotective agents acting through a cardiac P2X receptor. *J Med Chem* **53**, 2562-2576

107. El-Tayeb, A., Iqbal, J., Behrenswerth, A., Romio, M., Schneider, M., Zimmermann, H., Schrader, J., and Muller, C. E. (2009) Nucleoside-5'-monophosphates as prodrugs

of adenosine A(2A) receptor agonists activated by ecto-5'-nucleotidase. *J Med Chem* **52**, 7669-7677

108. Hurt, J. K., and Zylka, M. J. PAPupuncture has localized and long-lasting antinociceptive effects in mouse models of acute and chronic pain. *Mol Pain* **8**, 28

109. Goldman, N., Chen, M., Fujita, T., Xu, Q., Peng, W., Liu, W., Jensen, T. K., Pei, Y., Wang, F., Han, X., Chen, J. F., Schnermann, J., Takano, T., Bekar, L., Tieu, K., and Nedergaard, M. Adenosine A1 receptors mediate local anti-nociceptive effects of acupuncture. *Nat Neurosci* **13**, 883-888

110. Rittiner, J. E., Korboukh, I., Hull-Ryde, E. A., Jin, J., Janzen, W. P., Frye, S. V., and Zylka, M. J. AMP is an adenosine A1 receptor agonist. *J Biol Chem* **287**, 5301-5309

111. Korboukh, I., Hull-Ryde, E. A., Rittiner, J. E., Randhawa, A. S., Coleman, J., Fitzpatrick, B. J., Setola, V., Janzen, W. P., Frye, S. V., Zylka, M. J., and Jin, J. Orally active adenosine A(1) receptor agonists with antinociceptive effects in mice. *J Med Chem* **55**, 6467-6477

112. Cordeaux, Y., Ijzerman, A. P., and Hill, S. J. (2004) Coupling of the human A1 adenosine receptor to different heterotrimeric G proteins: evidence for agonist-specific G protein activation. *Br J Pharmacol* **143**, 705-714

113. Sowa, N. A., Street, S. E., Vihko, P., and Zylka, M. J. Prostatic acid phosphatase reduces thermal sensitivity and chronic pain sensitization by depleting phosphatidylinositol 4,5-bisphosphate. *J Neurosci* **30**, 10282-10293

114. Klotz, K. N., Hessling, J., Hegler, J., Owman, C., Kull, B., Fredholm, B. B., and Lohse, M. J. (1998) Comparative pharmacology of human adenosine receptor subtypes - characterization of stably transfected receptors in CHO cells. *Naunyn Schmiedebergs Arch Pharmacol* **357**, 1-9

115. Vittori, S., Lorenzen, A., Stannek, C., Costanzi, S., Volpini, R., AP, I. J., Kunzel, J. K., and Cristalli, G. (2000) N-cycloalkyl derivatives of adenosine and 1-deazaadenosine as agonists and partial agonists of the A(1) adenosine receptor. *J Med Chem* **43**, 250-260

116. Linden, J., Thai, T., Figler, H., Jin, X., and Robeva, A. S. (1999) Characterization of human A(2B) adenosine receptors: radioligand binding, western blotting, and coupling to G(q) in human embryonic kidney 293 cells and HMC-1 mast cells. *Mol Pharmacol* **56**, 705-713

117. Gao, Z., Chen, T., Weber, M. J., and Linden, J. (1999) A2B adenosine and P2Y2 receptors stimulate mitogen-activated protein kinase in human embryonic kidney-293 cells. cross-talk between cyclic AMP and protein kinase c pathways. *J Biol Chem* **274**, 5972-5980

118. Feoktistov, I., and Biaggioni, I. (1995) Adenosine A2b receptors evoke interleukin-8 secretion in human mast cells. An enprofylline-sensitive mechanism with implications for asthma. *J Clin Invest* **96**, 1979-1986

119. Simmons, M. A. (2005) Functional selectivity, ligand-directed trafficking, conformation-specific agonism: what's in a name? *Mol Interv* **5**, 154-157

120. Gay, E. A., Urban, J. D., Nichols, D. E., Oxford, G. S., and Mailman, R. B. (2004) Functional selectivity of D2 receptor ligands in a Chinese hamster ovary hD2L cell line: evidence for induction of ligand-specific receptor states. *Mol Pharmacol* **66**, 97-105

121. Chen, X., Sassano, M. F., Zheng, L., Setola, V., Chen, M., Bai, X., Frye, S. V., Wetsel, W. C., Roth, B. L., and Jin, J. Structure-functional selectivity relationship studies of beta-arrestin-biased dopamine D(2) receptor agonists. *J Med Chem* **55**, 7141-7153

122. Rives, M. L., Rossillo, M., Liu-Chen, L. Y., and Javitch, J. A. 6'-Guanidinonaltrindole (6'-GNTI) is a G protein-biased kappa-opioid receptor agonist that inhibits arrestin recruitment. *J Biol Chem* **287**, 27050-27054

123. Kaya, A. I., Onaran, H. O., Ozcan, G., Ambrosio, C., Costa, T., Balli, S., and Ugur, O. Cell contact-dependent functional selectivity of beta2-adrenergic receptor ligands in stimulating cAMP accumulation and extracellular signal-regulated kinase phosphorylation. *J Biol Chem* **287**, 6362-6374

124. Busnelli, M., Sauliere, A., Manning, M., Bouvier, M., Gales, C., and Chini, B. Functional selective oxytocin-derived agonists discriminate between individual G protein family subtypes. *J Biol Chem* **287**, 3617-3629

125. Atwood, B. K., Wager-Miller, J., Haskins, C., Straiker, A., and Mackie, K. Functional selectivity in CB(2) cannabinoid receptor signaling and regulation: implications for the therapeutic potential of CB(2) ligands. *Mol Pharmacol* **81**, 250-263

126. Verzijl, D., and Ijzerman, A. P. Functional selectivity of adenosine receptor ligands. *Purinergic Signal* **7**, 171-192

127. Tupone, D., Madden, C. J., and Morrison, S. F. Central Activation of the A1 Adenosine Receptor (A1AR) Induces a Hypothermic, Torpor-Like State in the Rat. *J Neurosci* **33**, 14512-14525

128. Luttrell, L. M., and Lefkowitz, R. J. (2002) The role of beta-arrestins in the termination and transduction of G-protein-coupled receptor signals. *J Cell Sci* **115**, 455-465

129. van Blitterswijk, W. J., and Houssa, B. (2000) Properties and functions of diacylglycerol kinases. *Cell Signal* **12**, 595-605

130. Sakane, F., Imai, S., Kai, M., Yasuda, S., and Kanoh, H. (2007) Diacylglycerol kinases: why so many of them? *Biochim Biophys Acta* **1771**, 793-806

131. Jose Lopez-Andreo, M., Gomez-Fernandez, J. C., and Corbalan-Garcia, S. (2003) The simultaneous production of phosphatidic acid and diacylglycerol is essential for the translocation of protein kinase Cepsilon to the plasma membrane in RBL-2H3 cells. *Mol Biol Cell* **14**, 4885-4895

132. Lucas, P., Ukhanov, K., Leinders-Zufall, T., and Zufall, F. (2003) A diacylglycerol-gated cation channel in vomeronasal neuron dendrites is impaired in TRPC2 mutant mice: mechanism of pheromone transduction. *Neuron* **40**, 551-561

133. Gregg, L. C., Jung, K. M., Spradley, J. M., Nyilas, R., Suplita, R. L., 2nd, Zimmer, A., Watanabe, M., Mackie, K., Katona, I., Piomelli, D., and Hohmann, A. G. Activation of type 5 metabotropic glutamate receptors and diacylglycerol lipase-alpha initiates 2-arachidonoylglycerol formation and endocannabinoid-mediated analgesia. *J Neurosci* **32**, 9457-9468

134. Jenkins, G. H., Fisette, P. L., and Anderson, R. A. (1994) Type I phosphatidylinositol 4-phosphate 5-kinase isoforms are specifically stimulated by phosphatidic acid. *J Biol Chem* **269**, 11547-11554

135. Merida, I., Avila-Flores, A., and Merino, E. (2008) Diacylglycerol kinases: at the hub of cell signalling. *Biochem J* **409**, 1-18

136. Baum, A. E., Akula, N., Cabanero, M., Cardona, I., Corona, W., Klemens, B., Schulze, T. G., Cichon, S., Rietschel, M., Nothen, M. M., Georgi, A., Schumacher, J., Schwarz, M., Abou Jamra, R., Hofels, S., Propping, P., Satagopan, J., Detera-Wadleigh, S. D., Hardy, J., and McMahon, F. J. (2008) A genome-wide association study implicates diacylglycerol kinase eta (DGKH) and several other genes in the etiology of bipolar disorder. *Mol Psychiatry* **13**, 197-207

137. Takata, A., Kawasaki, H., Iwayama, Y., Yamada, K., Gotoh, L., Mitsuyasu, H., Miura, T., Kato, T., Yoshikawa, T., and Kanba, S. Nominal association between a polymorphism in DGKH and bipolar disorder detected in a meta-analysis of East Asian case-control samples. *Psychiatry Clin Neurosci* **65**, 280-285

138. Weber, H., Kittel-Schneider, S., Gessner, A., Domschke, K., Neuner, M., Jacob, C. P., Buttenschon, H. N., Boreatti-Hummer, A., Volkert, J., Herterich, S., Baune, B. T., Gross-Lesch, S., Kopf, J., Kreiker, S., Nguyen, T. T., Weissflog, L., Arolt, V., Mors, O., Deckert, J., Lesch, K. P., and Reif, A. Cross-disorder analysis of bipolar risk genes: further evidence of DGKH as a risk gene for bipolar disorder, but also unipolar depression and adult ADHD. *Neuropsychopharmacology* **36**, 2076-2085

139. Yosifova, A., Mushiroda, T., Kubo, M., Takahashi, A., Kamatani, Y., Kamatani, N., Stoianov, D., Vazharova, R., Karachanak, S., Zaharieva, I., Dimova, I., Hadjidekova, S., Milanova, V., Madjirova, N., Gerdjikov, I., Tolev, T., Poryazova, N., O'Donovan, M. C., Owen, M. J., Kirov, G., Toncheva, D., and Nakamura, Y. Genome-wide

association study on bipolar disorder in the Bulgarian population. *Genes Brain Behav* **10**, 789-797

140. Squassina, A., Manchia, M., Congiu, D., Severino, G., Chillotti, C., Ardau, R., Piccardi, M., and Zompo, M. D. (2009) The diacylglycerol kinase eta gene and bipolar disorder: a replication study in a Sardinian sample. *Mol Psychiatry* **14**, 350-351

141. Zeng, Z., Wang, T., Li, T., Li, Y., Chen, P., Zhao, Q., Liu, J., Li, J., Feng, G., He, L., and Shi, Y. Common SNPs and haplotypes in DGKH are associated with bipolar disorder and schizophrenia in the Chinese Han population. *Mol Psychiatry* **16**, 473-475

142. Moya, P. R., Murphy, D. L., McMahon, F. J., and Wendland, J. R. Increased gene expression of diacylglycerol kinase eta in bipolar disorder. *Int J Neuropsychopharmacol* **13**, 1127-1128

143. Murakami, T., Sakane, F., Imai, S., Houkin, K., and Kanoh, H. (2003) Identification and characterization of two splice variants of human diacylglycerol kinase eta. *J Biol Chem* **278**, 34364-34372

144. Klauck, T. M., Xu, X., Mousseau, B., and Jaken, S. (1996) Cloning and characterization of a glucocorticoid-induced diacylglycerol kinase. *J Biol Chem* **271**, 19781-19788

145. Sakai, H., and Sakane, F. Recent progress on type II diacylglycerol kinases: the physiological functions of diacylglycerol kinase delta, eta and kappa and their involvement in disease. *J Biochem* **152**, 397-406

146. Nakano, T., Iravani, A., Kim, M., Hozumi, Y., Lohse, M., Reichert, E., Crotty, T. M., Stafforini, D. M., and Topham, M. K. Diacylglycerol kinase eta modulates oncogenic properties of lung cancer cells. *Clin Transl Oncol*

147. Catapano, L. A., and Manji, H. K. (2007) G protein-coupled receptors in major psychiatric disorders. *Biochim Biophys Acta* **1768**, 976-993

148. Pantazopoulos, H., Stone, D., Walsh, J., and Benes, F. M. (2004) Differences in the cellular distribution of D1 receptor mRNA in the hippocampus of bipolars and schizophrenics. *Synapse* **54**, 147-155

149. Young, L. T., Li, P. P., Kish, S. J., Siu, K. P., Kamble, A., Hornykiewicz, O., and Warsh, J. J. (1993) Cerebral cortex Gs alpha protein levels and forskolin-stimulated cyclic AMP formation are increased in bipolar affective disorder. *J Neurochem* **61**, 890-898

150. Rao, J. S., Rapoport, S. I., and Kim, H. W. (2009) Decreased GRK3 but not GRK2 expression in frontal cortex from bipolar disorder patients. *Int J Neuropsychopharmacol* **12**, 851-860

151. Friedman, E., and Wang, H. Y. (1996) Receptor-mediated activation of G proteins is increased in postmortem brains of bipolar affective disorder subjects. *J Neurochem* **67**, 1145-1152

152. Avissar, S., Schreiber, G., Danon, A., and Belmaker, R. H. (1988) Lithium inhibits adrenergic and cholinergic increases in GTP binding in rat cortex. *Nature* **331**, 440-442

153. Hahn, C. G., Umapathy, Wang, H. Y., Koneru, R., Levinson, D. F., and Friedman, E. (2005) Lithium and valproic acid treatments reduce PKC activation and receptor-G protein coupling in platelets of bipolar manic patients. *J Psychiatr Res* **39**, 355-363

154. Luo, J., Busillo, J. M., and Benovic, J. L. (2008) M3 muscarinic acetylcholine receptor-mediated signaling is regulated by distinct mechanisms. *Mol Pharmacol* **74**, 338-347

155. Sherrill, J. D., Stropes, M. P., Schneider, O. D., Koch, D. E., Bittencourt, F. M., Miller, J. L., and Miller, W. E. (2009) Activation of intracellular signaling pathways by the murine cytomegalovirus G protein-coupled receptor M33 occurs via PLC-{beta}/PKC-dependent and -independent mechanisms. *J Virol* **83**, 8141-8152

156. Kanoh, H., Sakane, F., and Yamada, K. (1992) Diacylglycerol kinase isozymes from brain and lymphoid tissues. *Methods Enzymol* **209**, 162-172

157. Ohanian, J., and Heagerty, A. M. (1994) Membrane-associated diacylglycerol kinase activity is increased by noradrenaline, but not by angiotensin II, in arterial smooth muscle. *Biochem J* **300 (Pt 1)**, 51-56

158. Tobin, A. B., Lambert, D. G., and Nahorski, S. R. (1992) Rapid desensitization of muscarinic m3 receptor-stimulated polyphosphoinositide responses. *Mol Pharmacol* **42**, 1042-1048

159. Tobin, A. B., and Nahorski, S. R. (1993) Rapid agonist-mediated phosphorylation of m3-muscarinic receptors revealed by immunoprecipitation. *J Biol Chem* **268**, 9817-9823

160. Shockley, M. S., Tolbert, L. M., Tobin, A. B., Nahorski, S. R., Sadee, W., and Lameh, J. (1999) Differential regulation of muscarinic M1 and M3 receptors by a putative phosphorylation domain. *Eur J Pharmacol* **377**, 137-146

161. Thangaraju, A., and Sawyer, G. W. Comparison of the kinetics and extent of muscarinic M1-M5 receptor internalization, recycling and downregulation in Chinese hamster ovary cells. *Eur J Pharmacol* **650**, 534-543

162. Rumenapp, U., Asmus, M., Schablowski, H., Woznicki, M., Han, L., Jakobs, K. H., Fahimi-Vahid, M., Michalek, C., Wieland, T., and Schmidt, M. (2001) The M3 muscarinic acetylcholine receptor expressed in HEK-293 cells signals to phospholipase D via G12 but not Gq-type G proteins: regulators of G proteins as tools

to dissect pertussis toxin-resistant G proteins in receptor-effector coupling. *J Biol Chem* **276**, 2474-2479

163. Yamada, K., Sakane, F., Imai, S., Tsushima, S., Murakami, T., and Kanoh, H. (2003) Regulatory role of diacylglycerol kinase gamma in macrophage differentiation of leukemia cells. *Biochem Biophys Res Commun* **305**, 101-107

164. Tewson, P. H., Quinn, A. M., and Hughes, T. E. A Multiplexed Fluorescent Assay for Independent Second-Messenger Systems: Decoding GPCR Activation in Living Cells. *J Biomol Screen* **18**, 797-806

165. Jackson, T. R., Patterson, S. I., Thastrup, O., and Hanley, M. R. (1988) A novel tumour promoter, thapsigargin, transiently increases cytoplasmic free Ca2+ without generation of inositol phosphates in NG115-401L neuronal cells. *Biochem J* **253**, 81-86

166. Verkhratsky, A. (2005) Physiology and pathophysiology of the calcium store in the endoplasmic reticulum of neurons. *Physiol Rev* **85**, 201-279

167. Venkatachalam, K., van Rossum, D. B., Patterson, R. L., Ma, H. T., and Gill, D. L. (2002) The cellular and molecular basis of store-operated calcium entry. *Nat Cell Biol* **4**, E263-272

168. Smyth, J. T., Hwang, S. Y., Tomita, T., DeHaven, W. I., Mercer, J. C., and Putney, J. W. Activation and regulation of store-operated calcium entry. *J Cell Mol Med* **14**, 2337-2349

169. Matsutomo, D., Isozaki, T., Sakai, H., and Sakane, F. Osmotic shock-dependent redistribution of diacylglycerol kinase eta1 to non-ionic detergent-resistant membrane via pleckstrin homology and C1 domains. *J Biochem* **153**, 179-190

170. Kelly, E., Bailey, C. P., and Henderson, G. (2008) Agonist-selective mechanisms of GPCR desensitization. *Br J Pharmacol* **153 Suppl 1**, S379-388

171. Krasel, C., Dammeier, S., Winstel, R., Brockmann, J., Mischak, H., and Lohse, M. J. (2001) Phosphorylation of GRK2 by protein kinase C abolishes its inhibition by calmodulin. *J Biol Chem* **276**, 1911-1915

172. Blumberg, P. M. (1988) Protein kinase C as the receptor for the phorbol ester tumor promoters: sixth Rhoads memorial award lecture. *Cancer Res* **48**, 1-8

173. Tang, H., Shirai, H., and Inagami, T. (1995) Inhibition of protein kinase C prevents rapid desensitization of type 1B angiotensin II receptor. *Circ Res* **77**, 239-248

174. Gereau, R. W. t., and Heinemann, S. F. (1998) Role of protein kinase C phosphorylation in rapid desensitization of metabotropic glutamate receptor 5. *Neuron* **20**, 143-151

175. Rodriguez-Rodriguez, R., Yarova, P., Winter, P., and Dora, K. A. (2009) Desensitization of endothelial P2Y1 receptors by PKC-dependent mechanisms in pressurized rat small mesenteric arteries. *Br J Pharmacol* **158**, 1609-1620

176. Thibault, D., Albert, P. R., Pineyro, G., and Trudeau, L. E. Neurotensin triggers dopamine D2 receptor desensitization through a protein kinase C and beta-arrestin1-dependent mechanism. *J Biol Chem* **286**, 9174-9184

177. Leaney, J. L., Dekker, L. V., and Tinker, A. (2001) Regulation of a G protein-gated inwardly rectifying K+ channel by a Ca(2+)-independent protein kinase C. *J Physiol* **534**, 367-379

178. Nishizuka, Y. (1984) The role of protein kinase C in cell surface signal transduction and tumour promotion. *Nature* **308**, 693-698

179. Keranen, L. M., Dutil, E. M., and Newton, A. C. (1995) Protein kinase C is regulated in vivo by three functionally distinct phosphorylations. *Curr Biol* **5**, 1394-1403

180. Newton, A. C. (2003) Regulation of the ABC kinases by phosphorylation: protein kinase C as a paradigm. *Biochem J* **370**, 361-371

181. Brown, S. G., Thomas, A., Dekker, L. V., Tinker, A., and Leaney, J. L. (2005) PKC-delta sensitizes Kir3.1/3.2 channels to changes in membrane phospholipid levels after M3 receptor activation in HEK-293 cells. *Am J Physiol Cell Physiol* **289**, C543-556

182. Sumandea, M. P., Rybin, V. O., Hinken, A. C., Wang, C., Kobayashi, T., Harleton, E., Sievert, G., Balke, C. W., Feinmark, S. J., Solaro, R. J., and Steinberg, S. F. (2008) Tyrosine phosphorylation modifies protein kinase C delta-dependent phosphorylation of cardiac troponin I. *J Biol Chem* **283**, 22680-22689

183. Iwabu, A., Smith, K., Allen, F. D., Lauffenburger, D. A., and Wells, A. (2004) Epidermal growth factor induces fibroblast contractility and motility via a protein kinase C delta-dependent pathway. *J Biol Chem* **279**, 14551-14560

184. Violin, J. D., Zhang, J., Tsien, R. Y., and Newton, A. C. (2003) A genetically encoded fluorescent reporter reveals oscillatory phosphorylation by protein kinase C. *J Cell Biol* **161**, 899-909

185. Dickson, E. J., Falkenburger, B. H., and Hille, B. Quantitative properties and receptor reserve of the IP(3) and calcium branch of G(q)-coupled receptor signaling. *J Gen Physiol* **141**, 521-535

186. Kong, K. C., Butcher, A. J., McWilliams, P., Jones, D., Wess, J., Hamdan, F. F., Werry, T., Rosethorne, E. M., Charlton, S. J., Munson, S. E., Cragg, H. A., Smart, A. D., and Tobin, A. B. M3-muscarinic receptor promotes insulin release via receptor phosphorylation/arrestin-dependent activation of protein kinase D1. *Proc Natl Acad Sci U S A* **107**, 21181-21186

187. Malhotra, R., D'Souza, K. M., Staron, M. L., Birukov, K. G., Bodi, I., and Akhter, S. A. G alpha(q)-mediated activation of GRK2 by mechanical stretch in cardiac myocytes: the role of protein kinase C. *J Biol Chem* **285**, 13748-13760

188. Yang, X. L., Zhang, Y. L., Lai, Z. S., Xing, F. Y., and Liu, Y. H. (2003) Pleckstrin homology domain of G protein-coupled receptor kinase-2 binds to PKC and affects the activity of PKC kinase. *World J Gastroenterol* **9**, 800-803

189. Crotty, T., Cai, J., Sakane, F., Taketomi, A., Prescott, S. M., and Topham, M. K. (2006) Diacylglycerol kinase delta regulates protein kinase C and epidermal growth factor receptor signaling. *Proc Natl Acad Sci U S A* **103**, 15485-15490

190. Cai, J., Crotty, T. M., Reichert, E., Carraway, K. L., 3rd, Stafforini, D. M., and Topham, M. K. Diacylglycerol kinase delta and protein kinase C(alpha) modulate epidermal growth factor receptor abundance and degradation through ubiquitin-specific protease 8. *J Biol Chem* **285**, 6952-6959

191. van Baal, J., de Widt, J., Divecha, N., and van Blitterswijk, W. J. Diacylglycerol kinase theta counteracts protein kinase C-mediated inactivation of the EGF receptor. *Int J Biochem Cell Biol* **44**, 1791-1799

192. Friedman, E., Hoau Yan, W., Levinson, D., Connell, T. A., and Singh, H. (1993) Altered platelet protein kinase C activity in bipolar affective disorder, manic episode. *Biol Psychiatry* **33**, 520-525

193. Wang, H. Y., Markowitz, P., Levinson, D., Undie, A. S., and Friedman, E. (1999) Increased membrane-associated protein kinase C activity and translocation in blood platelets from bipolar affective disorder patients. *J Psychiatr Res* **33**, 171-179

194. Hahn, C. G., and Friedman, E. (1999) Abnormalities in protein kinase C signaling and the pathophysiology of bipolar disorder. *Bipolar Disord* **1**, 81-86

195. Zarate, C. A., and Manji, H. K. (2009) Protein kinase C inhibitors: rationale for use and potential in the treatment of bipolar disorder. *CNS Drugs* **23**, 569-582

196. Kulkarni, J., Garland, K. A., Scaffidi, A., Headey, B., Anderson, R., de Castella, A., Fitzgerald, P., and Davis, S. R. (2006) A pilot study of hormone modulation as a new treatment for mania in women with bipolar affective disorder. *Psychoneuroendocrinology* **31**, 543-547

197. Bebchuk, J. M., Arfken, C. L., Dolan-Manji, S., Murphy, J., Hasanat, K., and Manji, H. K. (2000) A preliminary investigation of a protein kinase C inhibitor in the treatment of acute mania. *Arch Gen Psychiatry* **57**, 95-97

198. Zarate, C. A., Jr., Singh, J. B., Carlson, P. J., Quiroz, J., Jolkovsky, L., Luckenbaugh, D. A., and Manji, H. K. (2007) Efficacy of a protein kinase C inhibitor (tamoxifen) in the treatment of acute mania: a pilot study. *Bipolar Disord* **9**, 561-570

199. Yildiz, A., Guleryuz, S., Ankerst, D. P., Ongur, D., and Renshaw, P. F. (2008) Protein kinase C inhibition in the treatment of mania: a double-blind, placebo-controlled trial of tamoxifen. *Arch Gen Psychiatry* **65**, 255-263

200. Berridge, M. J. (1989) The Albert Lasker Medical Awards. Inositol trisphosphate, calcium, lithium, and cell signaling. *JAMA* **262**, 1834-1841

201. Nahorski, S. R., Ragan, C. I., and Challiss, R. A. (1991) Lithium and the phosphoinositide cycle: an example of uncompetitive inhibition and its pharmacological consequences. *Trends Pharmacol Sci* **12**, 297-303

202. Harwood, A. J. (2005) Lithium and bipolar mood disorder: the inositol-depletion hypothesis revisited. *Mol Psychiatry* **10**, 117-126

203. Manchia, M., Squassina, A., Congiu, D., Chillotti, C., Ardau, R., Severino, G., and Del Zompo, M. (2009) Interacting genes in lithium prophylaxis: preliminary results of an exploratory analysis on the role of DGKH and NR1D1 gene polymorphisms in 199 Sardinian bipolar patients. *Neurosci Lett* **467**, 67-71

204. Winder, W. W., and Hardie, D. G. (1999) AMP-activated protein kinase, a metabolic master switch: possible roles in type 2 diabetes. *Am J Physiol* **277**, E1-10

205. Swoap, S. J., Rathvon, M., and Gutilla, M. (2007) AMP does not induce torpor. *Am J Physiol Regul Integr Comp Physiol* **293**, R468-473

206. Jinka, T. R., Toien, O., and Drew, K. L. Season primes the brain in an arctic hibernator to facilitate entrance into torpor mediated by adenosine A(1) receptors. *J Neurosci* **31**, 10752-10758

207. Street, S. E., Kramer, N. J., Walsh, P. L., Taylor-Blake, B., Yadav, M. C., King, I. F., Vihko, P., Wightman, R. M., Millan, J. L., and Zylka, M. J. Tissue-nonspecific alkaline phosphatase acts redundantly with PAP and NT5E to generate adenosine in the dorsal spinal cord. *J Neurosci* **33**, 11314-11322

208. Keiser, M. J., Setola, V., Irwin, J. J., Laggner, C., Abbas, A. I., Hufeisen, S. J., Jensen, N. H., Kuijer, M. B., Matos, R. C., Tran, T. B., Whaley, R., Glennon, R. A., Hert, J., Thomas, K. L., Edwards, D. D., Shoichet, B. K., and Roth, B. L. (2009) Predicting new molecular targets for known drugs. *Nature* **462**, 175-181

209. Bosier, B., Muccioli, G. G., Hermans, E., and Lambert, D. M. Functionally selective cannabinoid receptor signalling: therapeutic implications and opportunities. *Biochem Pharmacol* **80**, 1-12

210. Deliganis, A. V., Pierce, P. A., and Peroutka, S. J. (1991) Differential interactions of dimethyltryptamine (DMT) with 5-HT1A and 5-HT2 receptors. *Biochem Pharmacol* **41**, 1739-1744

211. Smith, R. L., Canton, H., Barrett, R. J., and Sanders-Bush, E. (1998) Agonist properties of N,N-dimethyltryptamine at serotonin 5-HT2A and 5-HT2C receptors. *Pharmacol Biochem Behav* **61**, 323-330

212. Abbracchio, M. P., Burnstock, G., Boeynaems, J. M., Barnard, E. A., Boyer, J. L., Kennedy, C., Knight, G. E., Fumagalli, M., Gachet, C., Jacobson, K. A., and Weisman, G. A. (2006) International Union of Pharmacology LVIII: update on the P2Y G protein-coupled nucleotide receptors: from molecular mechanisms and pathophysiology to therapy. *Pharmacol Rev* **58**, 281-341

213. Pacher, P., Batkai, S., and Kunos, G. (2006) The endocannabinoid system as an emerging target of pharmacotherapy. *Pharmacol Rev* **58**, 389-462

214. Saxe, J. P., Wu, H., Kelly, T. K., Phelps, M. E., Sun, Y. E., Kornblum, H. I., and Huang, J. (2007) A phenotypic small-molecule screen identifies an orphan ligand-receptor pair that regulates neural stem cell differentiation. *Chem Biol* **14**, 1019-1030

215. Wilson, S., Bergsma, D. J., Chambers, J. K., Muir, A. I., Fantom, K. G., Ellis, C., Murdock, P. R., Herrity, N. C., and Stadel, J. M. (1998) Orphan G-protein-coupled receptors: the next generation of drug targets? *Br J Pharmacol* **125**, 1387-1392

216. Szekeres, P. G. (2002) Functional assays for identifying ligands at orphan G protein-coupled receptors. *Receptors Channels* **8**, 297-308

217. Olkkola, K. T., and Ahonen, J. (2008) Midazolam and other benzodiazepines. *Handb Exp Pharmacol*, 335-360

218. Danysz, W., and Parsons, C. G. (1998) Glycine and N-methyl-D-aspartate receptors: physiological significance and possible therapeutic applications. *Pharmacol Rev* **50**, 597-664

219. Dilly, S., Lamy, C., Marrion, N. V., Liegeois, J. F., and Seutin, V. Ion-channel modulators: more diversity than previously thought. *Chembiochem* **12**, 1808-1812

220. Conn, P. J., Christopoulos, A., and Lindsley, C. W. (2009) Allosteric modulators of GPCRs: a novel approach for the treatment of CNS disorders. *Nat Rev Drug Discov* **8**, 41-54

221. Brauner-Osborne, H., Wellendorph, P., and Jensen, A. A. (2007) Structure, pharmacology and therapeutic prospects of family C G-protein coupled receptors. *Curr Drug Targets* **8**, 169-184

222. Roth, B. L., Sheffler, D. J., and Kroeze, W. K. (2004) Magic shotguns versus magic bullets: selectively non-selective drugs for mood disorders and schizophrenia. *Nat Rev Drug Discov* **3**, 353-359

223. Belmonte, S. L., and Blaxall, B. C. G protein coupled receptor kinases as therapeutic targets in cardiovascular disease. *Circ Res* **109**, 309-319

224. DeWire, S. M., Ahn, S., Lefkowitz, R. J., and Shenoy, S. K. (2007) Beta-arrestins and cell signaling. *Annu Rev Physiol* **69**, 483-510

225. Hollinger, S., and Hepler, J. R. (2002) Cellular regulation of RGS proteins: modulators and integrators of G protein signaling. *Pharmacol Rev* **54**, 527-559

226. Yasuda, S., Kai, M., Imai, S., Takeishi, K., Taketomi, A., Toyota, M., Kanoh, H., and Sakane, F. (2009) Diacylglycerol kinase eta augments C-Raf activity and B-Raf/C-Raf heterodimerization. *J Biol Chem* **284**, 29559-29570